2013

The Effects of Hydrostatic Pressure on Early Endothelial Tubulogenic Processes

Ryan M. Underwood
University of Kentucky, ryan.underwood@uky.edu

STUDENT AGREEMENT:

I represent that my thesis or dissertation and abstract are my original work. Proper attribution has been given to all outside sources. I understand that I am solely responsible for obtaining any needed copyright permissions. I have obtained and attached hereto needed written permission statements(s) from the owner(s) of each third-party copyrighted matter to be included in my work, allowing electronic distribution (if such use is not permitted by the fair use doctrine).

I hereby grant to The University of Kentucky and its agents the non-exclusive license to archive and make accessible my work in whole or in part in all forms of media, now or hereafter known. I agree that the document mentioned above may be made available immediately for worldwide access unless a preapproved embargo applies.

I retain all other ownership rights to the copyright of my work. I also retain the right to use in future works (such as articles or books) all or part of my work. I understand that I am free to register the copyright to my work.

REVIEW, APPROVAL AND ACCEPTANCE

The document mentioned above has been reviewed and accepted by the student's advisor, on behalf of the advisory committee, and by the Director of Graduate Studies (DGS), on behalf of the program; we verify that this is the final, approved version of the student's dissertation including all changes required by the advisory committee. The undersigned agree to abide by the statements above.

Ryan M. Underwood, Student

Dr. Hainsworth Y. Shin, Major Professor

Dr. Abhijit Patwardhan, Director of Graduate Studies

THE EFFECTS OF HYDROSTATIC PRESSURE ON EARLY ENDOTHELIAL TUBULOGENIC PROCESSES

THESIS

A thesis submitted in partial fulfillment of the requirements
for the degree of Master of Science in Biomedical Engineering
in the College of Engineering
at the University of Kentucky

By

Ryan M. Underwood

Director: Dr. Hainsworth Y. Shin, Professor of Biomedical Engineering

Lexington, Kentucky

2013

ABSTRACT OF THESIS

THE EFFECTS OF HYDROSTATIC PRESSURE ON EARLY ENDOTHELIAL TUBULOGENIC PROCESSES

The effects of mechanical forces on endothelial cell function and behavior are well documented, but have not been fully characterized. Specifically, fluid pressure has been shown to elicit physical and chemical responses known to be involved in the initiation and progression of endothelial cell-mediated vascularization. Central to the process of vascularization is the formation of tube-like structures. This process—tubulogenesis—is essential to both the physiological and pathological growth of tissues. Given the known effects of pressure on endothelial cells and its ubiquitous presence in the vasculature, we investigated pressure as a magnitude-dependent parameter for the regulation of endothelial tubulogenic activity. To accomplish this, we exposed two- and three-dimensional bovine aortic endothelial cell (BAEC) cultures to static pressures of 0, 20, and 40 mmHg for 3 and 4 days. The most significant findings were: (1) cells in two-dimensional culture exposed to 20, but not 40, mmHg exhibited significantly ($p < 0.05$) increased expression of both VEGF-C and VEGFR-3, and (2) cells in three-dimensional culture exposed to 20, but not 40, mmHg exhibited significant ($p > 0.05$) increases in endothelial sprouting. These findings evince the utility of pressure as a selective modulator of tissue microvascularization *in vitro* and implicate pressure as factor in pathological tubulogenesis *in vivo*.

KEYWORDS: angiogenesis, lymphangiogenesis, pressure, mechanotransduction, tissue-engineering

_____

_____

THE EFFECTS OF HYDROSTATIC PRESSURE ON EARLY ENDOTHELIAL TUBULOGENIC PROCESSES

by

Ryan Underwood

Master of Science in Biomedical Engineering
in the College of Engineering at the University of Kentucky

_____
Dr. Hainsworth Shin, Director of Thesis

_____
Dr. Abhijit Patwardhan, Director of Graduate Studies

_____
Date

Acknowledgements

I would like to acknowledge Dr. Hainsworth Shin for his consistent support, patience, and enthusiasm throughout the research discussed herein. I would also like to thank Dr. David Puleo (University of Kentucky) and Dr. Thomas Dziubla (University of Kentucky) for serving on my thesis committee and their thoughtful comments.

Furthermore, I would like to thank Dr. Steven Lai-Fook (University of Kentucky) for his assistance with and providing equipment for the pressure system.

I would like to thank Dr. Xiaoyan Zhang for her assistance with the flow cytometry experiments. I would also like to thank Xingjian Lei for completing extra experiment replicates where needed.

Table of Contents

List of Figures viii

List of Tables xi

1. Introduction 1

1.1 Fundamentals of Tissue Engineering 2

1.2 The Vasculature: Structure and Hemodynamics 4

Blood Vessels 4

Endothelial Cells 5

Mechanoenvironment of Endothelial Cells 8

1.3 Tubulogenesis 9

Tubulogenesis In Vivo 9

Tubulogenesis In Vitro 12

Clinical Implications 14

1.4 Tubulogenic Growth Factor Signaling 14

Vascular Endothelial Growth Factors (VEGFs) 15

Fibroblast Growth Factors (FGFs) 18

FGF and VEGF Synergy in Angiogenesis and Lymphangiogenesis 19

1.5 Effects of Pressure on Endothelial Cells 20

2. Rationale 22

3. Materials and Methods **24**

3.1 Cell Substrates 24

3.2 Cell Lines, Culture Conditions, and Passaging 25

3.3 Cell Storage 26

3.4 Cell Seeding 27

Two-Dimensional Substrates: Seeding in Multi-well Tissue Culture Plates 27

Three-Dimensional Substrates: Seeding on Cytodex3™ Microcarrier Beads 27

3.5 Pressure System 28

3.6 Proliferation Assay 32

Seeding and Pressure Exposure 32

Fixation, Labeling, and Quantification 33

3.7 Flow Cytometric Analysis of VEGFR-3 and VEGF-C Expression 34

Seeding and Pressure Exposure 34

Immunofluorescence Labeling of Cells 34

3.8 Three-Dimensional Collagen Gel Assays 35

Preparation of Endothelialized Beads 35

Collagen Gel Formulation 36

Gel Polymerization 37

Two-Layer Gel Polymerization 38

Single-Layer Gel Polymerization 39

3.9 Imaging 40

3.10 Migration/Invasion Assay Analysis 41

3.11 Tube Formation Assay Analysis 43

3.12 Statistical Analysis 44

4. Results 45

4.1 BAEC Culture on Two-Dimensional Substrates 45

4.2 Crystal Violet Uptake by BAEC 46

4.3 BAEC Seeding on Cytodex3™ Microcarrier Beads 46

4.4 Generation of Sustained Hydrostatic Pressures 47

4.5 Increase of BAEC Cell Density by Stimulation with Basic Fibroblast Growth Factor 50

4.6 Effect of Sustained Hydrostatic Pressure on BAEC Population Growth 51

4.7 Effect of Sustained Hydrostatic Pressure on BAEC Morphology 54

4.8 Role of VEGFR-3 in the Mediation of Pressure-Induced Endothelial Proliferation 55

4.9 Effects of Pressure on VEGF-C and VEGFR-3 Expression 56

4.10 Effects of Pressures on BAEC Migration and Invasion of a Three-Dimensional Collagen Matrix 57

4.11 Effects of Local Growth Factor Concentrations on BAEC Tubulogenesis 60

4.12 Effects of a 20 mmHg Sustained Hydrostatic Pressure on BAEC Tubulogenesis 65

4.13 Effects of a 40 mmHg Sustained Hydrostatic Pressure on BAEC Tubulogenesis 69

5. Discussion 74

5.1 Physiological Relevance of the Hydrostatic Pressures Used 74

5.2 Selection of Cell Type and Three-Dimensional Matrix Composition 75

5.3 Experimental Setup for Pressure Experiments 77

5.4 Confirmation of Cellular Responses of BAEC Grown in Two-Dimensional

Culture to Sustained Hydrostatic Pressures 79

Pressure Upregulates Proliferation at 20 mmHg, but not 40 mmHg, after Three Days of Exposure 79

Pressure Induces Morphological Changes in Endothelial Cells 82

MAZ-51 Inhibitor Blocks Increased Proliferation in Response to Pressure 82

Increased VEGF-C and VEGFR-3 Expression to Sustained Pressure Exposure 85

5.5 Investigation of the Effects of Sustained Pressure on Endothelial Migration and Invasion 85

5.6 Investigation of the Effect of Sustained Pressures on Endothelial Tube Formation 90

5.7 Concluding Remarks 97

References **100**

Vita **104**

List of Figures

Figure 1.2a – Progression of Sprouting Angiogenesis 10

Figure 3.5a – Three-Dimensional Model of Pressure Chambers 30

Figure 3.5b – Schematic Representation of the Pressure System 31

Figure 3.8b – 2-Layer Gel Polymerization 39

Figure 3.8c – Single-Layer Gel Polymerization 40

Figure 3.10a –InvasiQuant ImageJ Macro Code 42

Figure 4.1a – BAEC Cultured on Two-Dimensional Surface 45

Figure 4.2a – BAEC Stained with Crystal Violet 46

Figure 4.3a – BAEC Seeded on Cytodex3^{TM} Microcarrier Bead 47

Figure 4.4a – Pressure Measurement Methods 48

Figure 4.4b – Pulsatile Pressure Measurement 49

Figure 4.5a – Effect of Exogenous FGF-2 on Cell Density 50

Figure 4.6a – Effects of 20 and 40 mmHg Pressures on Cell Density (72 hours) 51

Figure 4.6b – Comparison of Effects of 20 and 40 mmHg Pressures on Cell Density (72 hours) 53

Figure 4.7a – Morphological Effect of Pressure on Cells Grown on Two-Dimensional Tissue Culture Surfaces 54

Figure 4.8a – Pressure Response-Blocking Effect of MAZ51 55

Figure 4.9a – Pressure Up-regulation of VEGF-C and VEGFR-3 Expression 56

Figure 4.10a –Migration Assay Images Processed Using InvasiQuant ImageJ Macro 57

Figure 4.10b –Effect of Exogenous Growth Factors on Endothelial Migration After 72and 96 Hours 58

Figure 4.10c –Effect of 20 and 40 mmHg Hydrostatic Pressures on Endothelial Migration After 72 and 96 Hours 59

Figure 4.11a –Example Image of Tubulogenic Sprouting and Measurement 61

Figure 4.11b –Representative Images of Tubulogenic Sprouting under Control Pressure Under Various Growth Factor Conditions 61

Figure 4.11c –Effects of FGF-2, VEGF-A, and FGF-2+VEGF-A on BAEC Sprouting 63

Figure 4.11d –Effects of FGF-2, VEGF-A, and FGF-2+VEGF-A on BAEC Sprout Length 64

Figure 4.12a –Representative Images of the Effect of 20 mmHg on Tubulogenic Sprouting (72 Hours) 65

Figure 4.12b –Representative Images of the Effect of 20 mmHg on Tubulogenic Sprouting (96 Hours) 66

Figure 4.12c –Effect of 20 mmHg Hydrostatic Pressure on the Total Number of Sprouts Formed per Bead (72/96 Hours) 66

Figure 4.12d –Effect of 20 mmHg Hydrostatic Pressure on the Number of Sprouts per Bead of Length Greater than 75 µm (72/96 Hours) 67

Figure 4.12e –Effect of 20 mmHg Hydrostatic Pressure on the Number of Sprouts per Bead of Length Greater than 150 µm (72/96 Hours) 68

Figure 4.12f – Effect of 20 mmHg Hydrostatic Pressure on the Mean Sprout Length per Bead (72/96 Hours) 69

Figure 4.13a –Representative Images of the Effect of 40 mmHg on Tubulogenic Sprouting (72 Hours) 70

Figure 4.13b –Representative Images of the Effect of 40 mmHg on Tubulogenic Sprouting (96 Hours) 71

Figure 4.13c –Effect of 40 mmHg Hydrostatic Pressure on the Total Number of Sprouts Formed per Bead (72/96 Hours) 71

Figure 4.13d –Effect of 40 mmHg Hydrostatic Pressure on the Number of Sprouts per Bead of Length Greater than 75 µm (72/96 Hours) 72

Figure 4.13e –Effect of 40 mmHg Hydrostatic Pressure on the Number of Sprouts per Bead of Length Greater than 150 µm (72/96 Hours) 73

Figure 4.13f – Effect of 20 mmHg Hydrostatic Pressure on the Mean Sprout Length per Bead (72/96 Hours) 73

Figure 5.1a – Local Blood Pressure Levels Throughout the Circulatory System 74

Figure 5.5a – Representative Images of Migration Assay Image Processing 86

Figure 5.6a – Growth Factor Signaling Pathway Diagram and Pressure Effect 94

List of Tables

Table 1.4a – Table of Known Pro-Tubulogenic Effects of VEGF-A 16

Table 1.4b – Table of Known Pro-Tubulogenic Effects of VEGF-C 17

Table 1.4c – Table of Known Pro-Tubulogenic Effects of FGF-2 18

Table 3.8a – Collagen Gel Formulation 36

Table 5.6a – Summary of Significant ($p > 0.05$) Differences between Pressure and Control Cultures 93

1. Introduction

Vascularization and blood flow are critical elements of any viable, living tissue whether the tissue is grown *in vitro* or *in vivo*. Blood vessels are the first organ developed during embryogenesis and eventually becomes the largest organ in the human body [1]. The most important function of the vascular system is the delivery of oxygen and nutrients to and the removal of waste products from peripheral tissues [2]. Mammalian cells require a constant supply of oxygen and blood-borne nutrients for survival [3]. The most predominant limiting factor in the clinical application of tissue engineering is the inability to generate microvasculature *de novo* [3]. Tissue constructs greater than one to two millimeters thick require a capillary network for the maintenance and function of cells within them [3]. Below this threshold thickness, cells receive oxygen by simple diffusion. In tissues thicker than one to two millimeters, the lack of a capillary network connected to the host tissue limits the generation of synthetic tissue constructs to thicknesses that are generally too thin for clinical applications [3]. Except for cartilage, tissues in the body can overcome insufficient perfusion by constructing capillary networks that provide conduits for convective transport of nutrients, dissolved gases, and waste products to and from tissues [3]. Inducing and controlling this process in tissue-engineered constructs presents a unique challenge in mass transport that must be overcome in order to produce clinically viable tissues beyond the one-to-two millimeter thickness limitation, such as large tissue masses and whole organs [3]. In addition to the challenges it presents in the tissue engineering context, abnormal or insufficient vessel growth plays a major role in human health and the pathogenesis of many congenital (e.g.

vascular malformations, DiGeorge syndrome) and non-congenital disorders (e.g., atherosclerosis, cancer, macular degeneration, Compartment Syndrome) [1].

1.1. Fundamentals of Tissue Engineering

Tissue engineering is a multidisciplinary field in which significant advances in biochemistry, cell biology, genetics, biomedical engineering and materials science have made possible the use of synthetic or naturally derived, engineered biomaterials to replace damaged or defective tissues, such as bone, skin, and even organs [4].

Tissue engineering involves the culture of mammalian cells (e.g., skin, muscle, cartilage, bone, endothelial, and stem cells) on a large scale in order to create new tissues and functional organs [4]. A typical tissue engineering application may consist of a biological or synthetic "scaffold" that when implanted in the body—as a temporary structure—provides a template that allows the body's own cells to grow and form new tissues while the scaffold is gradually absorbed [4]. Currently, there are three approaches to optimize nutrient transport in these scaffolds: (1) stimulating rapid vessel growth in avascular implants with angiogenic factors; (2) seeding biodegradable polymer scaffolds, which provide bulk, with endothelial cells and angiogenic factors; and (3) pre-vascularizing the artificial tissue before implantation [5]. Each of these approaches has exhibited promising results, but only the third approach—pre-vascularization with the expectation that the new microvessel network will rapidly integrate with the host microcirculation—eliminates the need for vascularization *in situ* post-implantation [5]. Implanting pre-vascularized tissues is, thus, anticipated to ensure uninterrupted fluid transport and long-term survival of cells at the center of the tissue [5].

Initiation of the self-assembly of blood vessels when pre-vascularizing tissues is a complex endeavor. *Schechner et al.* (2000) have shown that endothelial cells will form "cords"—non-luminal cell-cell structural connections—in fibronectin gels *in vitro* that will integrate with the host's vascular system after implantation *in vivo* [6]. *Nehls and Drenkhan* (1995) showed that endothelial cells grown on microcarrier beads embedded in collagen will form "capillary-like" structures when co-cultured with supporting cell types that express pro-angiogenic growth factors [7]. *Dietrich and Lelkes* (2005) showed that endothelial cells are also capable of forming the same "capillary-like" structures when co-cultured with angiogenesis-supporting cell types in collagen matrices [8]. However, thick tissues will require fully formed capillaries containing lumens and these structures do not, or rarely do, form and cannot be sustained in collagen matrices [5]. Thus, the formation of fully functioning, sustainable microvasculature will require a matrix composed of a multi-component extracellular matrix containing cells types that support angiogenesis.

To this point, tissue engineering applications have been severely limited to constructs that are two millimeters in thickness or less due to the difficulty in generating native vascular networks in tissue-engineered constructs [5]. Current tissue-engineered constructs are predominantly avascular, with the delivery of nutrients and removal of waste occurring by diffusion [9]. Because the diffusion distance of oxygen is 100-200 microns, avascular tissues grown *in vitro* are limited to this thickness range [3]. Mammalian cells must be located within the oxygen diffusion range (100-200 microns) of a blood vessel *in vivo* so as to satisfy their nutritional needs for proper functioning [3]. Growing larger, more complex structures *in vitro* will require a vascular network that

supports cellular viability and function with vessels furnishing overlapping regions of tissues with the essential gas and nutrient supply [3].

The limitations imposed by the inability of current strategies to successfully prevascularize tissue-engineered constructs must be overcome as the current organ transplant waitlist stands at over 100,000 patients [9]. Currently, approximately 2,000 patients die per year while waiting on a donor organ transplants, as current capacity only allows roughly 50% of patients to receive the vital organ transplants they need to survive [9]. *In vitro* grown organs, though a distant goal, is nonetheless one significant way that deaths from donor organ shortages can be eliminated. Furthermore, tissue-engineered replacement organs can avoid many of the problems that patients face upon receiving donor tissues. By using a patient's own cells to cultivate tissues to replace those that are damaged and diseased, the risk of rejection is significantly attenuated and the need for immunosuppressive drugs may be eliminated [4]. These combined effects reduce both the cost of medical treatment as well as patient mortality rates. The ultimate goal is totally replacing the need for donor organs with tissue-engineered organs, but technical obstacles must first be overcome [4]. All in all, it is estimated that tissue-engineering solutions potentially could address diseases and disorders accounting for about half of the nation's total healthcare costs [4].

1.2 The Vasculature: Structure and Hemodynamics

Blood Vessels

Blood vessel is a term that encompasses, generally, every type of blood-carrying conduit within an organism. Their primary function is the efficient transport of blood to

downstream tisues so as to promote the exchange of oxygen and nutrients for carbon dioxide and cellular waste within the tissues that they infiltrate [2, 10]. Blood vessels typically extend throughout an organism in a branched network wherein large, thick-walled vessels empty into incrementally smaller, thinner-walled vessels ultimately culminating in capillaries which are comprised of only a single layer of endothelial cells wrapped with a monolayer of perivascular cells [2, 10]. In humans, the morphology of the circulatory network consists of a branching of arteries into smaller arterioles from which a dense network of capillaries branch. The capillaries then coalesce into venules and then larger veins responsible for returning blood back to the heart [10].

In the larger vessels, the endothelial monolayer is supported by two thick outer layers of connective tissue capable of sustaining the large, pulsatile pressures characteristic of the macrocirculation. The outermost layer, the *tunica adventitia*, is a zone of connective tissue composed of collagenous and elastic fibers that enable a vessel's elasticity [2]. The layer in between the outermost and innermost layers, onto which the endothelial cells attach, is the *tunica media*, which is composed of alternating layers of elastic fibers and smooth muscle cells (SMCs) [2].

Endothelial Cells

The average adult human body contains approximately 1×10^{13} endothelial cells [11] Endothelial cells comprise the non-thrombogenic cellular monolayer that lines the interior surface of all blood and lymphatic vessels [2]. The endothelium is versatile and multifunctional and has many synthetic and metabolic roles, including the regulation of thrombosis and thrombolysis, platelet adherence, modulation of vascular tone and blood flow, and regulation of immune and inflammatory responses by controlling leukocyte and

platelet interactions with the vessel wall [11]. These functions are modulated by endothelial cells themselves in response to the continually changing chemical environment as well as the forces generated by the circulation of blood (or lymph in the lymphatic system) [2, 12].

Endothelial cells all derive from the same endothelial progenitor cell, but they may terminally differentiate into different phenotypes. For example, endothelial cells can differentiate into either arterial or venous endothelial cells during embryonic development and display remarkable phenotypic plasticity depending on their location in the body [1, 11]. Reportedly, it is possible that there might be as many different endothelial cell types as there are organs in the body [1,11]. For example, it has been shown that the expression and activity of Angiopoietin-1 (Ang-1) and vascular endothelial growth factor-A (VEGF-A), two potent angiogenic factors, vary greatly in different tissues depending on their vascularity [1, 11]. As another example of the phenotypic diversity of endothelial cells, the ability of Ang-1 to promote endothelial cell proliferation and survival is also organ- or tissue-specific [1, 13]. Notably, it has been shown that Ang-1 stimulates angiogenesis in the skin, but exerts the opposite effect in the heart where it suppresses vascular growth [13]. Such a difference is likely due to the fact that blood vessel remodeling and reconstruction is much more prevalent in epidermal tissues than cardiac tissues. The realization of such location-specific endothelial phenotypes provides opportunities for specialized angiogenic and vasculogenic therapies [1].

In addition to providing mechanical strength, the endothelial monolayer serves as a permeability barrier between the blood circulating in the vascular system and the

surrounding extravascular tissues [1]. The intercellular junctions between cells enable the mechanical strength and selective permeability properties of the endothelial cell monolayer. In quiescent vessels, the presence of adherens and tight junctions determine the mechanical strength and barrier properties of the endothelium [1]. Moreover, intercellular junctions not only create the structural barrier between the blood and the tissues, but also transmit signals critical for endothelial cell survival and intercellular signaling [1]. These junctions also dissolve during vessel spouting to allow individual cells to migrate, but are then reestablished during vessel construction [1]. Generally, VEGF signaling results in a "loosening" of these intercellular junctions and Ang-1 signaling results in "tightening" of these junctions [1].

Endothelial cells also engage in both autocrine and paracrine cell signaling with the smooth muscle cells to regulate vascular tone during blood flow control [11]. They also communicate through inflammatory mediators with the circulating white blood cells and platelets to modulate the immune response and the blood coagulation cascade [11]. But one of the most vital roles of endothelial cells is neovascularization and vascular remodeling. Endothelial cells are largely responsible for the initiation of angiogenic and lymphangiogenic processes. Despite the fact that endothelial cells are elongated, thin, and fragile cells, they are able to construct conduits capable of withstanding the mechanical forces generated as the heart drives blood throughout the vascular network [11]. And though the formation of large blood and lymphatic vessels also requires the actions of other cell types such as pericytes, fibroblasts, and smooth muscle cells (SMCs), the formation of the smallest blood vessels, capillaries, is mediated by endothelial cells [2, 11].

Mechanoenvironment of Endothelial Cells

Endothelial cells exist as a thin monolayer on a deformable substrate and are in contact with a dynamic, incompressible, flowing fluid [12]. External forces applied to endothelial cells are caused by the hydrodynamic and hydrostatic forces applied by blood and lymph and extrinsic stresses and strains caused by muscle contraction or vessel compliance [2]. These physiological conditions result in the exposure of endothelial cells to three predominant external mechanical forces: hydrodynamic pressure, fluid shear stress, and tensile stress [2, 14].

The effect of hemodynamic stresses—those resulting from the flow of blood or lymph—in modulating both normal and pathological endothelial functions is supported by ample evidence [2]. Studies of the effects of mechanical forces on vascular remodeling have been focused primarily on shear stress and substrate strain. Shear stress (i.e., wall shear stress) results from the frictional drag imparted on endothelial cells as blood flows over the monolayer surface [2]. Substrate strain (also, substrate tension or substrate stretch) is the circumferential stretch of the vessel wall, to which the endothelial monolayer is attached, caused by the pressure gradient between the blood vessel lumen and the vessel exterior [2]. Both shear stress and substrate strain have been the subject of both *in vitro* and *in vivo* studies. *In vivo* studies have demonstrated that each of the aforementioned mechanical stimuli promotes different types of angiogenesis [2]. Substrate tension initiates or upregulates sprouting angiogenesis and shear stress initiates or upregulates intussusceptive angiogenesis [2]. The discovery of different angiogenic responses to different mechanical stimuli could indicate that these mechanical signals are transduced through different biochemical pathways [2]. Such a possibility lends credence

to proposition that the endothelial response to hydrostatic pressure, in isolation from the other hemodynamic forces, could involve a unique intracellular mechanotransduction pathway.

1.3. Tubulogenesis

Tubulogenesis In Vivo

Tubulogenesis encompasses the process by which endothelial tubes are formed and stabilized with the eventual development into a microvascular network. The three types of tubulogenic processes mediated by endothelium include: angiogenesis, lymphangiogenesis, and vasculogenesis. Angiogenesis, generally, is the vascular process by which new blood vessels are formed from preexisting blood vessels [2]. Lymphangiogenesis is a process analogous to angiogenesis, but describes the process as it occurs for lymphatic vessels [15]. Vasculogenesis is defined as the process by which endothelial precursor cells called angioblasts differentiate into endothelial cells and form a primitive vascular network *de novo* [16]. Angiogenesis and vasculogenesis were initially considered discrete and independent events; however, it is now recognized that neovascularization is a more complex process that may involve both types of vessel formation within a single microenvironment [17].

With respect to angiogenesis (and lymphangiogenesis), there are two sub-types of vessel formation: sprouting angiogenesis and intussusceptive angiogenesis [2, 18]. The process of

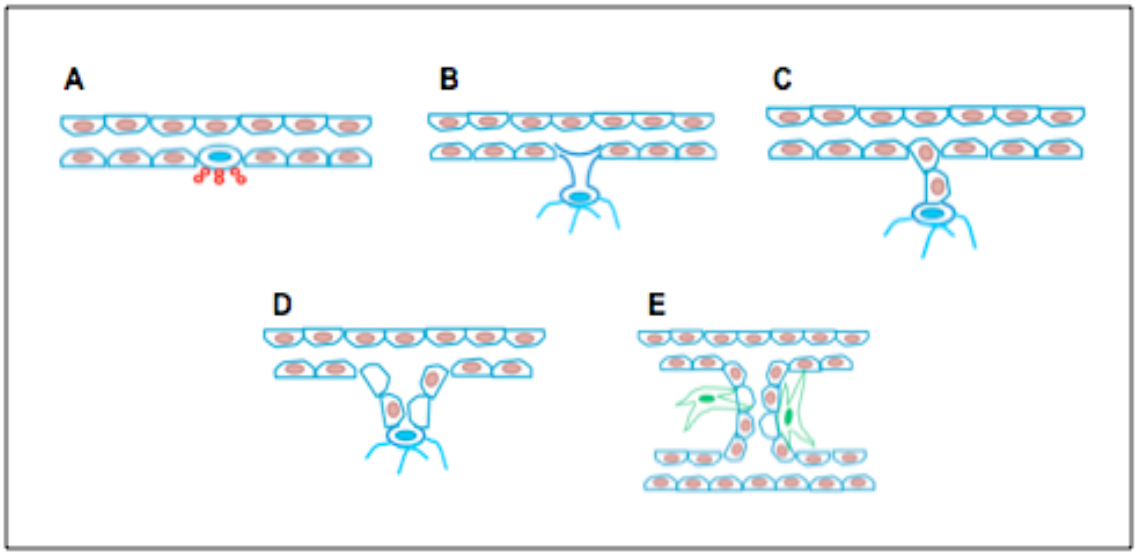

***Figure 1.2a* – Progression of sprouting angiogenesis. (A) Endothelial cell (EC) is stimulated by pro-angiogenic growth factors, (B) EC ("tip cell") degrades local extracellular matrix (ECM) elongates and migrates into the surrounding tissue space, (C) Other ECs ("trunk cells") follow the "tip cell" in invasion of the ECM, (D) ECs form multi-cellular sprout and begin forming a luminal structure, and (E) ECs for a patent lumen, recruit supporting cell types, and anastomose with other capillary structures.**

sprouting tubulogenesis is shown in *Figure 1.2a*. In both angiogenesis and lymphangiogenesis, endothelial cells are predominantly responsible for the initiation and progression of tube formation [2, 18]. The type of angiogenesis of interest in this study is sprouting angiogenesis, a process that consists of five sequential steps:

(1) dissolution of the basement membrane and detachment of pericytes at the site of branching;

(2) migration of endothelial cells toward the extracellular space and formation of a multicellular sprout;

(3) proliferation of endothelial cells ("trunk cells") behind a leading cell ("tip cell");

(4) morphological differentiation and formation of a lumen in the endothelial sprout;

(5) recruitment of supporting cell types (e.g., pericytes, fibroblasts, smooth muscle cells) and formation of the basement membrane around the new vessel [2, 18].

Steps 1 – 4 constitute what could be defined as "early tubulogenic activity" [2, 18, 19]. These early tubulogenic activities are followed by the arrest of proliferation and vessel stabilization with the formation of a basement membrane around the new tube and the recruitment of pericytes [2, 18]. The stabilization phase is essential to vessel development, as early-stage endothelial tubes will rapidly undergo apoptosis and regression without stabilization. [2, 18].

The role that the extracellular matrix (ECM) plays in both the direction of vessel growth and the preservation of new vessels cannot be understated. The ECM regulates the formation of new vessel sprouts and, when vascular cells migrate to form new sprouts, this matrix network is proteolytically broken down and its composition altered. [1]. Prior to vessel stabilization, the provisional extracellular matrix composed of fibronectin, fibrin, and other components provides a support scaffold, guiding endothelial cells to their targets [1]. Vessel stabilization is greatly enabled by supporting interstitial cells types (e.g., pericytes, fibroblasts, SMCs) and extracellular matrix (ECM) proteins [1]. The ECM provides the necessary contacts between endothelial cells and the surrounding tissue that prevent vessels from collapsing [1, 2]. Quiescent, stable vessels are encased by a basement membrane comprised of Type IV collagen, laminin, and other proteins [1, 2]. Surrounding this membrane is an interstitial matrix of Type I collagen and elastin, which provides viscoelasticity and strength to the vessel wall [2].

Tubulogenesis in Vitro

Tubulogenesis was first observed *in vitro* by Judah Folkman and Christian Haudenschild in 1980 [20]. Folkman, known as the "Father of Angiogenesis", and Haudenschild demonstrated that microvascular endothelial cells were capable of forming capillary-like structures *in vitro* in the absence of blood flow and supporting cell types [2, 16]. To date, several different types of *in vitro* tubulogenic assays have proven capable of generating capillary-like structures from the culture of endothelial cells alone. The types of *in vitro* tubulogenesis assays that have been developed can be divided into two categories: two-dimensional (2-D) and three-dimensional (3-D).

Two-dimensional *in vitro* tubulogenesis assays are those in which endothelial cells are seeded onto the surfaces of hydrogels (e.g., collagen, fibrin, Matrigel) or plastic culture-treated dishes on which they form sprouts or capillary-like structures within the two-dimensional plane of the culture surface [2]. However, to ensure that the cells form an interconnected network of tubes or endothelial cords instead of a confluent monolayer on 2-D culture surfaces, endothelial cells must be sparsely seeded on the surface and the underlying substrate must consist of select basement membrane proteins—mainly laminin and type IV collagen [2]. Earlier studies have shown that endothelial cells grown on the surface of a collagen gel form a monolayer on the surface and, absent treatment with angiogenic activity-inducing chemicals (e.g., phorbol esters), do not invade the underlying matrix [21]. Thus, 2-D assays are not the best model of the essential early tubulogenic processes in the absence of artificial stimulation.

Though 2-D assays have been widely used, they present two issues that raise concerns about their accuracy as models of angiogenesis. First, sprouting occurs from

individual cells or cell aggregates and not from an endothelial monolayer, as is the case *in vivo*. Second, the endothelial tubes or sprouts are in contact with fluid on the outside and any existing lumens contain extracellular matrix material on the inside—the inverse of what occurs *in vivo* [21]. Two-dimensional assays, on the other hand, have several benefits such as the ability to easily and quickly culture, image, and quantify tube formation [21]. Although 2-D angiogenesis models have greatly contributed to the understanding of the role of the extracellular matrix in vascular and lymphatic morphogenesis, these models do not encompass all of the steps of physiological tubulogenesis [16, 18].

Three-dimensional models of tubulogenesis consist of those assays in which individual endothelial cells, endothelial cell aggregates, or endothelial cell-coated microcarrier beads are embedded in a gelatinous matrix [2]. These models provide the best portrayal of endothelial cell migration and ECM invasion as it occurs in sprouting angiogenesis *in vivo* [2]. The assay that employs the use of endothelial cell-coated microcarrier beads, initially developed by *Nehls and Drenkhahn* in 1995 [7], has become one of the most widely used three-dimensional models. *Nehls and Drenkhahn* (1995) recognized that 2-D angiogenesis assays did not accurately reproduce *in situ* conditions. They also recognized that, though 3-D angiogenesis assays consisting of animal aortic segments embedded in hydrogels could produce capillary-like structures, it had not been shown that these structures were predominantly composed of endothelial cells. [7]. Thus, the need to investigate endothelial tubulogenic activity in isolation from other cell types, and to do so in an efficient and accurate manner, prompted the development of the embedded endothelial cell-coated microcarrier bead assay. By using this assay, *Nehls and*

Drenkhahn were able to show that intercellular adhesion, in addition to proliferation and migration, represented an essential step in the tubulogenic process [7].

Clinical Implications

Physiologically accurate *in vitro* models of tubulogenesis have immense clinical value. They allow for (1) clinical testing of pro- or anti-tubulogenic drug therapies; (2) modeling of pathological conditions such as intimal hyperplasia and intimal injury caused by surgical intervention (e.g., angioplasty); (3) studying of the discrete process of endothelial cell differentiation, migration, lumen formation, and vascular inoculation; and (4) elucidating the molecular and mechanosensitive mechanisms associated with tubulogenesis [18]. Much research has gone into the design of *in vitro* assays that more accurately reflect *in vivo* tubulogenic activity and, indeed, this still remains an important goal for the future [16].

1.4. Tubulogenic Growth Factor Signaling

Tubulogenesis is controlled by the balance between pro- and anti-tubulogenic factors [22]. The presence of greater levels of growth-promoting factors rather than growth-inhibiting factors "flips" the physiological "switch" and induces a tubulogenic endothelial phenotype [22]. The most potent, well-known, and well-characterized tubulogenic growth factors come from the vascular endothelial growth factor (VEGF) and fibroblast growth factor (FGF) growth factor families [2, 22]. In the presence of these growth factors, endothelial cells engage in proliferation, extracellular proteolytic activity, invasion of the extracellular matrix, and formation of capillary-like tubular structures [22]. In addition to their general involvement in endothelial tubulogenesis, members of

the VEGF and FGF families have been implicated in the transduction of mechanical signals (mechanotransduction), which is the subject of the study herein.

Vascular Endothelial Growth Factors (VEGFs)

Vascular endothelial growth factors (VEGFs) are mitogenic proteins derived from the vascular and lymphatic circulatory systems [23]. Growth factors from the VEGF family are unique to vascular and lymphatic endothelial cells in that they do not have any appreciable growth-promoting effect on other cell types [23]. The VEGF family includes five structurally similar growth factors: VEGF-A, VEGF-B, VEGF-C, VEGF-D, and placental growth factor (PlGF) [24]. These molecules differentially interact with and bind to a corresponding family of cell surface receptors VEGFR-1, VEGFR-2, and VEGFR-3 [24]. The two VEGF-related growth factor ligands pertinent to the present study are VEGF-A and VEGF-C.

VEGF-A is a potent mitogenic growth factor that is specific to vascular endothelial cells and is involved in both the physiological and pathological growth of blood vessels [23]. The potency of VEGF-A as an angiogenic factor and its importance in vascular development was demonstrated by two studies showing that a genetic mutation resulting in the loss of a single VEGF-A allele results in early lethality in mouse embryos [25, 26]. VEGF-A has also been implicated in pathological angiogenesis associated with tumor growth and retinal ischemia [23]. The vital role that VEGF-A plays in angiogenesis is shown in *Table 1.4a*.

***Table 1.4a* - Table of Known Pro-Tubulogenic Effects of VEGF-A on Endothelial Cells**

Name	Function
VEGF-A	Stimulates tubulogenesis *in vitro* and *in vivo* [2]
	Increases endothelial cell permeability [2, 24]
	Promotes endothelial cell survival (inhibits apoptosis) [24]
	Stimulates endothelial cell proliferation [22, 24]
	Enhances endothelial cell migration and invasion [2, 22]
	Stimulates endothelial cell production of matrix proteases and protease inhibitors [2, 22]
	Stimulates the activity and production of endothelial nitric oxide synthase (vasodilation) [2, 23]

The pro-tubulogenic effects of VEGF-A listed in *Table 1.4a* above are elicited when it binds to its high-affinity receptor VEGFR-2, a transmembrane tyrosine kinase [2]. Interestingly, cellular expression of VEGF-A and VEGFR-2 are both tied to local tissue oxygen concentration [2]. Chronic hypoxia upregulates VEGF-A and VEGFR-2 expression in parallel [2]. VEGF-A binding to VEGFR-2 causes endothelial cell proliferation, extracellular matrix invasion, and tube formation presumably to vascularize and oxygenate the hypoxic tissue [2]. The VEGF-A/VEGFR-2 pathway is capable of stimulating the entire angiogenic process, and thus, is a key mediator of tissue perfusion and the physiologic response to tissue ischemia [2].

The other pro-tubulogenic VEGF-family ligand of interest to this study is VEGF-C. VEGF-C has been primarily implicated in lymphangiogenesis, the formation of new lymphatic vessels [27]. However, VEGF-C also plays a role in angiogenesis and the formation of new blood vessels [24]. VEGF-C binds to both the VEGFR-2 and VEGFR-3 receptors [27]. The importance of VEGF-C has been demonstrated by studies

investigating its high-affinity receptor, VEGFR-3, and the effect of VEGF-C/VEGFR-3 binding on angiogenesis *in vitro* [28, 29]. The results of these studies have shown that VEGF-C/VEGFR-3 signaling is essential for both physiological and pathological angiogenesis [28]. The known effects of VEGF-C on endothelial tubulogenesis are listed in *Table 1.4b*.

Table 2.4b **- Table of Known Pro-Tubulogenic Effects of VEGF-C on Endothelial Cells**

Name	Function
VEGF-C	Stimulates tubulogenesis *in vitro* and *in vivo* [30]
	Stimulates endothelial cell proliferation [29, 31]
	Enhances endothelial cell migration and invasion [29, 30]
	Stimulates production of matrix proteases [29, 30]
	Promotes endothelial cell survival (inhibits apoptosis) [29]

Much like VEGF-A, previous studies using *Vegfr3*-gene knockout mouse embryos that were unable to express the high-affinity receptor to VEGF-C, VEGFR-3, exhibited significant defects in both arterial and venous vascular development and remodeling resulting in embryonic lethality [28]. Based on the essential role that VEGF-C/VEGFR-3 signaling plays in lymphangiogenesis, it is anticipated that lymphatic development and remodeling would also be substantially impaired by *Vegfr3*-gene knockout [24]. Indeed, it has been demonstrated that suppression of VEGF-C levels in tumor-bearing mice with neutralizing VEGF-C antibodies or a soluble form of VEGFR-3 elicited a predominantly anti-*lymphangiogenic*, rather than an anti-angiogenic, effect [29].

Studies have also demonstrated the pro-angiogenic effect of VEGF-C/VEGFR-3 binding *in vitro*. Blocking VEGFR-2, the high-affinity receptor for VEGF-A and low-

affinity receptor for VEGF-C, while stimulating endothelial cells cultured on the surface of three-dimensional collagen gels with VEGF-C, did not completely extinguish the *in vitro* angiogenic response [29]. As shown in the study by *Persaud et al*. (2004), VEGF-C was capable of eliciting an angiogenic response in vascular endothelial cells in the absence of VEGF-A/VEGFR-2 and VEGF-C/VEGFR-2 binding, thus advocating for the role of VEGF-C in angiogenesis [29]. These previous reports substantiate the essential role that VEGF-C/VEGFR-3 signaling plays in both forms of tubulogenesis—angiogenesis and lymphangiogenesis.

Fibroblast Growth Factors (FGFs)

The FGF ligand family was among the first discovered pro-angiogenic factors [2]. Though FGFs are similar to VEGFs in that they promote endothelial cell activity crucial to *in vivo* angiogenesis and the formation of capillary-like structures *in vitro*, they are unlike VEGFs in that they do not exclusively act on endothelial cells [2]. The effects of FGF-2, also known as basic fibroblast growth factor (bFGF), on endothelial cells are shown in *Table 1.4c* below.

***Table 3.6c* - Table of Known Pro-Tubulogenic Effects of FGF-2 on Endothelial Cells**

Name	Function
FGF-2	Stimulates tubulogenesis *in vitro* and *in vivo* [2, 22, 32]
	Stimulates endothelial cell proliferation [2, 14, 22]
	Enhances endothelial cell migration and invasion [2, 22]
	Stimulates the production of matrix proteases in endothelial cells [2, 22]
	Promotes endothelial cell survival (inhibits apoptosis) [33]

The effects of FGF-family growth factors are elicited through binding to four receptor tyrosine kinases: FGFR-1, FGFR-2, FGFR-3, and FGFR-4. FGF-2 binds to

FGFR-1, which induces both proliferation and migration [34, 35]. Previous studies have also shown that FGF-2/FGFR-1 binding, alone, is capable of eliciting angiogenic and lymphangiogenic sprouting [34, 35]. FGF-2 also binds to FGFR-2 and induces several of the essential early endothelial tubulogenic activities (e.g., migration, proliferation, matrix protease production). [36]. Though redundant receptor-ligand specificity is characteristic of the FGF/FGFR signaling pathways, blockade of either FGFR-1 or FGFR-2 inhibits vascular development and results in death during early embryonic development [33, 36].

FGF and VEGF Synergy in Angiogenesis and Lymphangiogenesis

Though it has been shown that FGF-2, VEGF-A, and VEGF-C are each capable of inducing tubulogenesis on their own, the combined tubulogenic effects of FGF-2 and VEGF-A or FGF-2 and VEGF-C have shown to be greater than the sum of their individual effects [35, 37]. Studies have shown both interdependency and synergism between FGF-2 and either VEGF-A or VEGF-C. *Mandriota and Pepper* (1997) showed that sequestration of FGF-2 prevented VEGF-A-induced angiogenesis *in vitro* [37]. Furthermore, it has been shown that VEGF-A and FGF-2 elicit a synergistic angiogenic response both *in vitro* and *in vivo*, and it has been surmised that this results from FGF-2-induced upregulation of VEGFR-2, the high-affinity VEGF-A receptor.

Cao et al. (2012) recently demonstrated that, although FGF-2 is capable of inducing lymphatic endothelial cell proliferation and migration *in vitro*, FGF-2 stimulation in the absence of VEGF-C/VEGFR-3 signaling was unable to induce lymphangiogenic sprouting *in vivo* [35]. It must also be noted that VEGF-A/VEGFR-2 signaling is not restricted to angiogenesis and VEGF-C/VEGFR-3 signaling is not restricted to

lymphangiogenesis. VEGF-A and VEGF-C have been shown to be involved in both angiogenesis and lymphangiogenesis [29, 38].

1.5. Effects of Pressure on Endothelial Cells

Several previous studies have suggested that endothelial cell responses to hydrostatic pressure are distinct from other hemodynamic forces to which endothelial cells are exposed *in vivo* [39]. The known effects of pressure on endothelial cells, to this point, have primarily implicated the FGF-2/FGFR-1/2 and VEGF-C/VEGFR-3 pathways. *Acevedo et al.* (1994) demonstrated that sustained pressures induced the release of nuclear and cytosolic stores of FGF-2 [14]. This release resulted in increased proliferation and morphological restructuring of endothelial cells in two-dimensional culture [14]. In a later study, *Shin et al.* (2004) demonstrated that cyclic pressure-induced increases in endothelial cell proliferation were also mediated by FGF-2/FGFR-2 signaling [40]. This later study, however, found that the endothelial response to the applied pulsatile pressure was not FGF-2 dependent, but rather, somehow tied to FGFR-2 activity. The exact function of the FGF-2/FGFR-2 pathway in the transduction of pressure is still unclear.

Pressure has also been shown to upregulate the expression of VEGF-C. *Shin et al*. (2002) showed that VEGF-C gene transcription (*Vegfc*) was upregulated in endothelial cells exposed to pressure [31]. This increase in VEGF-C transcription resulted in increased VEGF-C expression and, concomitantly, increased endothelial cell proliferation [31]. A similar study showed alterations of intercellular connectivity and modulation of the endothelial barrier function in response to cyclic pressure exposure [39].

These previous studies and results involve endothelial functions and growth factors that have been implicated in both angiogenesis and lymphangiogenesis. Thus, early evidence suggests that pressure may have an effect on endothelial tubulogenesis and such effect may be transduced through the mechanosensitive growth factor signaling pathways related to FGF-2 and VEGF-C.

2. Rationale

To date, studies of the effects of mechanical forces on endothelial tubulogenesis have been confined to those resulting from shear stress and substrate tension. The literature has generally neglected to investigate the effects of hydrostatic pressure in isolation on endothelial tubulogenesis in comparison to the effects of the other hemodynamic mechanical forces, despite the fact that endothelial cells are constantly exposed to varying levels of pressure under normal and pathological conditions. The demonstrated relationship between hydrostatic pressure exposure and the expression, upregulation, or release of certain pro-angiogenic and pro-lymphangiogenic growth factors begs the question of whether hydrostatic pressure has an effect on endothelial tubulogenic processes.

The present Master's thesis-related research exposed bovine aortic endothelial cells to sustained hydrostatic pressures known to stimulate the pro-tubulogenic activity of endothelial cells. The goal was to substantiate the hypothesis that pressure is a magnitude-dependent modulator of early endothelial tube formation processes. Along this line, the objectives of the present study were to develop a method for subjecting endothelial cells in three-dimensional culture to sustained hydrostatic pressures and evaluate the *in vitro* tubulogenic responses of endothelial cells. For this purpose, a system for subjecting endothelial cells in 2-D and 3-D cell cultures was developed and employed to verify the effects of pressure on endothelial proliferation and morphology established by previous studies and to assess the effects of pressure on the early endothelial tubulogenic processes (e.g., migration, tube formation). Using this system, the present

study also aimed to elucidate a novel VEGFR-3-mediated pathway that links pressure exposure encountered in the physiological mechanoenvironment of the endothelial cell to capillary-like tube formation.

By using a combined biomedical engineering and experimental biological approach, the present study addressed key issues regarding the angiogenic response of vascular endothelial cells to sustained hydrostatic pressure and laid the groundwork for future studies investigating the effects of various pressure regimes and growth factors on endothelial tube formation. The knowledge gained from this study not only expounds upon endothelial mechanical signal transduction and the effects of pressure on endothelial cells, but also provides new information that could eventually lead to improvements in the generation of pre-vascularized tissues *in vitro* and the treatment of pressure-related pathological conditions.

3. Materials and Methods

3.1 Cell Substrates

The two-dimensional substrates used in the present study consisted of polystyrene tissue culture substrates in the form of multi-well tissue culture plates. Prior to seeding, tissue culture surfaces, on which cells were grown, were coated with sterile 0.2% gelatin (Sigma-Aldrich) in aqueous solution and incubated for a minimum of fifteen minutes. The gelatin solution was removed prior to cell seeding.

For three-dimensional cultures, commercially available Cytodex3™ microcarrier beads (GE Healthcare®) were used. Cytodex3™ beads are spherical cross-linked polystyrene beads with diameters ranging from 141-211 microns that have a layer of denatured collagen chemically bonded to their surfaces. The beads were prepared for cell culture by submerging them in Phosphate Buffered Solution (PBS) in a siliconized glass bottle at a concentration of 100 g/mL in PBS. Cytodex3™ beads were allowed to remain in PBS for three hours permitting them to swell and hydrate. To ensure proper saturation of the beads, two drops of Tween 80 were added per 100 mL of PBS during this first hydration rinse to overcome the effect of surface tension that would prevent the beads from hydrating. After three hours in the initial PBS rinse, the supernatant was removed and 50 mL of fresh PBS per gram of beads was added. The bead solution was then sterilized by steam autoclave at 115°C and 15 psi for 15 minutes. After autoclaving, the bead solution was stored at 4°C. Beads prepared in this fashion are stable for up to 1 year.

3.2 Cell Lines, Culture Conditions, and Passaging

Bovine aortic endothelial cells (BAEC) were generously provided by Dr. Shu Chien and Dr. Jason Haga from the Department of Bioengineering at the University of California – San Diego (La Jolla, CA) or were purchased from a commercial source (Invitrogen®). BAEC were subcultured on the gelatin-coated polystyrene tissue culture surfaces of either 25 cm^2 (T-25) or 75 cm^2 (T-75) vented cell culture flasks (BD Falcon®) in Dulbecco's Modified Eagle Medium (DMEM) (HyClone®) supplemented with 10% v/v fetal bovine serum (FBS) (HyClone®), 1% v/v penicillin/streptomycin/L-glutamine solution (HyClone®), and 5 U/mL heparan (Sigma®). Cells were maintained under standard tissue culture incubator conditions—humidified, 37°C, 5% carbon dioxide/95% air environment. During routine cell culture, the media was replaced every 2 to 3 days. Upon reaching confluence, BAEC cultures in T-25 or T-75 flasks were split (1:2 or 1:3 ratio) into new flasks. To do so, cell monolayers were rinsed once with PBS for 5 minutes. The PBS was then removed and 1 mL of 0.25% trypsin/1 mM EDTA (Sigma®) was added to flasks, which were then incubated for 1 to 2 minutes. After gentle agitation, cells would detach from the tissue culture surface of the flask and be suspended in fresh complete media. To remove the tripsyn/EDTA solution, cells suspended in complete media were centrifuged at 200G for 5 minutes at 25°C. After centrifugation, the supernatant solution was aspirated and the resulting cell pellet was resuspended in complete media and added to new T-25 or T-75 flasks. For every confluent population of cells within a single flask, two to three flasks of passaged cells were generated. Cells from passages 7 to 15 were used in all experiments in the present study.

3.3 Cell Storage

Confluent or near-confluent BAEC monolayers from T-75 cell culture flasks were cryopreserved for later use following standard cell culture procedures. Briefly, after rinsing BAEC monolayers in PBS for 5 minutes, cells were dissociated from tissue culture flask surfaces by incubation with 1 mL of 0.25% trypsin/1 mM EDTA for 1 to 2 minutes followed by gentle agitation and subsequent resuspension in complete culture. The resulting cell suspensions were then transferred to 15 mL centrifuge tubes (BD Falcon®) and pelleted by centrifugation at 200G for 5 minutes at 25°C. The cell pellet was then resuspended in 1.5 mL of freezing solution consisting of 10% dimethyl sulfoxide (DMSO) (Sigma®) in FBS and transferred to 2-mL cryogenic vials (BD Falcon), and stored at -80°C until needed or transferred to liquid-nitrogen cryogenic storage.

As needed, frozen cell suspensions in cryogenic vials were rapidly thawed by submersion in a 37°C water bath. Thawed cell solutions were then transferred to sterile 15-mL centrifuge tubes containing 5 mL of warm complete media, pelleted at 200G for 5 minutes at 25°C, resuspended in 5 mL of complete media. Cells suspended in complete media, now with freezing solution removed, were transferred to a T-75 cell culture flask containing 10 mL of complete media and cultured under standard cell culture conditions (as detailed in Section 3.2).

3.4 Cell Seeding

Two-Dimensional Substrates: Seeding in Multi-Well Tissue Culture Plates

For proliferation assays and analyses of VEGF-C and VEGFR-3 expression, cells were seeded in 10 cm^2 petridishes or individual wells of 6-well, 12-well or 96-well tissue culture polystyrene plates (BD Falcon®) that had been pre-coated with gelatin as described previously. Confluent or near-confluent BAEC were lifted, centrifuged, and resuspended in 10 mL of fresh media. The numbers of cells contained in two 10-µL aliquots of this suspension were then counted using a hemacytometer to determine the concentration of cells in a particular cell solution. Cell solutions were diluted with complete media such that an average of 20-50 cells would be counted per grid-square of the hemacytometer to ensure an accurate determination of concentration. After the concentration of cells in solution was determined, aliquots of cell solution were added to wells containing heparan-free complete media in order to obtain the desired number of cells per unit surface area in each well depending on the seeding density designated for each assay. For proliferation assays, cells were seeded at 5,000 cells/cm^2. After 16-24 hours, BAEC attached to the cell culture surfaces of the multi-well plates and media was replaced with fresh heparan-free media, with the addition of supplements (i.e., FGF-2, VEGF-A, MAZ51, DMSO) as needed for each experiment.

Three-Dimensional Substrates: Seeding on Cytodex3™ Beads

Prior to cell seeding, the concentration of beads in a stock solution of Cytodex3™ microcarrier beads in PBS was determined by counting and averaging the number of beads in three 10-µL droplets. The volume of stock solution containing the desired amount of beads was then determined and combined with 2 mL of warm serum-free

media. The tube was agitated briefly and then the beads were allowed to settle to the bottom so the PBS in solution could be aspirated for rinsing with fresh buffer. The beads were then rinsed one additional time in complete cell culture media.

To seed BAEC onto Cytodex3^{TM} microcarrier beads, cells were first lifted, pelleted, and resuspended in warm complete medium. The concentration of cells in solution was determined with a hemacytometer as described previously. A volume of this cell suspension was then added to the microbead solution to yield a ratio of 1×10^6 cells per 2,500 beads and incubated under standard cell culture conditions in an upright position. During this incubation, the cell-microbead suspension underwent periodic (i.e., once every 20 minutes) gentle agitation for an initial 4-hour duration to ensure uniform coverage of the bead surface with cells. After this initial 4-hour seeding period, the bead-cell solution was then carefully transferred to a T-25 flask containing 3 mL of cell culture media. The solution was then incubated for 24 hours in an upright position (vented cap facing upward) to prevent coated beads from adhering to the tissue culture-treated surface of the flask. After an overnight incubation, the beads were entirely covered in a confluent or nearly confluent layer of BAEC. During this time, some of the coated beads would become adhered to the inner surfaces of the flask. To address this, flask surfaces were gently agitated and rinsed with complete media to disassociate the beads from the plastic surfaces.

3.5 Pressure System

Cells grown on two-dimensional substrates and polymeric beads embedded in three-dimensional collagen gels were exposed to pressures above atmospheric using a

custom-designed pressure system capable of exposing cells grown in tissue culture plates to either static or pulsatile pressure stimuli. The system consisted of custom-fabricated polycarbonate chambers that were designed and fabricated to accommodate a multi-well cell culture plate or multiple chamber slides while minimizing the volume within the chamber. The chamber volume was minimized so that the change in volume required to generate a pressure pulse within the chamber would be minimized. As shown in the *Equation 3.5* below, as the volume of the chamber ($V_{chamber}$) governs the change in volume (ΔV) required to produce a pressure pulse within the chamber defined by a minimum (P_0) and maximum (P_E) pressure level.

$$P_E = \frac{\Delta V}{V_{chamber}} P_0 \qquad \text{[Equation 3.5]}$$

This change in volume (ΔV) can be either the volume of gas needed to bring the chamber pressure from 0 mmHg to the experimental pressure (i.e., 20 mmHg or 40 mmHg) or represents the change in volume required to oscillate the chamber pressure between two pressures (P_0 and P_E) for generating pulsatile pressures. Therefore, minimizing the chamber volume allows for the use of less gas to generate sustained pressures and lower stroke volumes to generate pulsatile pressures.

For pressure experiments, cell culture plates or dishes were placed between the two interlocking halves (shown in *Figure 3.5a*) and sealed by tightening six fasteners (not shown) that surround the perimeter of the chamber. Tightening the fasteners compresses an O-ring that forms an airtight seal between the inner compartment and the outside environment.

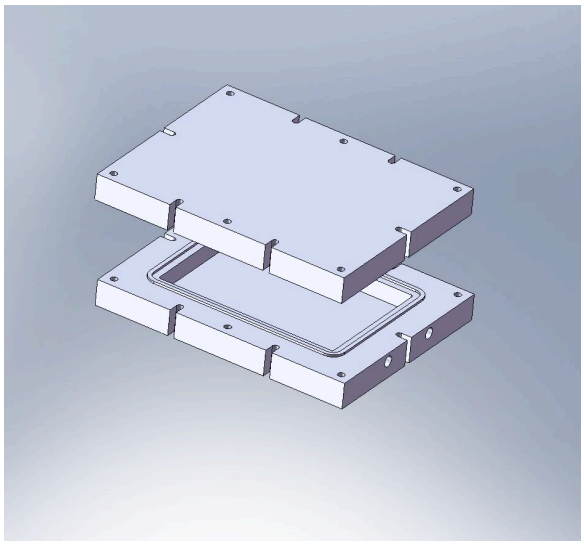

***Figure 3.5a* – Three-dimensional *SolidWorks*® model of the pressure chamber.**

Three ports on the sides of the chamber allow for connections to the supply gas mixture, instrumentation, a second chamber (in series or parallel), and relief valves.

The hydrodynamic pressure system is capable of exposing one plate to a sustained, static pressure or pulsatile pressure regime while maintaining a second downstream chamber at atmospheric pressure. For this configuration, a compressed gas tank supplies a pressurized 5% carbon dioxide, 95% air mixture through a humidifier and into a sealed polycarbonate chamber. The second downstream chamber (Chamber 2) passively receives a 5% carbon dioxide, 95% air gas mixture from the pressurized chamber; this gas is allowed to escape from the second chamber via a pressure port that is open to the atmosphere.

Sustained pressures were controlled (in the range of 0 to 100 mmHg) within the pressure chamber by controlling the depth of the pressure head tube in the column of

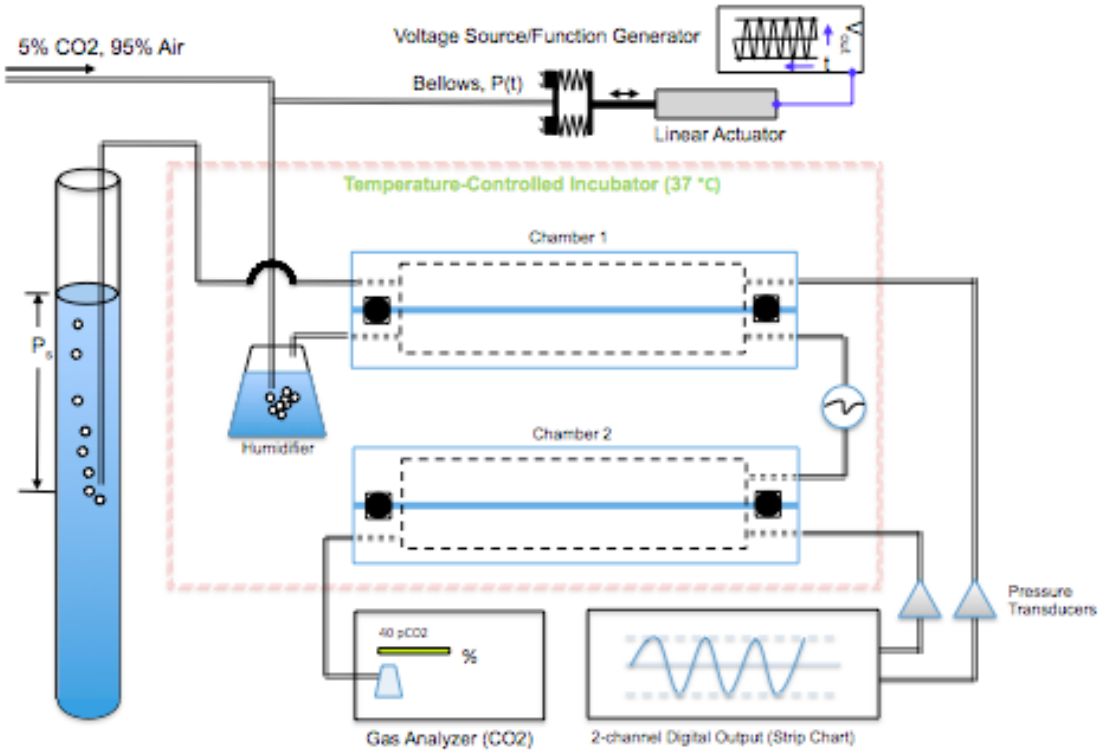

Figure 3.5b **- Schematic representation of the pressure system designed for the present study. As diagrammed in the figure, the system consists of a pressurized chamber (Chamber 1) in series with the control chamber (Chamber 2), which is maintained at 0 mmHg while Chamber 1 is maintained at an elevated, sustained pressure. The pulsatile component (bellows, linear actuator, voltage source, function generator) were not used in the present study.**

water (P_s in *Figure 3.2b*), which creates an upper limit on the pressure allowing for stable sustained pressures for long periods of time. The inflow rate of gas into the pressure chamber was controlled by adjusting the pressure regulator on the 5% carbon dioxide supply tank while the outflow rate was adjusted by modulating the resistance to gas flow between the pressure and control chambers using an adjustable valve. The resistance to gas flow between the two polycarbonate chambers ensured the generation of a static pressure level in the upstream chamber. The pressure in the control chamber (Chamber 2) was maintained at atmospheric pressure (0 mmHg) by adjusting the flow rate into the chamber from the pressurized chamber (Chamber 1) as well as the outflow from the

control chamber via a relief valve. The flow rate of gas from the 5% CO_2/95% air tank and the pressure head control were set so as to minimize the gas flow required to maintain the desired pressures and CO_2-content of each chamber. Each chamber was connected to a pressure transducer interfaced with a multi-channel digital output that allowed for continuous, real-time monitoring of the pressure in both chambers. A CO_2 gas analyzer was connected downstream from the control chamber to continuously monitor the gas mixture and ensure a 5% carbon dioxide content inside both chambers. Both chambers were maintained at 37^{o}C using a temperature-controlled incubator.

The pressure system was also set up with the capability to generate pulsatile pressures with pulse pressures ranging from 0 to 20 mmHg and frequencies of 0 to 2 Hz. Pulsatile pressures are generated using a bellows pump connected to a digitally controlled linear actuator driven by a DC power supply and function generator. This setup allowed for adjustment of the bellows displacement amplitude and frequency, which in turn controlled the pulse pressure and frequency of the applied pressure regime in the upstream polycarbonate chamber.

3.6 Proliferation Assay

Seeding and Pressure Exposure

Cells were enzymatically dissociated from culture surfaces and resuspended in media containing 10% FBS and 1% Pen/Strep/L-glutamine solution and seeded at densities of 5,000 cells/cm^2 in the wells of 96-well plates.[1] For these experiments, two

[1] 5,000 cells/cm^2 was determined to be the cell density at which cells would not reach 100% confluence by the end of the 72-hour experiment duration. Permitting the cells the reach confluence before the end of the 72-hour period would prevent observation or detection of differences in cell densities between cultures maintained under different culture conditions (i.e., pressure or growth factor supplementation).

identically seeded plates of cells were generated: one for a control and one for a pressure experiment. After an overnight incubation, the culture media in each of the wells containing cells was gently aspirated and replaced with 200 microliters of fresh complete media with or without 1 ng/mL FGF-2. Six wells were seeded per treatment per independent experiment. This yielded six wells for each of four different treatments that were prepared for control and pressure plates per independent experiment. Cell preparations were either maintained under atmospheric pressure in the control chamber or exposed to elevated hydrostatic pressures (20 or 40 mmHg) for 72 hours.

Fixation, Labeling, and Quantification of Cell Density

After experiments, the experimental cell preparations were immediately fixed with 2% paraformaldehyde/0.5% glutaraldehyde for 2 hours. The fixative was then removed and the cell monolayers were rinsed once with PBS. A Crystal Violet solution (0.5% w/w Crystal Violet and 20% methanol in PBS; a nuclear stain) was then added to each well and incubated for one hour at room temperature. The cell layers were then rinsed five times with PBS for five minutes each to remove excess, unbound dye. Finally, PBS at a volume of 100 µL was added to each well in preparation for quantifying dye uptake. Crystal violet uptake by BAEC layers was then quantified using a spectrophotometric microplate reader (Biotek® uQuant) at an absorbance wavelength of 570 nm. Experiments to assess the effects of pressure on BAEC proliferation were repeated five separate times (N = 5) for each condition tested.

3.7 Flow Cytometric Analysis of VEGFR-3 and VEGF-C Expression

Seeding and Pressure Exposure

Cells were enzymatically dissociated from culture surfaces and resuspended in media containing 10% FBS and 1% Pen/Strep/L-glutamine solution and seeded at 1/3 confluence in gelatin-coated, 10 cm^2 tissue culture plates and allowed to culture for 24 – 48 hours. Prior to experiments, the culture media in each plate was replaced with fresh complete media. These cell preparations were then either maintained under control (i.e., atmospheric) pressure conditions or exposed to the sustained hydrostatic pressures of interest (either 20 or 40 mmHg) for 72 hours using the custom pressure system (see section 3.5).

At the end of experiments, the cells were enzymatically released from substrates, rinsed with ice-cold PBS and immediately fixed with 0.25% p-formaldehyde in 0.1 M sodium phosphate.

Immunofluorescence Labeling of Cells

Fixed cells were washed 3 times in ice-cold PBS prior to labeling with fluorescence antibodies to either VEGFR-3 or VEGF-C. For VEGFR-3 staining, cells were labeled with mouse monoclonal antibodies to human VEGFR-3 (Millipore; cross-reactivity with bovine antigen) in 1% bovine serum albumin (BSA; blocking buffer; Sigma-Aldrich) at room temperature for 1 h. Cells bound with this antibody was fluorescently-labeled with goat anti-mouse IgG secondary antibodies conjugated to Alexa-Fluor®488 for 45 minutes.

Cellular VEGF-C on the fixed cells was labeled with goat anti-human VEGF-C (Santa Cruz Biotechnologies; cross-reactivity with bovine antigen) in 1% BSA in PBS supplemented with 0.1% saponin (a compound used to permeabilize the cells and allow cytosolic staining of the antigen of interest). The cells were then rinsed three times and stained with donkey anti-goat IgG conjugated to Alexa-Fluor® 488 in blocking buffer with 0.1% saponin for 45 minutes.

After fluorescent labeling for VEGFR-3 or VEGF-C, cells were rinsed of excess unbound antibodies in their respective blocking buffers and resuspended in 0.5% BSA. Binding of fluorescent antibodies to cells was quantified with an LSR II flow cytometer (Becton-Dickinson). For each sample, at least 10,000 cells were analyzed using FACsDiva (Becton-Dickinson). Histograms of fluorescence intensity (reflecting the numbers of antibodies bound to cells) were recorded for each sample and the mean fluorescence intensity was determined as a measure of antigen expression levels.

3.8 Three-Dimensional Collagen Gel Assays

Tube formation and invasion assays were conducted in the following chronology: preparation of cellularized beads, gel formulation, and gel polymerization. After these steps, endothelial tubulogenic activity under pressure was examined.

Preparation of Endothelialized Beads

BAEC were seeded on Cytodex3™ microcarrier beads as described in **Section 3.4 – Cell Seeding**. Cellularized beads were removed from T-25 tissue culture flasks, transferred to a 15-mL centrifuge tube, and allowed to settle to the bottom of the tube for

up to 10 min. At that time, the supernatant media was aspirated, and the beads were rinsed once in 2 mL of heparin-free complete media.

Collagen Gel Formulation

Since live BAEC were to be embedded into the collagen gels, the gel formulation had to consist of a precise balance of reagents in order to yield a three-dimensional environment in which the cells could survive and carry out the cellular processes of interest in the present study. The gel acidity, osmolarity, metabolite availability, and collagen concentration were taken into account when developing the gel formulation used in this experiment. Gel reagents and their respective ratios to the final solution volume are listed in *Table 3.8a* (on the following page)

Table 3.8a – Collagen Gel Formulation. Reagents and their respective ratios to the final solution (Ratio – X:1000). Reagents were added such that the concentrations of reagent were 1X DMEM, 2 mM L-glutamine, and 2.0 – 2.5 mg/mL Type I Collagen (rat tail).

Reagent	X:1000
Deionized Water (diH_2O)	527
200 mM L-glutamine	10
HC Collagen Type I (8-11 mg/mL)	291
0.1 N Sodium Hydroxide (aq.)	40
0.53 N Sodium Bicarbonate (aq.)	32
10X DMEM	100

Prior to and throughout the mixing process, all stock solutions and gel mixtures were maintained at 0° - 2° C in an ice bath. The gel solution was then generated according to the following procedure.

1. 10X DMEM (Sigma®), sterile distilled water (diH_2O), and L-glutamine (Sigma®) were added to a sterile 15-mL centrifuge tube.

2. Type I Collagen solution (8-11 mg/mL Type I collagen from rat tail tendon dissolved in 0.02 N acetic acid) (BD Biosciences®) was then added to the centrifuge tube and the solution was mixed thoroughly. Since the concentration of collagen in the commercially-available stock collagen solution varied between 8 and 11 mg/mL, it was necessary to adjust the ratios of gel reagents to yield the appropriate collagen concentration (2.0 – 2.5 mg/mL) and solution pH.
3. The 0.1 N sodium hydroxide solution and 0.53 N sodium bicarbonate solution were then added to the tube and the solution was thoroughly mixed by pipet aspiration and using a vortexer set at a low speed. The tube was then returned to the ice bath.
4. A volume of the solution of endothelialized Cytodex3™ beads (containing approximately 2,500 beads) in complete media (top layers) or an equivalent volume of heparan-free complete media containing no beads (to generate a bottom, acellular layer; *see Gel Polymerization* section below) was then added to and thoroughly mixed with the gel solution. If cellularized beads were added to the gel solution (top layers), the contents of the tube were mixed *gently* to distribute the cells throughout the gel solution without shearing them off of the bead surface.

Gel Polymerization

Gel polymerization was allowed to progress by raising the temperature and the pH of the gel solution since the collagen will remain in a viscous liquid state when maintained at 0-4°C (i.e., ice bath). The sodium hydroxide solution (0.1 N) and sodium bicarbonate solution (0.53 N), the final two reagents added to the collagen gel solution,

were used to neutralize the acidity of the gel solution. When maintained in an ice bath, the collagen gel solution would not polymerize. When the temperature of the solution was elevated to 37°C, the gel rapidly polymerized. By controlling the duration, location, and sequence of heat application, the polymerization of the gels within the tissue culture plate wells was precisely timed to guide gelation. Two gel polymerization protocols were used to yield two different gels. To ensure that the beads would not sink to the bottom of gels prior to polymerization, an acellular (not containing cells or beads) layer of gel was polymerized in each well and the gel solution containing BAEC-coated beads were overlaid on top of this acellular layer. It was determined in the current study that if the beads are allowed to sink to the bottom of the well, the cells will migrate off of the bead and onto the bottom of the well (the tissue-culture treated surface) and form a monolayer. The following procedures were, thus, designed to prevent this from happening.

Two-Layer Gel Polymerization

For the *Migration Assay* depicted in *Figure 3.4a*, an acellular gel solution (of the exact same formulation as the top layer, but not containing BAEC-coated Cytodex© beads) was added to the each well and allowed to completely polymerize by incubation at 37°C for ten to fifteen minutes. A top layer of gel containing cellularized beads was then added to each well and polymerized by incubation at 37°C for another fifteen minutes. After polymerization of the top layer, heparan-free complete media was added. *Figure 3.8b* on the following page displays the chronology of bi-layer gel polymerization.

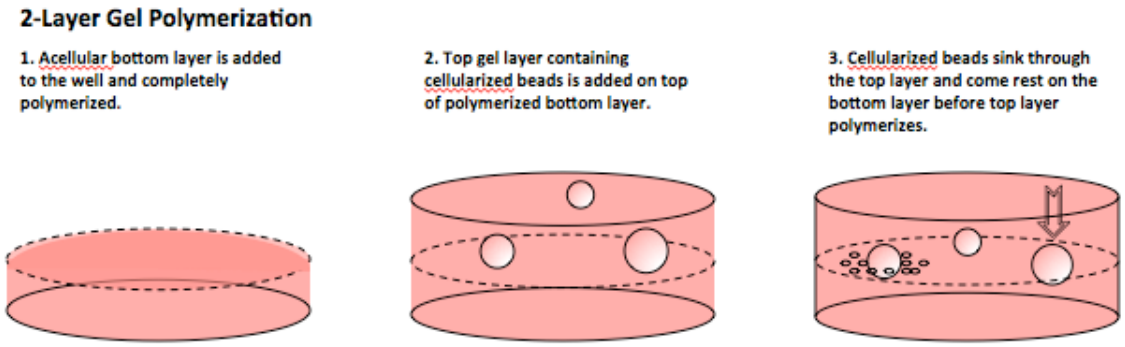

***Figure 3.8b* – 2-layer gel polymerization sequence. The top and bottom gel layers are added and allowed to polymerize independently by 10-15 minute incubation at 37 deg. C for each layer. The result is a non-continuous, dual-layer gel structure.**

As shown in *Figure 3.8b*, once the bottom gel layer was polymerized, it adhered to the bottom of the well allowing the top layer gel to be overlaid on top. Once polymerized, a "seam" was created between the two gel layers on which beads from the top layer rested and on which endothelial cells migrated off the bead during our migration assays.

Single-Layer Gel Polymerization

The gel polymerization sequence for the tube formation assay (shown in *Figure 3.8c* on the following page) creates a single, continuous gel layer within which the BAEC-coated Cytodex™ beads are suspended. A volume (0.250 mL) of acellular bottom layer gel solution was added to each well of a 24-well plate. The plate was then placed on a heating plate set to 37 deg. C and allowed to rest for one to two minutes. After addition of the bead-containing top layer of gel, the well plate was returned to the heating plate. The continuous application of heat to the bottom of the plate allowed the gel to

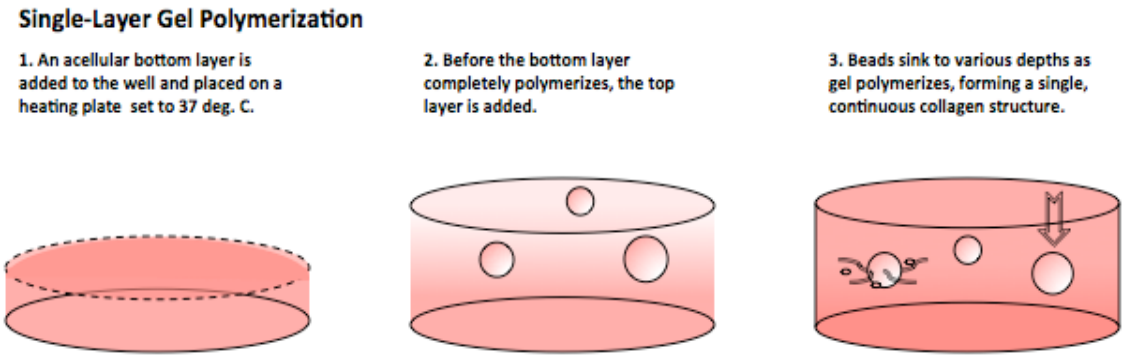

***Figure 3.8c* – Single-layer gel polymerization sequence. The acellular bottom layer gel is added to each well and the plate is placed on a heating plate at 37 deg. C. The bottom layer is allowed to partially polymerize, then the bead-containing top layer is added. The plate is then returned to the heating plate, causing top and bottom layers to completely polymerize. The result is a continuous, single-layer gel structure.**

progressively polymerize from the bottom to the top of the gel. This progressive polymerization from the bottom surface upward prevented beads from descending to the bottom of the well and allowed the sequentially added gel layers to form a continuous and homogenous gel layer. *Figure 3.8c* above shows how this process was carried out.

3.9 Imaging

High-resolution, bright field images of beads and their associated cells were captured digitally using an Olympus (Model IX-70) inverted light microscope equipped with a Hammamatsu camera, relief contrast, and a range of high-magnification (100X – 600X) objectives. Images of cell populations in three dimensional gel cultures were captured after 72 hours and 96 hours in culture. For the migration assay, images were captured at 100X magnification with the focal plane positioned at the interface between the two get layers. For the tube formation assay, images were captured at 100X

magnification with the focal plane positioned at the mid-plane of the bead. If cells or cellular structures formed out of the midplane of the bead (as was common in the tube formation assay), additional images would be captured on different focal planes in order to visualize these structures.

3.10 Migration/Invasion Assay Analysis

The migration and invasion assay images were analyzed using an image processing macro developed for the NIH ImageJ software. The program applied a high pass filter to gray-scale images of single beads with migrating cells to create a new black-and-white image based on a threshold frequency below which all low-frequency image components were converted to white and all high-frequency image components were converted to black. This conversion was accomplished using the ImageJ macro code shown in *Figure 3.9a* on the following page. After applying this procedure, the "Migration Index" was determined.

```
macro "InvasiQuant [f5]" {
run("8-bit");

rename("Original.tif");

run("Duplicate...", "title=Filter.tif");
selectWindow("Filter.tif");

run("Gaussian Blur...", "sigma=5");

run("Invert");

imageCalculator("Average create", "Original.tif","Filter.tif");
//run("Image Calculator...", "image1=Image1.tif operation=Average

setAutoThreshold("IsoData");
//run("Threshold...");

setThreshold(0, 118);
run("Make Binary", "thresholded remaining black");

run("Remove Outliers...", "radius=1 threshold=1 which=Dark");

run("Measure");

close();
close();
run("Open Next");
}
```

Figure 3.10a **– InvasiQuant ImageJ macro code. When the macro is run, a gray-scale image is converted to a binary (black and white) image wherein high-contrast areas of the image (i.e., cell borders) are converted to black and low-contrast areas (i.e., background noise, bead interior, out-of-focus elements) are converted to white pixels. The macro returns a numeric value that corresponds to the ratio of black pixels to white pixels ("Migration Index").**

Specifically, the Migration Index represented the ratio of the number of black pixels to white pixels within the processed image. In the processed image, high contrast elements (i.e., the outer edges or borders of cells) are filtered out and converted to black pixels. Image elements not meeting the preset threshold contrast are converted to white pixels. Accordingly, as the number and dispersion of cells increases the amount of cell borders in each image increases. An increase in the amount and dispersion of the cell borders in an image is represented by an increase in black pixels in the processed image. Theoretically, the number of black pixels in an image is directly related to the number and dispersion of cells in an image. An image containing a larger number and dispersion of cells as compared with an image having a smaller number will necessarily have a

greater number of black pixels and, correspondingly, a higher "Migration Index". A migration index was determined for 5 beads from each well of an experimental treatment and averaged as one independent measurement.

3.11 Tube Formation Assay Analysis

Images from the tube formation assay were analyzed by counting the number of tubes per bead and measuring the length of each tube counted. Tube length measurements were calibrated against features of known lengths at the same magnification as the tube formation assay images. For this purpose, a hemacytometer grid was used to calibrate length measurements.

A sprout or tube was classified as any multicellular projection, at least 50 μm in length, originating from the bead surface and consisting of multiple contiguous cells. Lengths of sprouts or tubes were measured from the bead surface to the tip of the sprout. Occasionally tubes with bifurcations were observed and in such instances a measurement of the length of the longest continuous cellular projection was made. An example the image analysis performed for the tube formation assay is shown on the following page in *Figure 3.11a*.

Sprouts (i.e., "tubes"), once counted and measured, were categorized such that the number of tubes greater than or equal to 50 μm, 75 μm, or 150 μm could be compared between treatment groups. The number of sprouts greater than 50 μm constitutes the total number of sprouts, as cellular projections not greater than or equal to 50 μm in length were not considered "sprouts". The average sprout length per bead was also calculated and used as a basis for comparison between treatment groups.

3.12 Statistical Analysis

Data were expressed as mean ± standard error. Activity of BAEC in the absence or presence of growth factor stimulation or small molecule inhibition under control (atmospheric) pressures was assessed using raw values to ascertain the baseline behavior. The means of these experimental treatments were compared using a Student's t-test with $p < 0.05$ delineating significant differences. Bonferroni adjustments were used to correct p-values when multiple comparisons were performed. Responses of BAEC to pressure were normalized to those of matched controls (i.e., cells under control pressure, but otherwise similar experimental conditions) and expressed as fold change to account for any affects due to the influence of exogenous chemicals on baseline activity. Significant fold changes were determined with a one-sample t-test. Fold-change values for control samples was 1.0 with $p < 0.05$ denoting a significant difference from this threshold value. Different pressure treatments were compared using Student's t-test with Bonferroni's adjustment for multiple comparisons, again with $p < 0.05$ denoting a significant difference.

4. Results

4.1. BAEC Culture on Two-Dimensional Substrates

Bovine aortic endothelial cells (BAEC) seeded sparsely (5,000 cells/cm^2) and cultured on two-dimensional tissue culture-treated polystyrene surfaces reached confluence within 2 to 3 days and exhibited a typical "cobblestone" morphology [12, 14]. *Figure 4.1a* shows BAEC after a 24-hour overnight incubation (left) and BAEC after three days in culture (right).

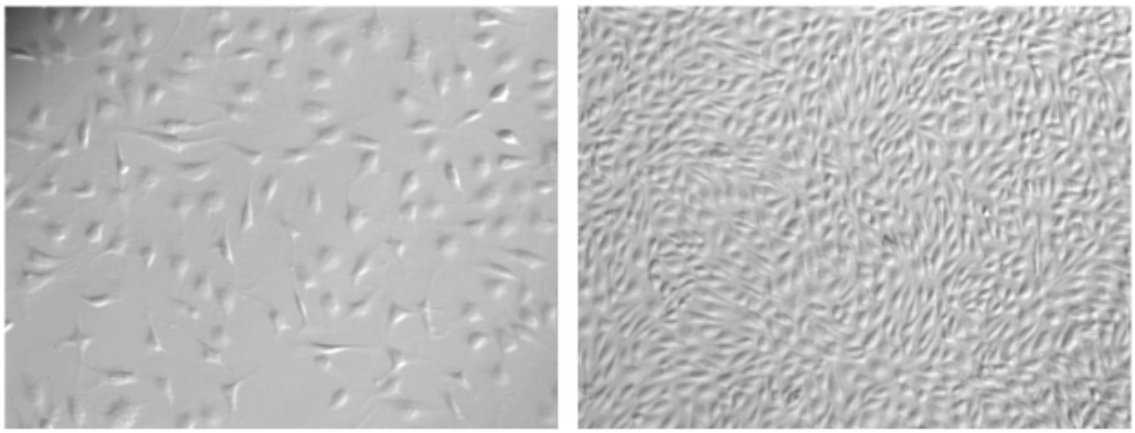

***Figure 4.1a* – BAEC shortly after 24 hour (left) and after 48 – 72 hour time periods in culture (right). Magnification 20X.**

4.2. Crystal Violet Uptake by BAEC

For proliferation experiments with BAE cells grown on two-dimensional substrates, cell layers labeled with Crystal Violet nuclear stain exhibited uniform uptake of crystal violet dye immediately upon removal from incubation. *Figure 4.2a* (below) shows fixed and stained BAE cells cultured on a two-dimensional substrate with crystal violet localized predominantly to the nucleus. Crystal violet uptake was quantified by spectrophotometry at a wavelength of 570 nm.

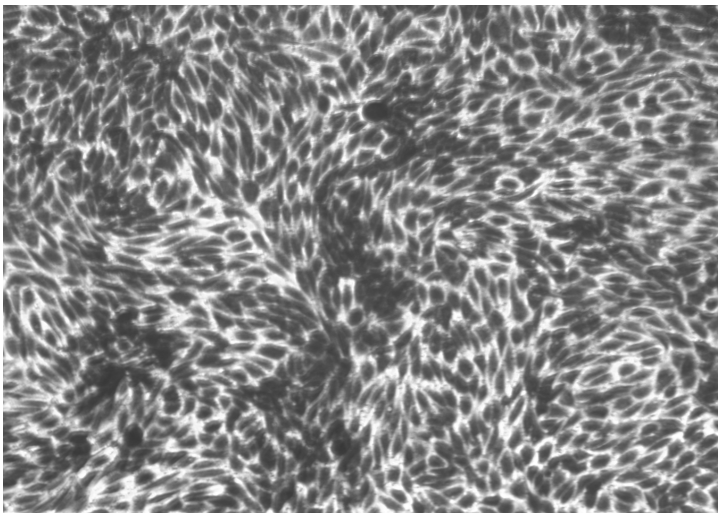

***Figure 4.2a* – Bovine aortic endothelial cell (BAEC) monolayer stained with Crystal Violet nuclear stain and rinsed with phosphate buffer solution (PBS). Magnification 20X.**

4.3. BAEC Seeding on Cytodex3^{TM} Microcarrier Beads

BAEC were seeded on Cytodex3^{TM} microcarrier beads according to the procedure described in **Section 3.4**. Endothelialization of the Cytodex3^{TM} beads used in the present study was confirmed by bright field and fluorescence microscopy as shown below in *Figure 4.3a*.

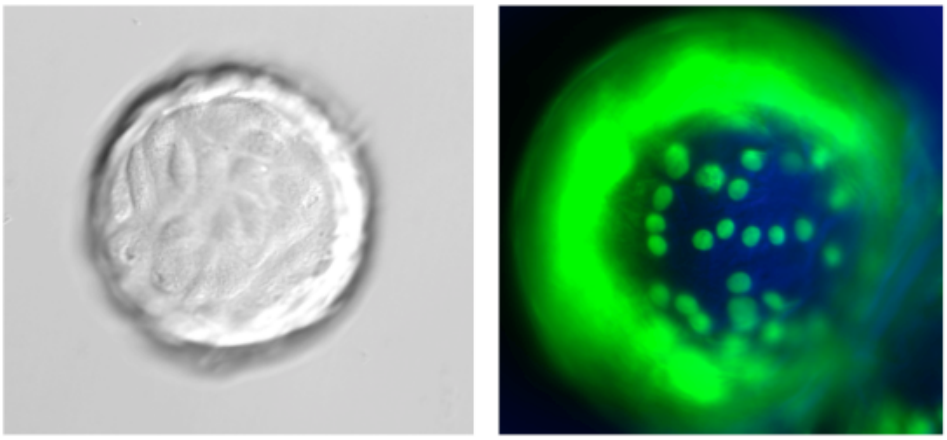

Figure 4.3a - Cytodex3™ microcarrier bead coated in BAE cells under bright-field view (left) and bead with cells labeled with nuclear stain, DAPI, and viewed under ultraviolet illumination (right). Magnification 100X.

The left panel of *Figure 4.3a* displays a representative bead whose outer surface has bean coated with a layer of BAE cells. The bright-field image on the left is focused on the top half of the bead and shows a near-confluent monolayer of cells on its surface. The image in the right panel of *Figure 3.4* shows a bead coated with BAEC labeled with DAPI nuclear stain. In line with bright-field images, endothelialized beads exhibited punctate staining of cell nuclei uniformly distributed along the bead surface.

4.4. Generation of Sustained Hydrostatic Pressures

Sustained hydrostatic pressures ranging from 0 to 120 mmHg were achieved for a single pressurized chamber. Moreover, when two chambers were connected in parallel, the system was also capable of achieving sustained hydrostatic pressures up to 40 mmHg. The images in *Figure 4.4a* show two pressure transducer digital outputs (20 and 40 mmHg) and the corresponding readings of a mercury barometer connected simultaneously to the same pressure chamber as the transducers.

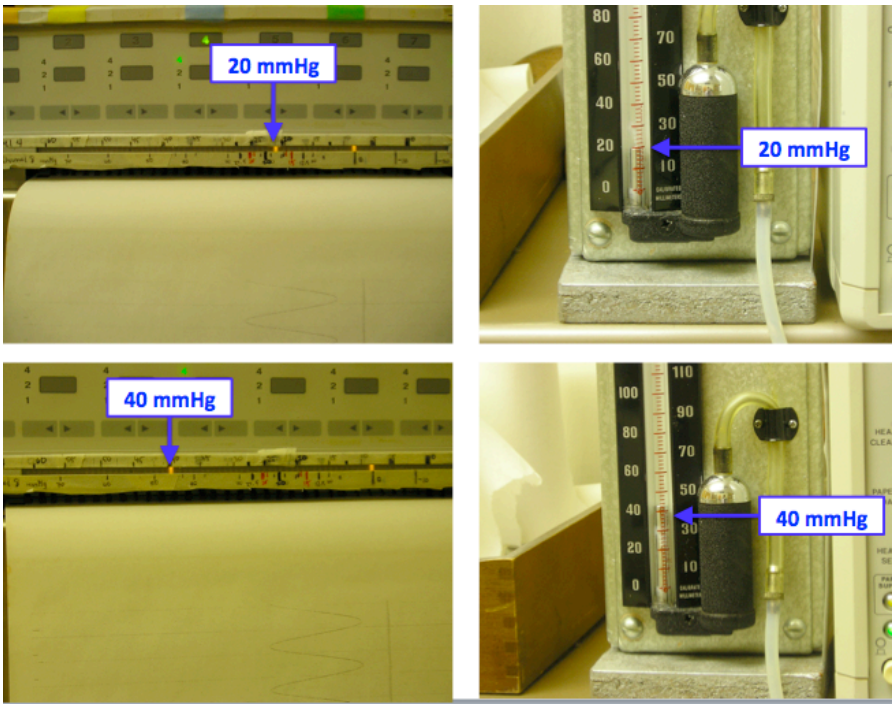

***Figure 4.4a* – Pressure transducer digital readouts (left) of 20 and 40 mmHg with corresponding, simultaneous mercury barometer readings (right).**

Though no cyclic pressure experiments were conducted as part of this study, the properties of the cyclic pressure profiles that the system was capable of generating were determined. The maximum pulse pressure of the system, with the components used in this study, was 20 mmHg at a mean pressure of 40 mmHg at 1 Hz pulse frequency. At 1 Hz, it was determined that the system was capable of generating a sinusoidal pressure profile with an upper limit pressure of 50 mmHg and a lower limit pressure of 30 mmHg. At mean pressures below 40 mmHg, the system was capable of generating sinusoidal pressure waves with frequencies between 0.5 and 2.5 Hz and pulse pressures up to 20 mmHg.

Shown in *Figure 4.4b* is an image of a pressure transducer strip chart readout of a 1 Hz sinusoidal pressure wave with a mean pressure of 40 mmHg and a pulse pressure of 20 mmHg.

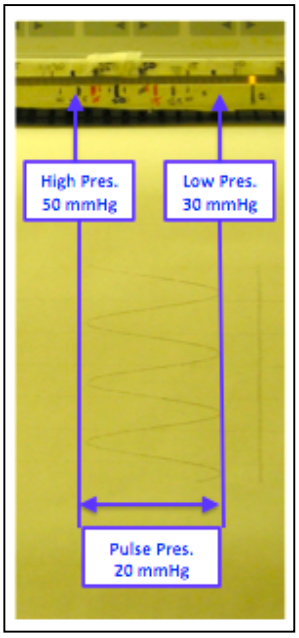

Figure 4.4b **– Pressure transducer strip chart readout depicting a 1 Hz sinusoidal pressure wave with a mean pressure of 40 mmHg and a pulse pressure of 20 mmHg, which alternates between high and low pressures of 50 mmHg and 30 mmHg, respectively.**

The pressure system proved to be capable of generating and sustaining pulsatile pressures for several days with a maximum pressure of 50 mmHg, maximum pulse pressure of 20 mmHg, and a maximum pulse frequency of 2 Hz.

4.5. Increase of BAEC Cell Density By Stimulation with Basic Fibroblast Growth Factor

The present study confirmed that a submaximal dose of 2.5 ng/mL FGF-2 significantly enhanced the proliferation rates of BAE cells. *Figure 4.5a* displays the average absorbance of light at 570 nm, which corresponds to cell density, of cultures maintained in cell culture media with and without either 1 or 2.5 ng/mL FGF-2 for 72

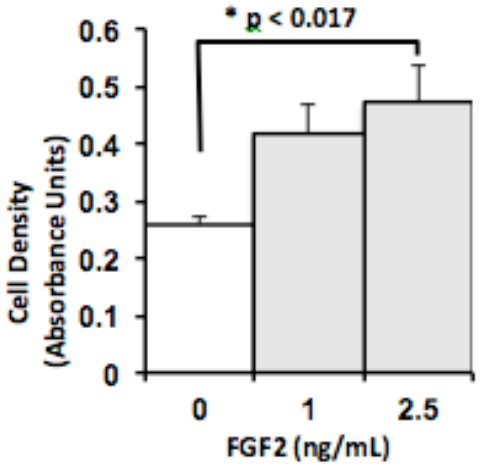

***Figure 4.5a* – Endothelial cell growth is dependent on the presence of local concentrations of fibroblast growth factor-2 (FGF-2) within a certain range of concentrations. Crystal violet light absorption at 570 nm (measure of cell density) of two-dimensional BAEC cultures was measured for cultures maintained in media alone (white bar) or in the presence of 1 and 2.5 ng/mL FGF-2 (gray bar). Bars in the figure are mean absorbance units ± standard error; n=3 independent experiments compared to control levels using a paired t-test with Bonferroni's correction (*p < 0.01; N = 3).**

hours. As shown in *Figure 4.5a*, BAEC cultured in DMEM containing 10% FBS and supplemented with 2.5 ng/mL but not 1 ng/mL FGF-2 exhibited a significantly ($p < 0.01$) increased level of crystal violet uptake compared to untreated cells.

4.6. Effect of Sustained Hydrostatic Pressure on BAEC Population Growth

BAEC were seeded on two-dimensional substrates at a cell density of 5,000 cells/cm^2 and exposed to sustained pressures of 20 mmHg or 40 mmHg for a period of 72 hours. The results of this experiment are shown in *Figure 4.6a.* After exposure to 20 mmHg sustained pressure for 72 hours, BAEC populations exhibited significant increases

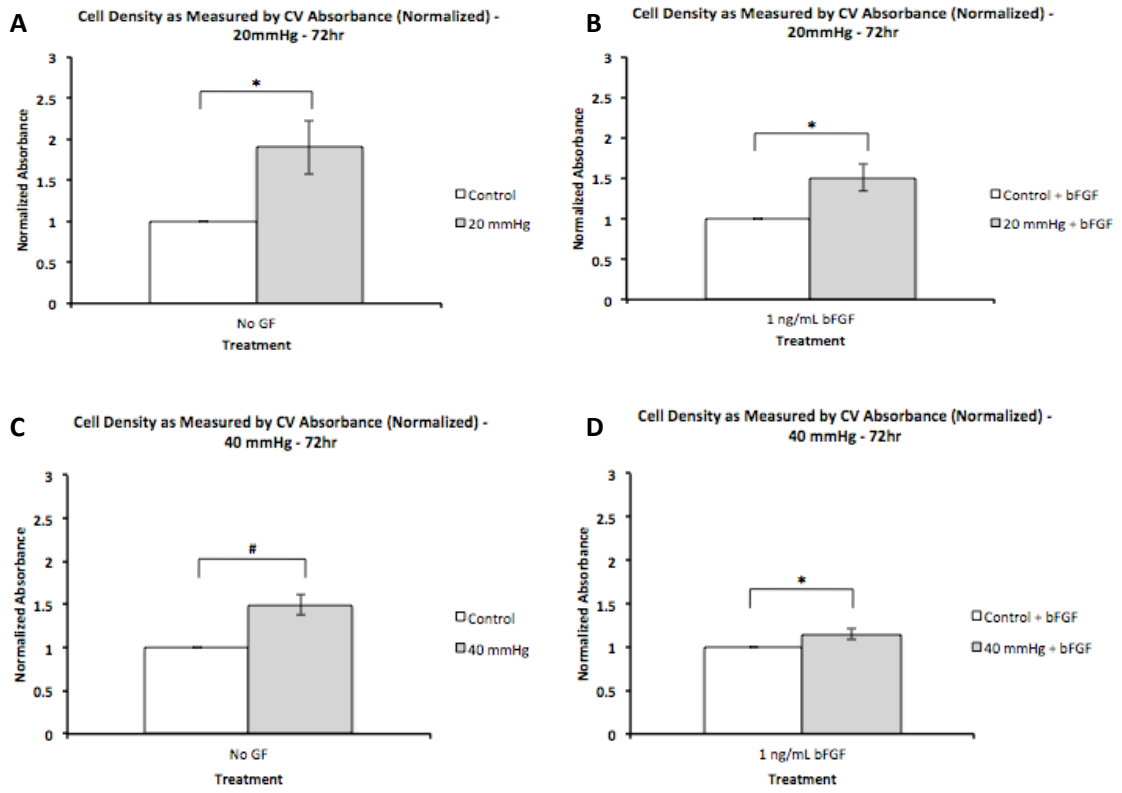

***Figure 4.6a* – Endothelial cell proliferation is responsive to both local hydrostatic pressures and local levels of FGF-2 (labeled as bFGF) in the supernatant media. Cell density was determined by measuring crystal violet light absorbance at 570 nm of two-dimensional BAEC cultures. Comparisons were made between cultures maintained at 0 mmHg (white bars) and an experimental hydrostatic pressure (gray bars). The graphs above depict comparisons between (A) 0 mmHg (control) and 20 mmHg pressures, each in standard media (no growth factor supplement); (B) 0mmHg (control) and 20 mmHg pressures, each in media supplemented with 1 ng/mL FGF-2; (C) 0 mmHg (control) and 40 mmHg pressures, each in standard media; (D) 0 mmHg (control) and 40 mmHg, each in media supplemented with 1 ng/mL FGF-2. Crystal violet uptake of pressurized cell cultures was normalized to those of cell cultures maintained under atmospheric (control) pressure, but otherwise similar experimental (i.e., with or without FGF-2) conditions, and expressed as fold change. Bars in each panel are mean fold change ± standard error; n=5 independent experiments compared to control levels assigned a value of 1 (dashed line) using one-sample t-test (*p < 0.05).**

(*$p < 0.05$) in cell density compared to cells maintained under control pressure (0 mmHg above atmospheric), but otherwise similar experimental conditions. *Figure 4.6a* (on the following page) displays two figures that show the effect of a 20 mmHg sustained pressure on BAEC proliferation in media that does not contain FGF-2 (left) and media that does contain FGF-2 (right) at a concentration 1 ng/mL. In both cases, cultures exposed to a 20 mmHg pressure exhibited a statistically significant increase in cell density with p-values of 0.018 and 0.049, respectively.

The same experiment was conducted with BAEC being exposed to a sustained hydrostatic pressure of 40 mmHg for 72 hours; this experiment was also repeated four times (N = 4). *Figure 4.6a* displays two figures that show the effect of a 40 mmHg sustained pressure on BAEC proliferation in media that does not contain FGF-2 (Panel C) and media that contains FGF-2 (Panel D) at a concentration 1 ng/mL. Pressurization elicited significant increases in cell density of cultures maintained in media containing 1 ng/mL FGF-2 but not in cultures containing no FGF-2 with p-values of 0.042 and 0.077, respectively.

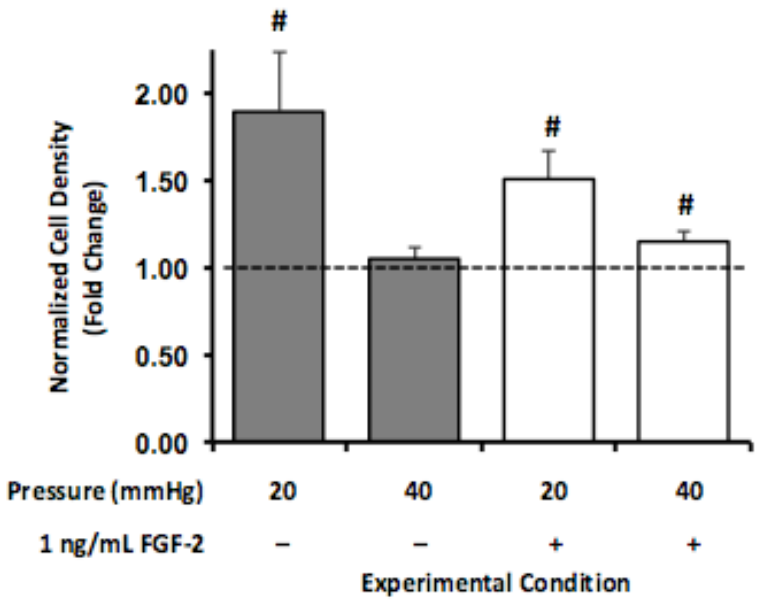

***Figure 4.6b* - Endothelial growth is a function of local hydrostatic pressure levels and extracellular levels of fibroblast growth factor-2 (FGF-2). Endothelial cell populations were maintained under atmospheric (control) pressure conditions as well as exposed to 20- and 40-mmHg hydrostatic pressures above atmospheric in the absence (white bars) and presence (gray bars) of 1 ng/mL FGF-2 for 3 days. Crystal violet uptake of pressurized cell cultures was normalized to those of cell cultures maintained under atmospheric (control) pressure, but otherwise similar experimental (i.e., with or without FGF-2) conditions, and expressed as fold change. Bars are mean fold change ± standard error; n=5 independent experiments compared to control levels assigned a value of 1 (dashed line) using one-sample t-test (#$p < 0.05$).**

The results presented in *Figure 4.6b* summarize the results shown in *Figure 4.6a* (on the previous page) but displayed in a manner that allows for comparison of the responses to 20 and 40 mmHg pressure and the effect of FGF-2 supplementation. Comparing the response at 20 mmHg (*Figure 4.6a*, Panel A/B) and experiments conducted at 40 mmHg (*Figure 4.6a*, Panel C/D) in *Figure 4.6b* reveals that a 20 mmHg sustained hydrostatic pressure appears to have a more potent proliferative effect.

4.7. Effect of Sustained Hydrostatic Pressure on BAEC Morphology

Compared to cells maintained under control pressure conditions, BAEC cultures exposed to 40 mmHg for 72 hours appeared to exhibit cell elongation. This effect was also observed for BAEC populations exposed to 40 mmHg in culture media supplemented with 5 ng/mL FGF-2 for 72 hours, as shown in *Figure 4.7* below.

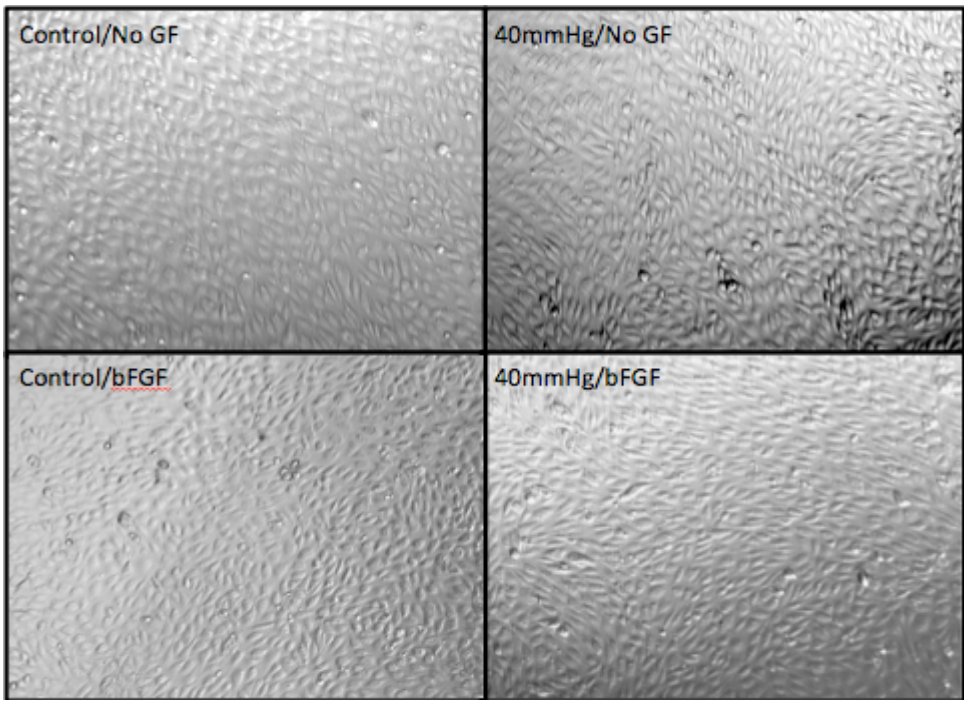

Figure 4.7a **- Images of BAEC cultures after 72 hours of exposure to pressure in the absence of presence of FGF-2 (labeled as bFGF). The two images to the left show cultures exposed to 40 mmHg for 72 hours and the cells in both images appear to be elongated without any predominant orientation and tightly-packed whereas the images to the right (controls) show cells that are more rounded.**

4.8. Role of VEGFR-3 in the Mediation of Pressure-Induced Endothelial Proliferation

The involvement of VEGF-C-related signaling in the proliferative responses of BAEC cultures to pressure stimulation was explored using MAZ51, a VEGFR-3 inhibitor. Under control (i.e., atmospheric pressure) conditions, BAEC cell density decreased linearly as a function of increasing MAZ51 concentration (*Figure 4.7a*). *Figure 4.7a* (Panel B) shows the effects of MAZ51 on BAEC population growth in response to exposure to 20 mmHg sustained pressure. As shown in the figure, MAZ51 at concentrations greater than 1 µM and up to 20 µm attenuated and eventually blocked the proliferative responses of BAEC cultures subjected to 20mmHg for 72 hours.

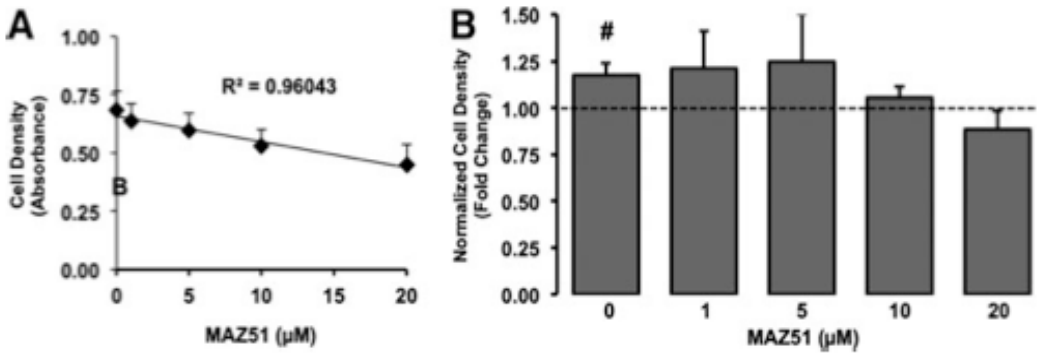

***Figure 4.8a* - Pressure-sensitive endothelial proliferative responses depend on VEGFR-3 activity. (A) We defined the relationship between MAZ51 and baseline endothelial proliferation under atmospheric pressures using linear regression analyses. Points in (A) are cell densities (reflected by absorbance of crystal violet at 570 nm) – standard error. MAZ51 concentration dependence of cell densities was assessed by linear regression. (B) We also examined the influence of 0–20 µM MAZ51 on the growth response of BAEC to 20-mmHg-pressure exposure. Crystal violet uptake of pressurized cells was normalized to those of cells maintained under atmospheric (control) pressure, but otherwise similar experimental (i.e., MAZ51) conditions, and expressed as fold change. Bars in (B) are mean ± standard error; n = 5. #p < 0.05 compared to levels of matched control assigned a value of 1 (dashed line) using one-sample t-test.**

4.9. Effects of Pressure on VEGF-C and VEGFR-3 Expression

To further explore a potential role of the VEGF-C/VEGFR-3 pathway, the expression of VEGF-C and VEGFR-3 by BAEC exposed to either 20 or 40 mmHg pressure were compared to those of cells maintained under control (atmospheric) pressure conditions. As shown in Panel A and Panel B, increases in the number of cells expressing VEGF-C and the number of cells expressing VEGFR-3, for one sample, were observed in BAEC exposed to 20 mmHg for three days. Repeating this experiment four to six more

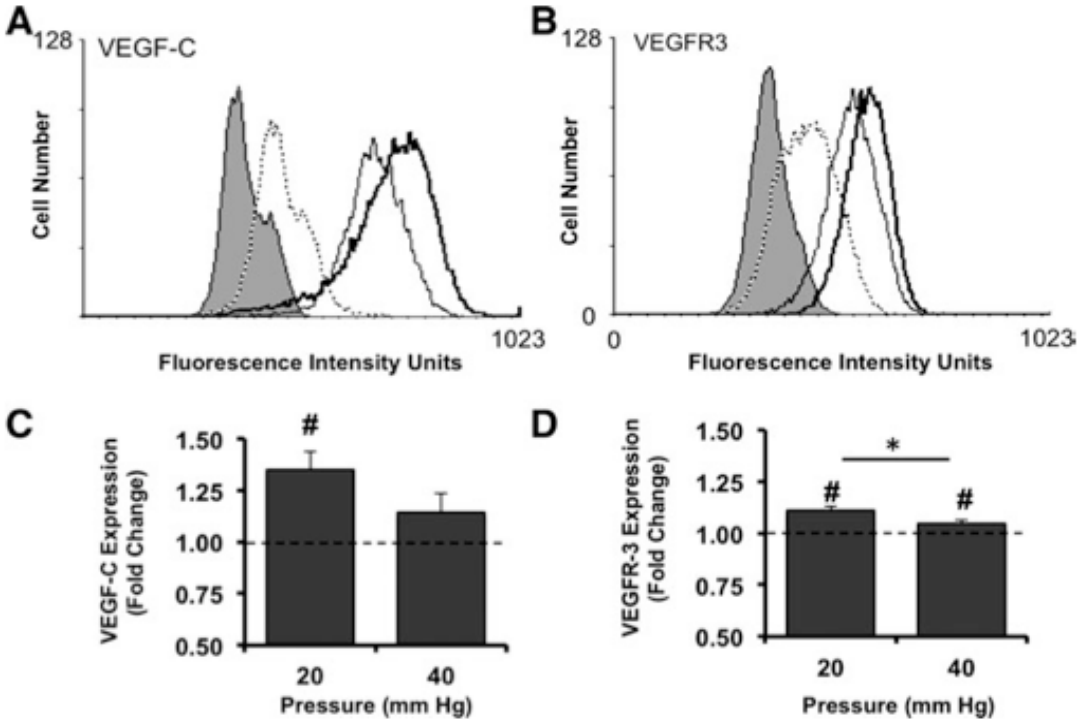

Figure 4.9a **- Pressure upregulates cellular levels of VEGF-C and membrane expression of its high-affinity receptor, VEGFR-3 (Panel A/B). Histograms of fluorescence intensity for either VEGF-C (Panel A) or VEGFR-3 (Panel B), were plotted for unlabeled BAEC (no- stain, filled curve) and cells labeled only with the appropriate species-specific secondary antibodies, Alexa^{TM} 488 conjugates (dotted line), as well as for control cells (thin black line) and cells exposed to 20 mmHg (thick black line) for 3 days and detected with antigen-specific primary antibodies. Mean fluorescence intensities reflecting bound antibodies for either VEGF- C (Panel C) or VEGFR-3 (Panel D) on BAEC exposed to either 20 or 40mmHg (20 or 40, respectively) were normalized to those of matched controls (dashed line) and expressed as fold change. Bars in Panel C and Panel D are mean ± standard error; n=4 to 6. #p<0.05 compared to control levels (dashed line) assigned a value of 1 (dashed line) using a one-sample t-test. *p<0.05 compared using Student's t-test. (*Shin et al.*, 2012).**

times (n = 4 – 6) for both 20 mmHg and 40 mmHg revealed some significant ($^{\#}p < 0.05$) differences as compared with control samples maintained at atmospheric (0 mmHg) pressure. As shown in *Figure 4.7b*, exposure of BAEC to 20 mmHg, but not 40 mmHg, sustained hydrostatic pressure for 72 hours significantly increased the expression of VEGF-C, as compared to controls. Significant increases ($^{\#}p < 0.05$) in response to pressure exposure were also observed in VEGFR-3 expression, the high-affinity VEGF-C receptor. Specifically, the number of cells expressing VEGFR-3 significantly increased after exposure to either a 20 or 40 mmHg sustained pressure for 3 days relative to time-matched controls.

4.10. Effects of Pressure on BAEC Migration and Invasion of Three-Dimensional Collagen Matrix

The effect of hydrostatic pressure on cell *invasiveness*, the characteristic representative of cell migration and invasion into the extracellular matrix, of BAEC was

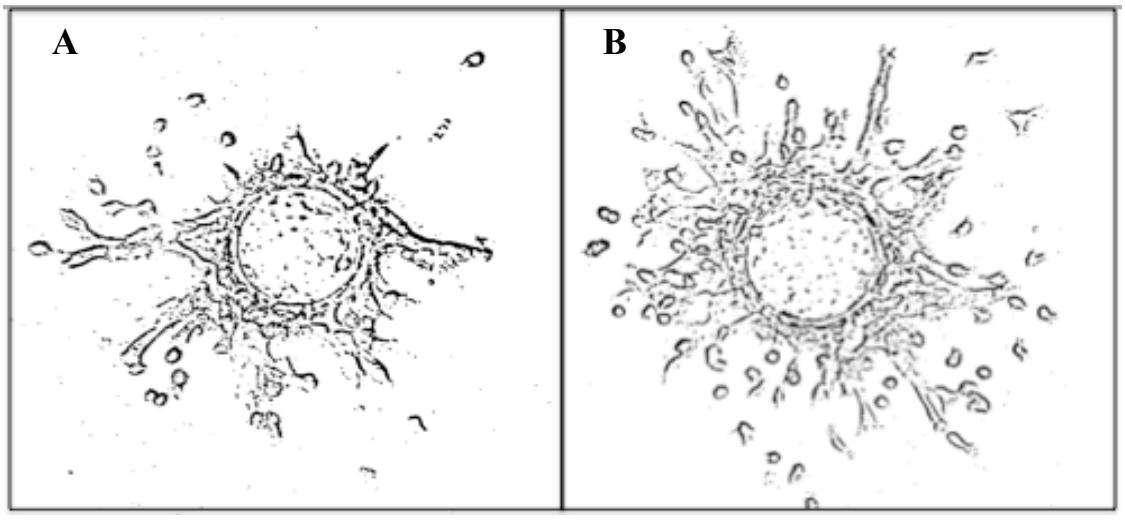

***Figure 4.10a* - Example of binary images filtered by the InvasiQuant macro written for the ImageJ software package. The image in Panel A (Migration Index = 9.371) displays a culture exhibiting less invasive activity than the image of the culture in Panel B (Migration Index = 14.256).**

investigated using a two-layer gel format (see **Section 3.8** on **Materials and Methods).** *Figure 4.10a* (on previous page) displays two representative images, each of a single cellularized bead, embedded in a two-layer collagen gel, after 72 hours in culture. These images were used to quantify Migration Indices (see **Section 3.9** of **Materials and Methods**). The Migration Index of the image on the left is 9.371 and the same quantity for the image on the right is 14.256.

Figure 4.10b displays the Migration Indices for BAEC populations on Cytodex3^{TM} beads that had been cultured under atmospheric pressure for 72 hours in the absence of the presence of either FGF-2 or VEGF-A. BAEC maintained in media supplemented with 2.5 mg/mL FGF-2 exhibited a significant increase ($p = 0.048$) in average Migration Index compared to untreated cells. In contrast, although BAEC cultures stimulated with 2.5 mg/mL VEGF-A exhibited an overall average increase in Migration Index over untreated cells, this effect did not result in a statistically significant

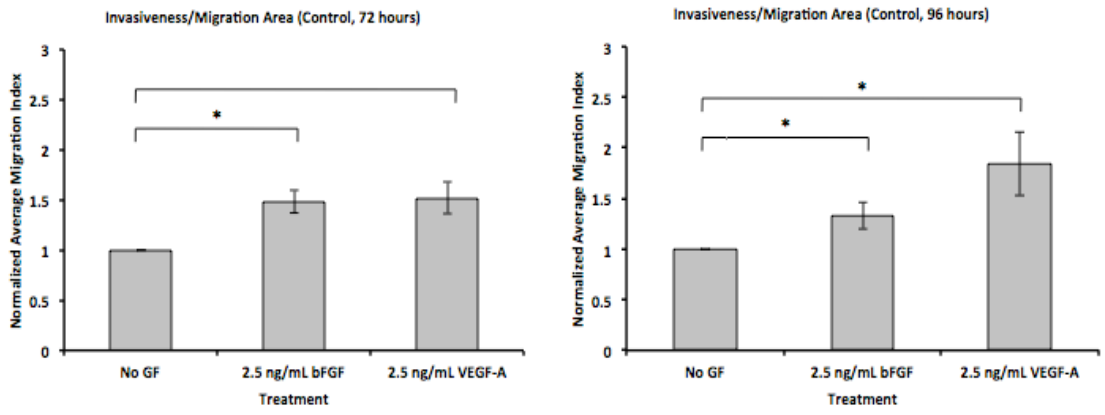

***Figure 4.10b* – Endothelial cell motility is affected by the local concentration of pro-angiogenic growth factors such as FGF-2 (labeled as bFGF) and VEGF-A. The migratory activity of BAEC were measured using the image processing technique and computation of the InvasiQuant ImageJ macro developed herein. All cultures were maintained at atmospheric (control) pressure conditions for 72-hour (left) and 96-hour (right) durations. The Average Migration Indices of cultures in media supplemented with FGF-2 and VEGF-A were normalized to and compared with cultures containing no added growth factor. The effect of each growth factor on migration was compared mathematically using paired Student's t-test in conjunction with Bonferroni's adjustment for multiple comparisons (*$p < 0.05$).**

difference. Finally, after a 96-hour incubation period, BAEC populations cultured in the presence of FGF-2 and VEGF-A exhibited significant increases ($p = 0.025$ and $p = 0.022$, respectively) in their respective Average Migration Indices compared with paired controls (no growth factor).

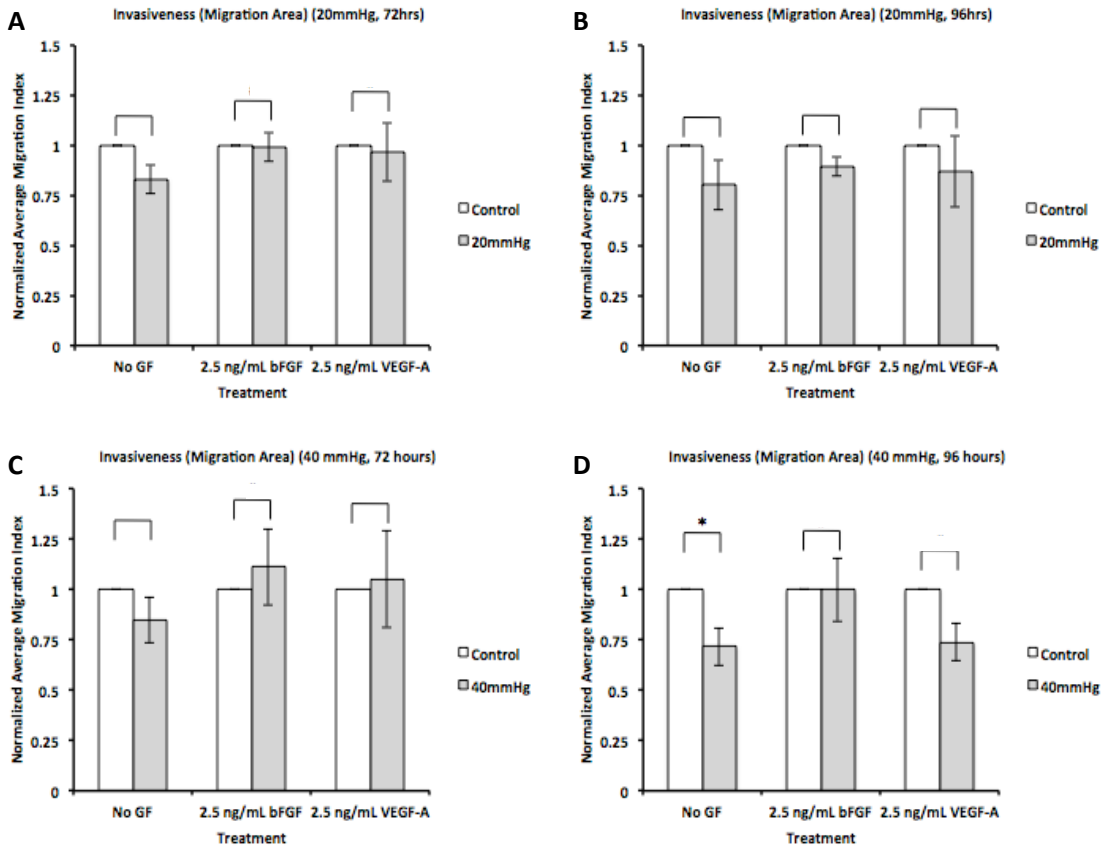

***Figure 4.10c* – Exposure to 20- and 40-mmHg hydrostatic pressures did not significantly enhance the invasive activity of BAEC. BAEC seeded on Cytodex3™ beads and suspended in bi-layer collagen gels for 72 and 96 hours were assessed for their ability to exhibit invasive activity (i.e., migration). The effect of pressure was compared across multiple pressures, experiment durations, and growth factor supplementation. Each experiment contained two growth factor treatment groups, 2.5 mg/mL FGF-2 (labeled as bFGF) and 2.5 mg/mL VEGF-A, and one untreated group (no growth factor). 3-D cultures were exposed to 20 mmHg for (A) 72 hours and (B) 96 hours and 40 mmHg for (C) 72 hours and (D) 96 hours. Bars in (A) and (B) represent comparisons within each growth factor group of mean fold-change in migration index ± standard error of cultures maintained at control (0 mmHg) pressure and 20 mmHg; n=3. #p > 0.05 using paired t-test. The same comparisons were performed for exposures to 40 mmHg in (C) and (D) (*p < 0.05, #p > 0.05).**

In terms of pressure experiments, BAEC either exposed to a 20 mmHg or maintained at control (atmospheric) pressure for 72 and 96 hours exhibited similar levels of migration in between gel layers. As shown in *Figure 4.10c*, when exposed to 40 mmHg, BAEC migration indices were significantly ($p<0.05$) reduced only after 96 hours in the absence of growth factors. Cells exposed to 40 mmHg in the presence of either 2.5 ng/mL FGF-2 or VEGF-A for either 72 or 96 hours displayed migration indices that were similar to time-matched controls (i.e., cells maintained under atmospheric pressure conditions in the absence of growth factor).

4.11. Effects of Local Growth Factor Concentrations on BAEC Tubulogenesis

The results in this section describe the effects of elevated hydrostatic pressures and local growth factor concentrations on BAEC tubulogenesis. The tube formation assay was conducted using the single-layer gel configuration obtained by following the protocol described in **Section 3.8** of the **Materials and Methods** section. Images were analyzed using the image processing method described in **Section 3.10 – Migration/Invasion Assay Analysis**.

In these experiments, BAEC were seeded on Cytodex3^{TM} microcarrier beads that were embedded in a single-layer collagen gel and maintained in media containing either FGF-2, VEGF-A, FGF-2 + VEGF-A, or no growth factors. During experiments, cells were expected to initiate the process of tube formation by engaging in cellular activities such as matrix degradation, migration, intercellular connection, and morphogenesis.

A visual example of how sprouts (or tubes) were measured, counted, and analyzed is shown in *Figure 4.8a*. Tube formation was quantified by counting the number of tubes

per bead and measuring the length of all tubes emanating from a bead. The number of tubes per bead was further categorized into the average number of tubes per bead of length greater than 50, 75, and 150 micrometers.

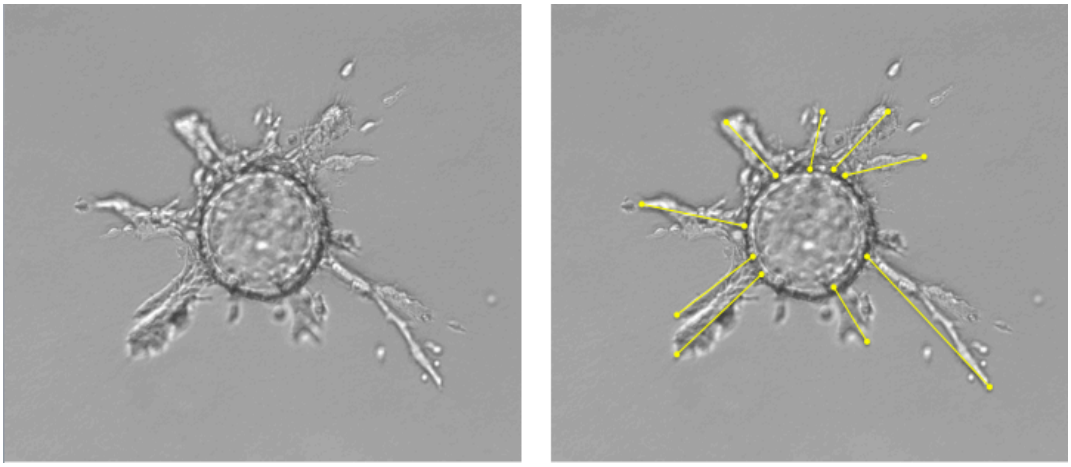

***Figure 4.11a* – Visual example of the sprout/tube counting and measurement process. The figure contains two identical images of a bead embedded in a 3-D single-layer collagen gel. After incubation for 3-4 days, BAEC would form cellular processes (i.e., tubes or sprouts) emanating from the bead surface. These processes would be counted and their length measured linearly from the bead surface to the end of the process. Lines (yellow) that demonstrate how tubes were measured overlay the image on the right. Magnification 60X.**

To verify the effects of the growth factors with known pro-tubulogenic influences used in this study, comparison of tubulogenic activity between groups maintained in media containing no growth factors and media supplemented with FGF-2, VEGF-A, or FGF-2 + VEGF-A. *Figure 4.11b* shows images of one bead from each of these growth factor treatments.

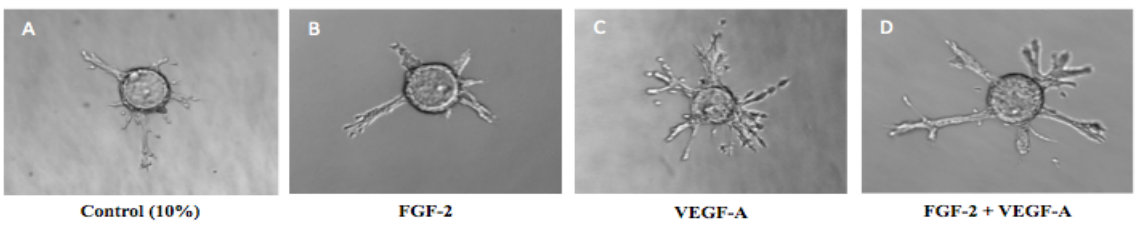

***Figure 4.11b*– Representative images of Cytodex3™ beads maintained in media containing no growth factor (Panel A), 2.5 ng/mL FGF-2 (Panel B), 2.5 ng/mL VEGF-A (Panel C), and 2.5 ng/mL of both FGF-2 and VEGF-A (Panel D). Bright field, magnification 60X.**

The images in *Figure 4.11b* display representative BAEC bead cultures maintained under atmospheric pressure condition in the absence (untreated controls) or presence of either 2.5 ng/mL FGF-2, 2.5 ng/mL VEGF-A, or both FGF-2 and VEGF-A in combination (2.5 ng/mL of each). Under all conditions tested, BAEC exhibited tubulogenic activity consistent with the formation of sprouts. Comparisons were performed for mean tube length per bead to determine whether the known pro-angiogenic properties of FGF-2 and VEGF-A have a detectable effect on tube length after 72 and 96 hours. *Figure 4.11c* on the following page displays the average total number of tubes above each length threshold (50, 75, 150 μm) formed within each growth factor treatment group after 72 hours (left, Panels A/C/E) and 96 hours (right, Panels B/D/F) under atmospheric pressure

As shown in *Figure 4.11c*, BAEC populations stimulated with either 2.5 ng/mL VEGF-A or 2.5 ng/mL of VEGF-A plus 2.5 ng/ml FGF-2, but not 2.5 ng/mL FGF-2 alone, exhibited a significant increase (*$p < 0.05$) in the mean number of sprouts per bead greater than 50 μm compared to untreated cells (no growth factor). After 96 hours of culture, BAE cells under all growth factor conditions (Figure 4.9b; Panel A) exhibited significantly increased numbers of tubes greater than 50 μm in length.

When examining the effects of growth factor concentrations on the formation of sprouts greater than 75 μm, only bead cultures maintained under atmospheric pressure conditions in VEGF-A for 96 hours failed to show a significant increase in the number of tubes. Compared to untreated cells, BAEC bead populations stimulated with FGF-2, VEGF-A, and FGF-2+VEGF-A) for 72 hours showed significant increases in the number of tubes greater than 75 μm in length, relative to controls. Furthermore, stimulation with

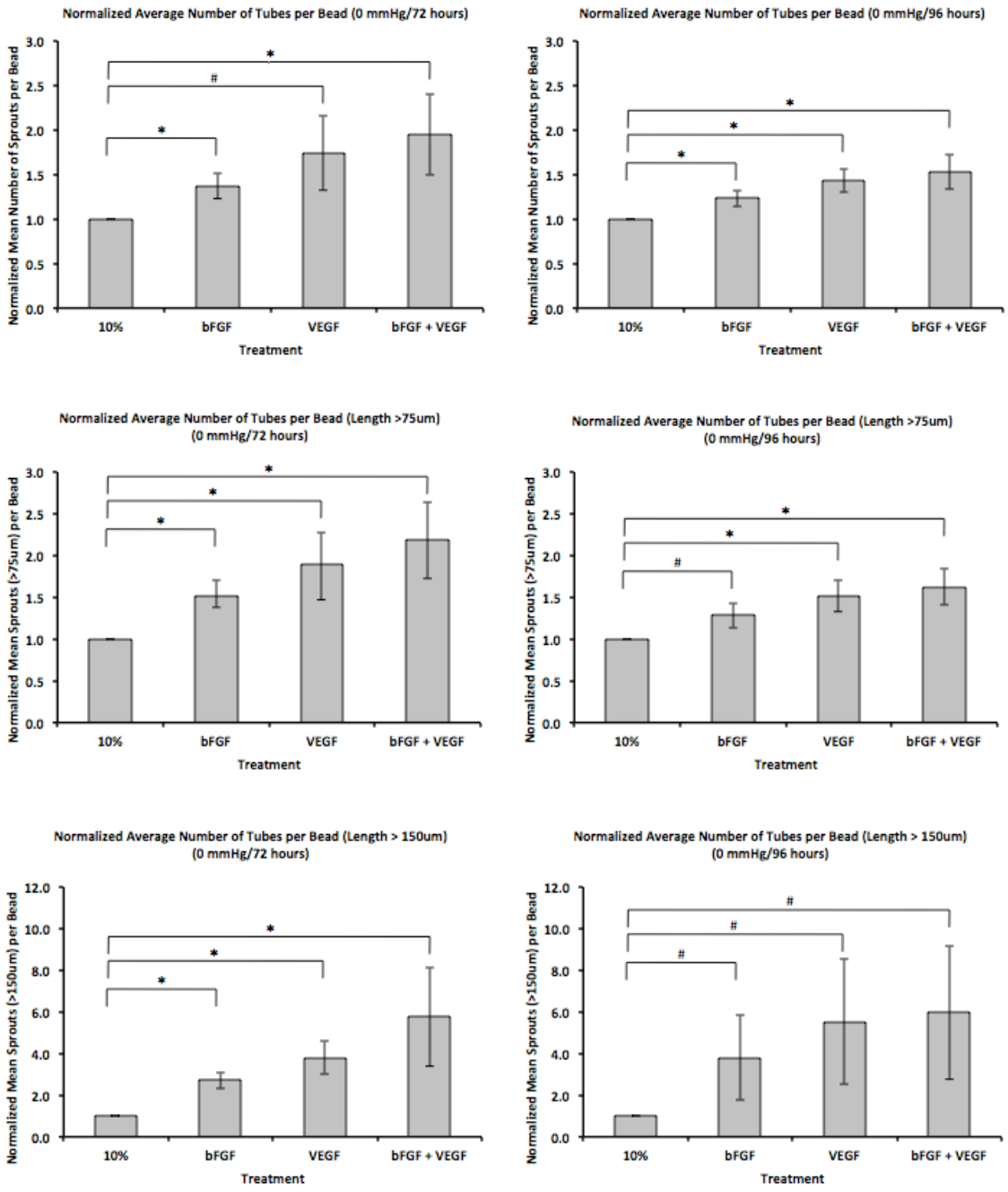

Figure 4.11c **– Graphs displaying a comparison of the number of tubes present of length greater than 0 µm (Panels A/B), 75 µm (Panels C/D), and 150 µm (Panels E/F) after maintenance in media containing no growth factor, 2.5 mg/mL FGF-2 (labeled as bFGF), 2.5 mg/mL VEGF-A (VEGF), 2.5 mg/mL of both FGF-2 and VEGF-A. Measurements were taken after both 72 hours (Panels A/C/E) and 96 hours (Panels B/D/F) of incubation under standard cell culture conditions. Bars in each graph represent the mean-fold change in the number of sprouts (i.e., tubes) counted greater than each threshold length (0, 75, or 150 µm) ± standard error of cultures maintained under each growth factor treatment; N=4. *p > 0.05 and #p > 0.05 using a paired Student's t-test with Bonferroni adjustment.**

VEGF-A and FGF-2 for 96 hours also induced significant increases the in the formation of tubes greater than 75 µm in length.

As shown in *Figure 4.11c* on the previous page, Panels E and F, BAEC stimulated with either FGF-2, VEGF-A, or both FGF-2 and VEGF-A for 72 hours exhibited significant increases (*$p < 0.05$) in the formation of sprouts per bead that were greater than 150 µm in length compared to untreated controls (no growth factor). Interestingly, the number of sprouts greater than 150 µm in length that were formed by BAEC bead cultures treated with either FGF-2, VEGF-A, or FGF-2 + VEGF-A for 96 hours were similar to those of untreated cells.

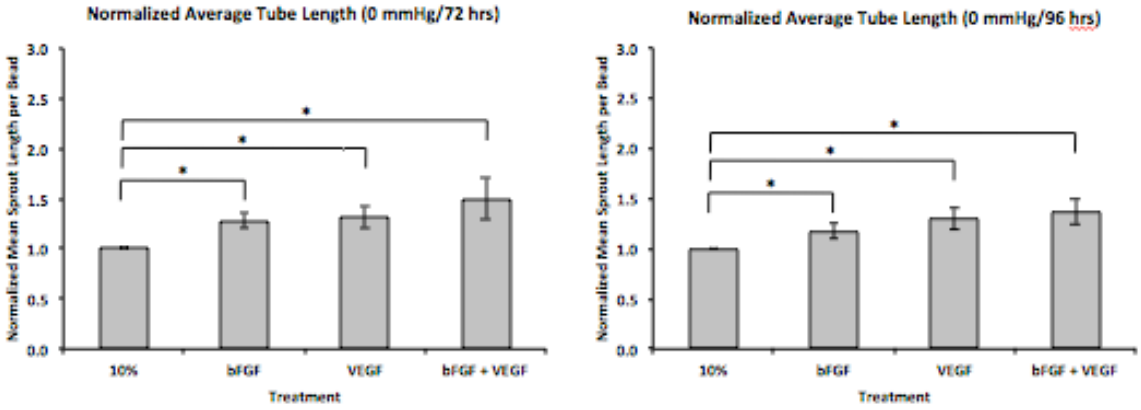

***Figure 4.11d* – Graphs displaying a comparison of the mean tube (i.e., sprout) length per bead between growth factor treatment groups after 72 hours (Panel A) and 96 hours (Panel B) of incubation. Bars in each graph above represents the fold change in mean tube length per bead ± standard error of cultures maintained under each growth factor treatment; N=4. *$p > 0.05$ using a paired Student's t-test with Bonferroni adjustment.**

Collectively, these results confirmed the utility of the Cytodex3^{TM} bead cultures tested in the present study to detect changes in the tubulogenic activity of BAEC.

4.12. Effects of a 20 mmHg Sustained Hydrostatic Pressure on BAEC Tubulogenesis

The results in this section describe the effects of exposure to 20 mmHg hydrostatic pressure levels in the absence and presence of the pro-tubulogenic growth factors FGF-2 and VEGF-A on BAEC tubulogenesis. *Figure 4.12a* and *Figure 4.12b* display representative images of beads with BAEC either maintained under control conditions or exposed to 20 mmHg hydrostatic pressures in the absence or presence of either FGF-2, VEGF-A or both FGF-2 + VEGF-A for 72 and 96 hours, respectively. As shown in the figures, endothelial sprouts or tubes formed under all media treatments and pressure conditions.

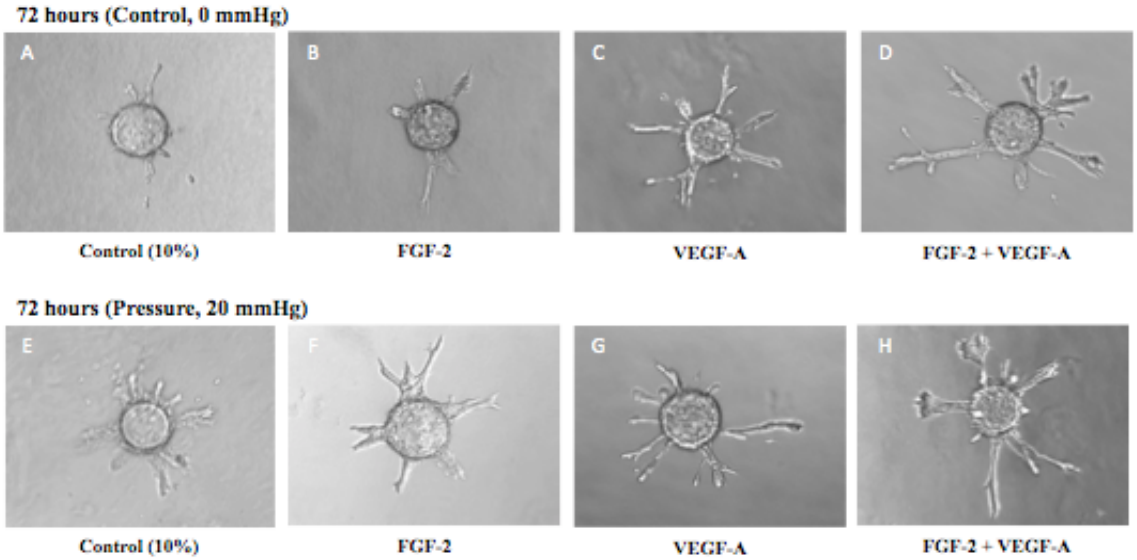

***Figure 4.12a* - Representative images of BAEC on Cytodex3^{TM} beads suspended in collagen gels and maintained under atmospheric (control) or 20 mmHg pressure conditions for 3 days. One representative image is provided for each growth factor treatment at either the control (0 mmHg) or 20 mmHg pressure condition. Images were acquired under 60X magnification.**

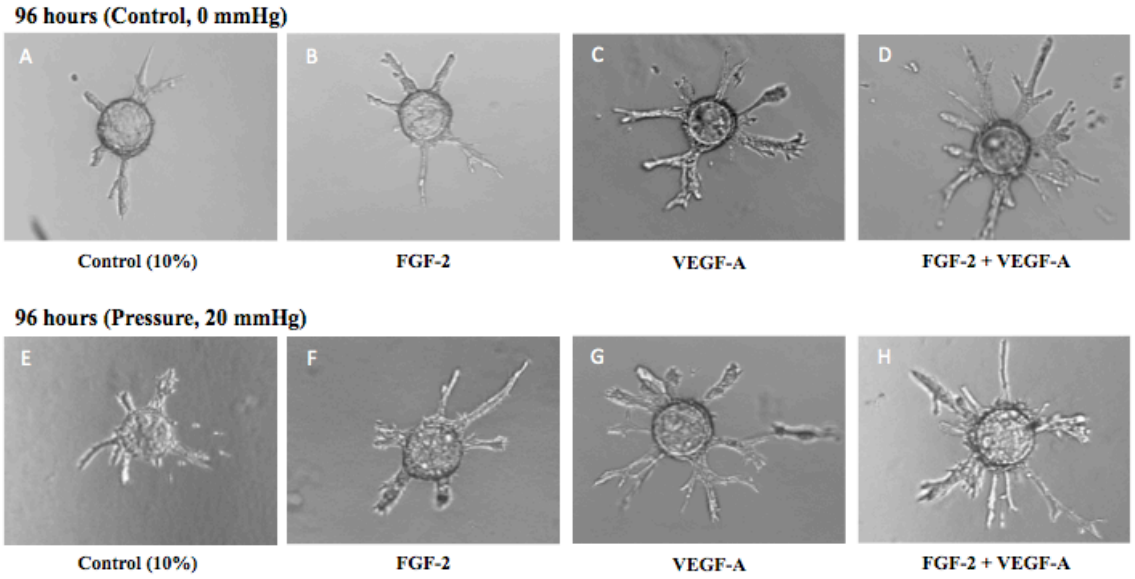

Figure 4.12b **- Representative images of BAEC on Cytodex3^{TM} beads suspended in collagen gels and maintained under atmospheric (control) or 20 mmHg pressure conditions for 4 days. One representative image is provided for each growth factor treatment at either the control (0 mmHg) or 20 mmHg pressure condition. Images were acquired under 60X magnification.**

When examining the numbers of sprouts formed by BAEC cultures, apparent differences were observed between those formed by either cells maintained under control conditions or exposed to pressure. Specifically, exposure to

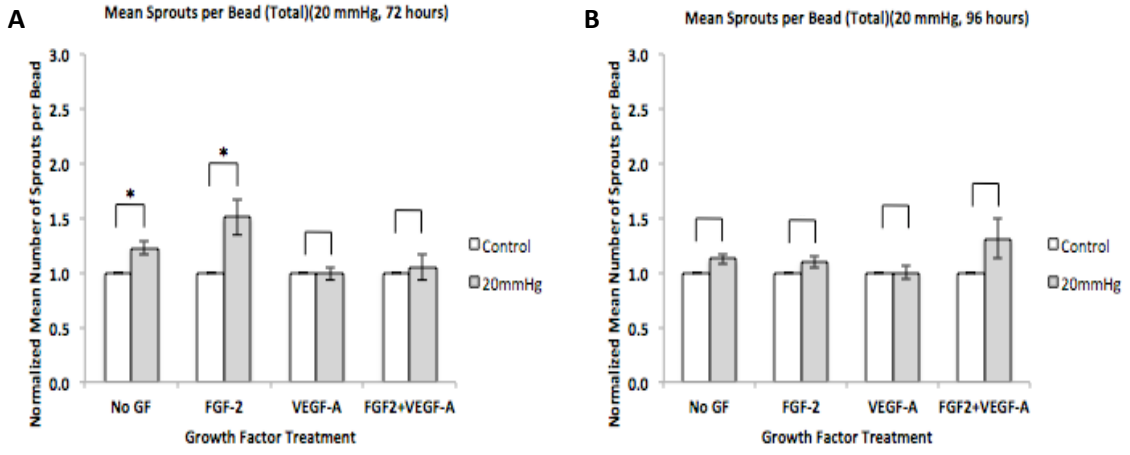

Figure 4.12c **– Graphs displaying the comparison of the mean number of tubes (i.e., sprouts) greater than 0 µm between control (0 mmHg) and 20 mmHg pressure-exposed cultures within each treatment group after 72 hours (Panel A) and 96 hours (Panel B) of incubation. Bars in each graph above represent the mean-fold change in the number of tubes greater than 0 µm per bead ± standard error of cultures maintained under each treatment; N=4. Comparisons were made using a paired Student's t-test (*p > 0.05, #p > 0.05).**

20 mmHg sustained hydrostatic pressure stimulated significant increases in the number of tubes greater than 0 µm (total number of tubes/sprouts) under the "no growth factor" and FGF-2 treatment groups after 72 hours of incubation. (*Figure 4.12c*, Panel A) All significant differences in tube formation between cells exposed to pressure or maintained under control conditions disappeared after 96 hours of incubation (*Figure 4.12c*, Panel B).

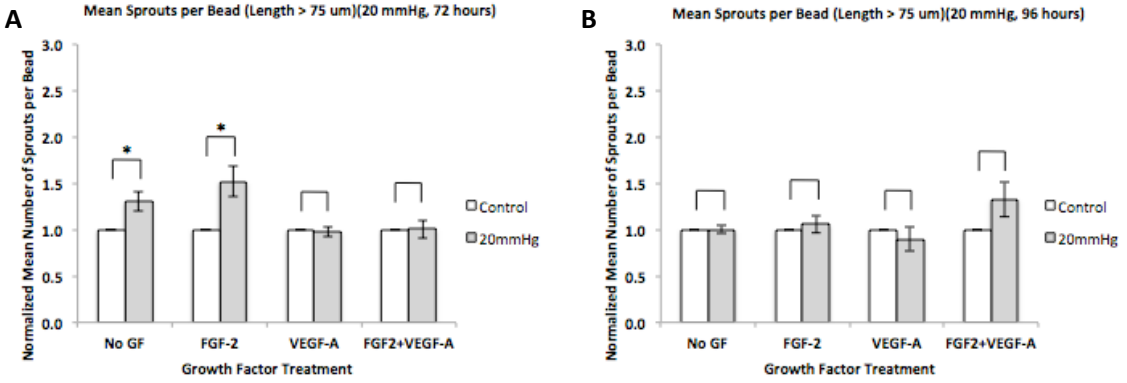

***Figure 4.12d* – Graphs displaying the comparison of the mean number of tubes (i.e., sprouts) greater than 75 µm between control (0 mmHg) and 20 mmHg pressure-exposed cultures within each treatment group after 72 hours (Panel A) and 96 hours (Panel B) of incubation. Bars in each graph above represent the mean-fold change in the number of tubes greater than 75 µm per bead ± standard error of cultures maintained under each treatment; N=4. Comparisons were made using a paired Student's t-test (*p < 0.05).**

Exposure to 20 mmHg sustained hydrostatic pressure for 72 hour also elicited significant increases in the number of tubes greater than 75 µm under the "no growth factor" (No GF) and FGF-2 treatment groups (*Figure 4.12d*). However, after 96 hours of exposure, pressurization produced no effect on the formation of sprouts greater than 75 µm for all conditions tested in the present study (*Figure 4.12d*).

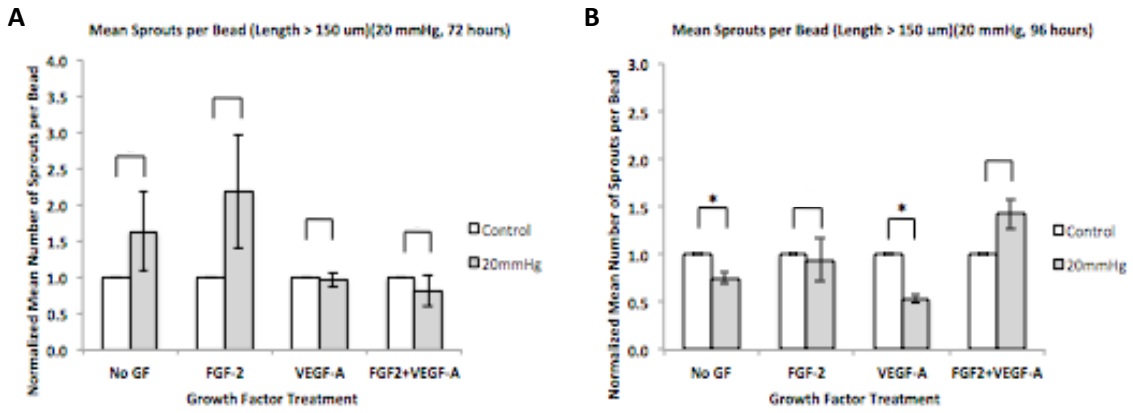

***Figure 4.12e* – Graphs displaying the comparison of the mean number of tubes (i.e., sprouts) greater than 150 µm between control (0 mmHg) and 20 mmHg pressure-exposed cultures within each treatment group after 72 hours (Panel A) and 96 hours (Panel B) of incubation. Bars in each graph above represent the mean-fold change in the number of tubes greater than 150 µm per bead ± standard error of cultures maintained under each treatment; N=4. Comparisons were made using a paired Student's t-test (*p > 0.05).**

As shown in *Figure 4.12e*, exposure to 20 mmHg pressure for 72 hours had no significant effect on the formation of sprouts greater than 150 µm in length compared to cells maintained under control pressure conditions. After 96 hours, significant ($p < 0.05$) reductions in the number of tubes greater than 150 µm in length were observed for BAE bead cultures in the absence or presence of VEGF-A (*Figure 4.12e*). There were no significant differences observed when cells were either exposed to pressure or maintained under control conditions in the presence of either the FGF-2 or FGF2 + VEGF-A group (see *Figure 4.12e*).

Figure 4.12f shows the results obtained when measuring mean sprout (or tube) length per bead. Only BAEC cultures stimulated with FGF-2 + VEGF-A exhibited a significant change ($p = 0.019$) in mean tube length (*Figure 4.12d*, Panel A). After 96 hours, significant ($p < 0.05$) changes in mean tube length were observed between cells either exposed to pressure or maintained under control condition in the presence of FGF-2 and VEGF-A (see *Figure 4.12d*, Panel B).

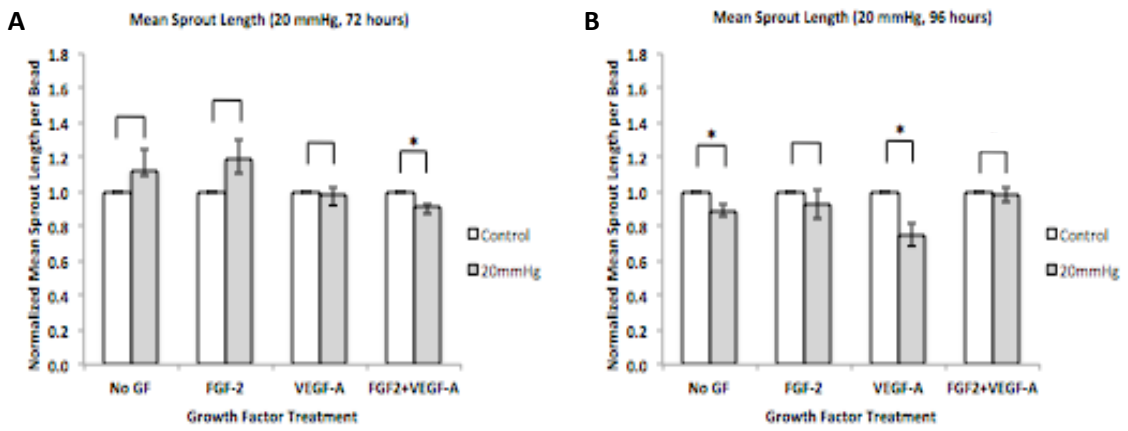

***Figure 4.12f* - Graphs displaying the comparison of mean tube (i.e., sprout) length between control (0 mmHg) and 20 mmHg pressure-exposed cultures within each treatment group after 72 hours (Panel A) and 96 hours (Panel B) of incubation. Bars in each graph above represent the mean-fold change in the mean tube length per bead ± standard error of cultures maintained under each treatment; N=4. Comparisons were made using a paired Student's t-test (*p > 0.05).**

Thus, it appeared that pressure had a modest effect on the mean length of sprouts formed by BAE bead cultures in both the absence and presence of growth factors.

4.13. Effects of a 40 mmHg Sustained Hydrostatic Pressure on BAEC Tubulogenesis

The results in this section display the effects of exposure to 40 mmHg hydrostatic pressure levels in the absence and presence of the pro-tubulogenic growth factors FGF-2 and VEGF-A on BAEC tubulogenesis. *Figure 4.11e* and *Figure 4.11f* display representative images of beads with BAE cells either maintained under control conditions or exposed to 40 mmHg hydrostatic pressures in the absence or presence of either FGF-2, VEGF-A or both FGF-2 + VEGF-A for 72 and 96 hours, respectively.

As shown in *Figure 4.13a* and *Figure 4.13b* (following page), sprout formation was observed under every media and pressure condition tested, both after 72 and 96 hours in culture. The figures that follow in the next page display the results of the tube formation assay using a 40 mmHg pressure.

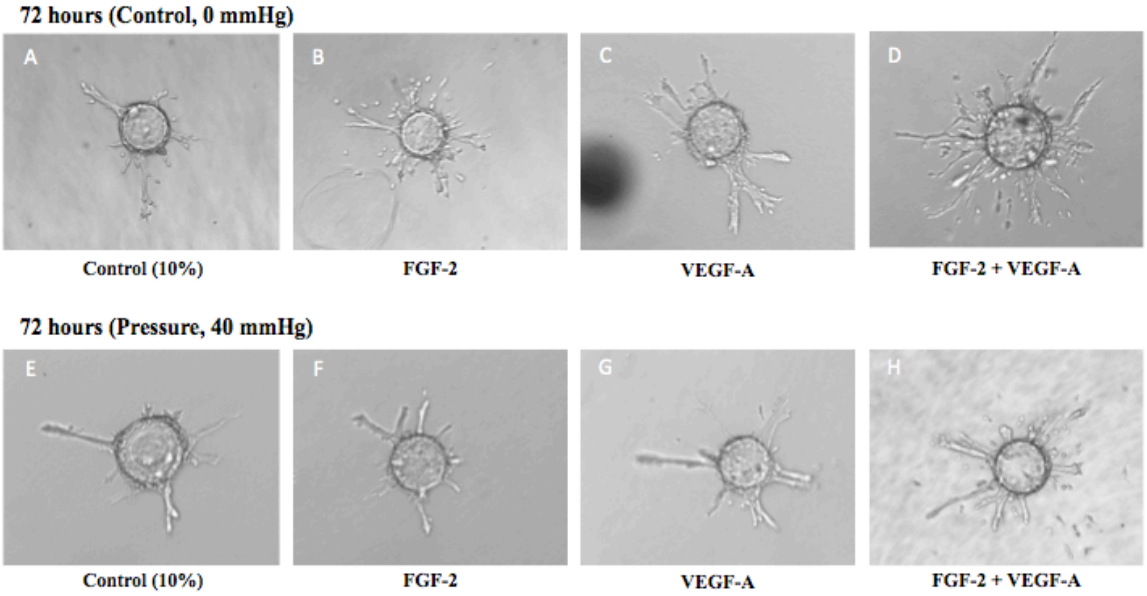

***Figure 4.13a* - Representative images of BAEC on Cytodex3^{TM} beads suspended in collagen gels and maintained under atmospheric (control) or 40 mmHg pressure conditions for 3 days. One representative image is provided for each growth factor treatment at either the control (0 mmHg) or 40 mmHg pressure condition. Images were acquired under 100X magnification. No significant differences were observed after 3-day exposure to 40 mmHg.**

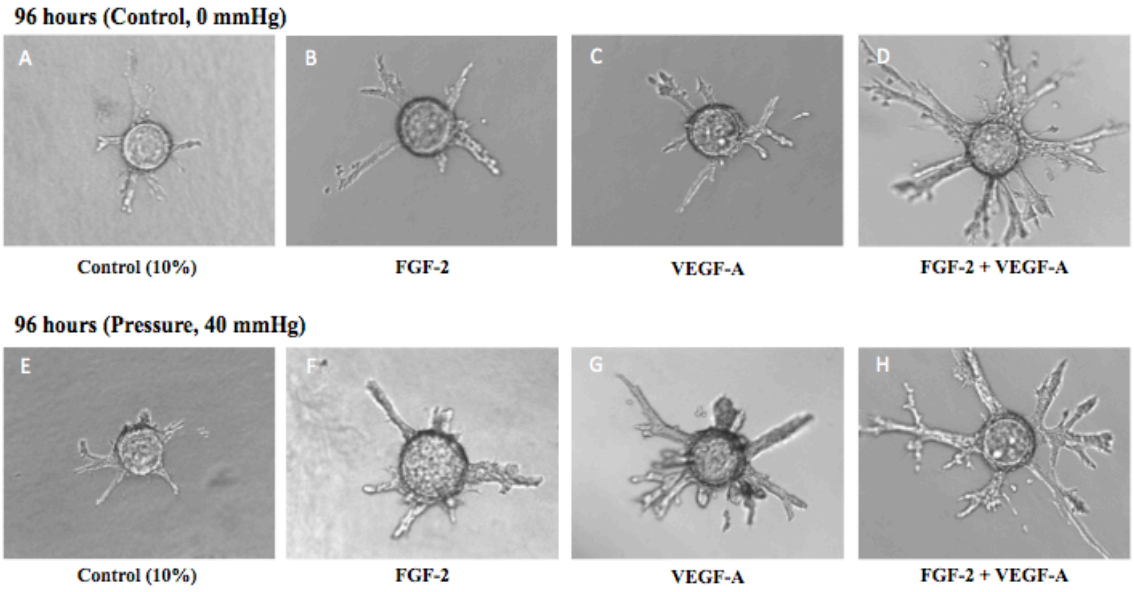

Figure 4.13b - **Representative images of BAEC on Cytodex™ beads suspended in collagen gels and maintained under atmospheric (control) or 40 mmHg pressure conditions for 4 days. One representative image is provided for each growth factor treatment at either the control (0 mmHg) or 40 mmHg pressure condition. Images were acquired under 100X magnification. The only significant difference between cultures maintained under control pressure and cultures exposed to 40 mmHg for 96 hours was the total number of sprouts (greater than 50 µm) in cultures maintained in media containing 2.5 ng/mL FGF-2 + 2.5 ng/mL VEGF-A (Panel D/H).**

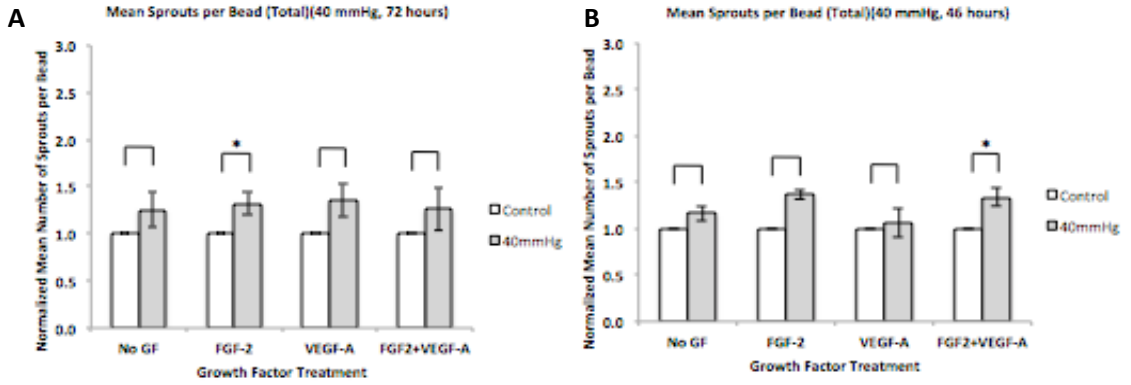

Figure 4.13c - **Graphs displaying the comparison of the mean number of tubes (i.e., sprouts) greater than 50 µm between control (0 mmHg) and 40 mmHg pressure-exposed cultures within each treatment group after 72 hours (Panel A) and 96 hours (Panel B) of incubation. Bars in each graph above represent the mean-fold change in the number of tubes greater than 50 µm per bead ± standard error of cultures maintained under each treatment; N=4. Comparisons were made using a paired Student's t-test (*p > 0.05).**

Figure 4.13c (previous page) displays the results when cultures were exposed to a 40 mmHg sustained hydrostatic pressure and the total number of tubes was counted. In this case, only BAEC bead cultures exposed to pressure in the presence of FGF-2 for 72 hours or FGF-2 + VEGF-A for 96 hours exhibited significant increases in total sprout numbers. When only counting tubes or sprouts greater than 75 µm in length, there was no statistically significant effect of pressure on sprout formation for all growth factor conditions.

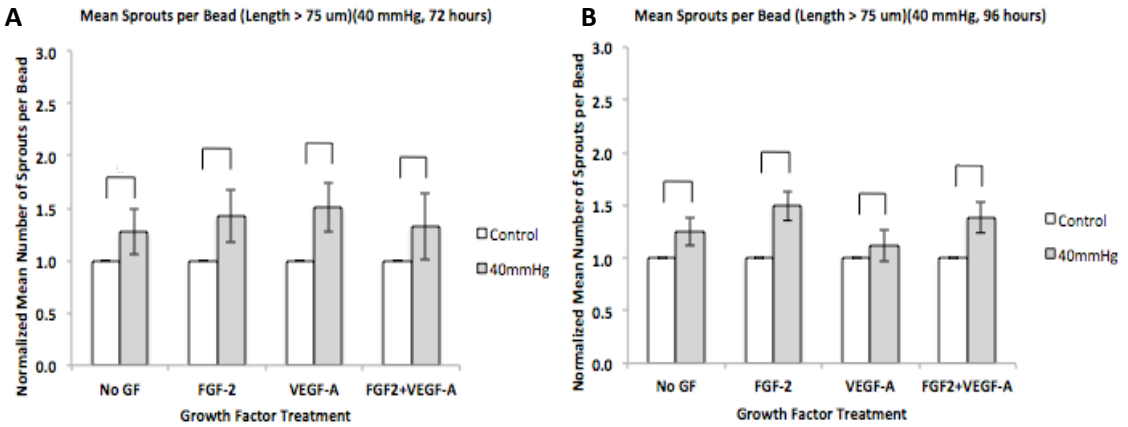

***Figure 4.13d* - Graphs displaying the comparison of the mean number of tubes (i.e., sprouts) greater than 75 µm between control (0 mmHg) and 40 mmHg pressure-exposed cultures within each treatment group after 72 hours (Panel A) and 96 hours (Panel B) of incubation. Bars in each graph above represent the mean-fold change in the number of tubes greater than 75 µm per bead ± standard error of cultures maintained under each treatment; N=4. Comparisons were made using a paired Student's t-test (*p > 0.05).**

Similarly, no significant differences in the number of tubes greater than 150 µm were elicited by subjecting cultures to a 40 mmHg sustained hydrostatic pressure (*Figure 4.13e*).

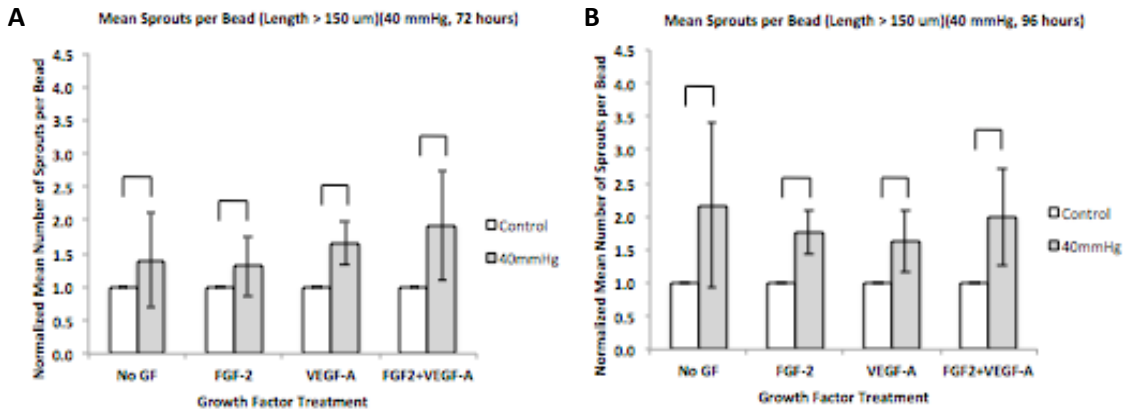

***Figure 4.13e* - Graphs displaying the comparison of the mean number of tubes (i.e., sprouts) greater than 150 µm between control (0 mmHg) and 40 mmHg pressure-exposed cultures within each treatment group after 72 hours (Panel A) and 96 hours (Panel B) of incubation. Bars in each graph above represent the mean-fold change in the number of tubes greater than 150 µm per bead ± standard error of cultures maintained under each treatment; N=4. Comparisons were made using a paired Student's t-test (*p > 0.05).**

Combined, these results provided evidence that exposure to BAEC tubulogenic activity is relatively insensitive to a 40 mmHg pressure stimulus. *Figure 4.13f* on the following page shows the results when mean tube lengths per bead were compared within growth factor treatment groups. No significant differences in mean tube length were detected for bead cultures either maintained under control conditions or exposed to 40 mmHg pressure for 72 or 96 hours for all media conditions tested.

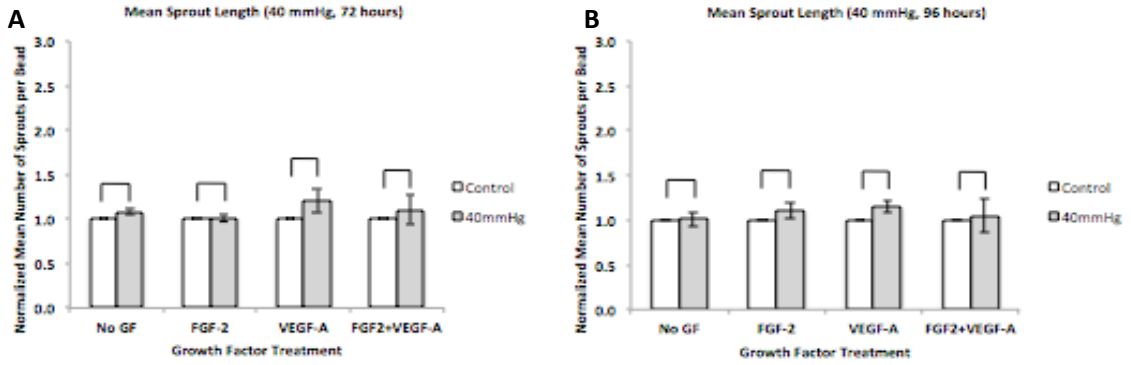

***Figure 4.13f* - Graphs displaying the comparison of mean tube (i.e., sprout) length between control (0 mmHg) and 40 mmHg pressure-exposed cultures within each treatment group after 72 hours (Panel A) and 96 hours (Panel B) of incubation. Bars in each graph above represent the mean-fold change in the mean tube length per bead ± standard error of cultures maintained under each treatment; N=4. Comparisons were made using a paired Student's t-test (*p > 0.05).**

5. Discussion

The research presented in this thesis is the first *in vitro* investigation of the hypothesis that sustained hydrostatic pressure exposure is a magnitude-dependent modulator of early endothelial sprout formation. The foundations of this study were the known effects of pressure on endothelial cell proliferation and morphology suggestive of a pro-tubulogenic phenotype. Based on the established links between pressure and 2-D cultures of endothelial cells, this study elucidates the effects of pressure on endothelial cells in a 3-D environment.

5.1. Physiological Relevance of the Hydrostatic Pressures Used

Within the human body, endothelial cells may be exposed to sustained hydrostatic blood pressures or pulsatile pressures that exhibit complex waveforms that vary in

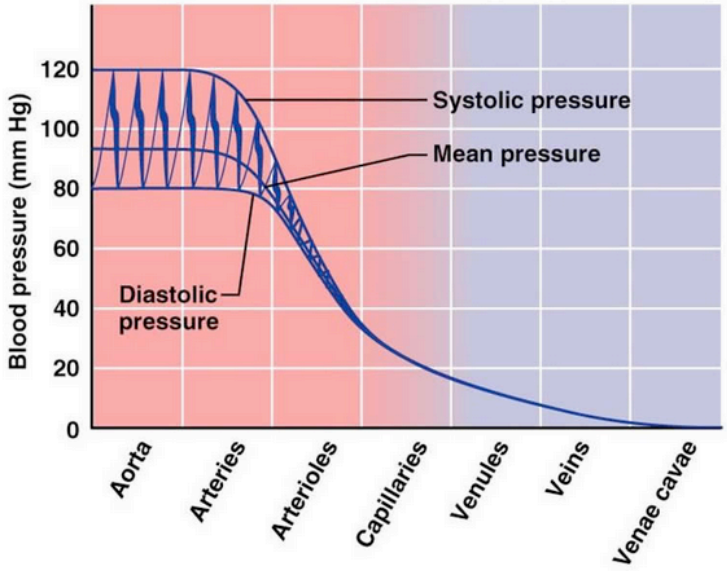

***Figure 5.1a* – Blood pressure levels throughout the circulatory system. As shown in the figure, capillary blood pressure ranges from approximately 18 mmHg to 38 mmHg. (*available at* http://classes.midlandstech.edu/carterp/Courses/bio211/chap19/chap19.html)**

amplitude and frequency depending on a particular cell's location in the vascular tree. The pressures used in this study, however, were consistent with the physiological pressures to which microvascular endothelial cells are exposed.[2] As shown in *Figure 5.1a* on the previous page, capillary pressures vary between approximately 18 mmHg and 38 mmHg. *Figure 5.1a* also shows that the pulsatile component of circulatory blood pressure found in the aorta and large arteries is largely eliminated by the time blood reaches the capillaries.

The two pressures examined in this thesis were 20 mmHg and 40 mmHg hydrostatic pressures—pressures similar to those that microvascular endothelial cells would be exposed *in vivo.* The 40 mmHg is slightly above that which would be encountered in the microcirculation under normal physiological conditions, however, pressures at this level or greater may be present under pathological conditions such as in the tumor interstitium, due to traumatic soft tissue injury, and during intraocular hypertension. These pressures are also similar to pressures used in previous studies[3] [12, 14], which allowed for comparison of results to verify the experimental setup used in this study.

5.2. Selection of Cell Type and Three-Dimensional Matrix Composition

The cell type selected for the experiments conducted herein was the bovine aortic endothelial cell (BAEC). This cell type was selected as it is a well-characterized, stable

[2] Capillary endothelial cells are exposed to pressures in the range of 18 mmHg to 40 mmHg under normal conditions. By the time blood reaches the capillaries, however, all or nearly all pulsatility in pressure has ceased. (*available at* http://classes.midlandstech.edu/carterp/Courses/bio211/chap19/chap19.html)

[3] *Sumpio et al.* (1994) used pressures 40-120 mmHg to investigate the effects of sustained hydrostatic pressures on endothelial cell proliferation and morphology. *Acevedo et al.* (1993) also explored endothelial cell responses to pressures of 1.1 and 7.4 mmHg. Both previous studies used pressures that are considered physiologically similar to the pressures studied in this section.

cell type that has been used in similar experiments in previous studies [8, 12, 29, 41]. The study by *Sumpio et al.* (1994) showed up-regulation of BAEC proliferation in response to sustained hydrostatic pressures, with possible implication of FGF-2 as the growth factor that transduced this effect [12]. The implication of FGF-2 as a modulating factor for endothelial cell proliferation is also supported by the study by *Acevedo et al*. (1993), which identified the pressure-induced release of FGF-2 by bovine pulmonary artery endothelial cells from intracellular stores with a concomitant increase in cell proliferative proliferation rates [14]. Both the individual and combined effects of FGF-2 and sustained hydrostatic pressures were examined in this study and are discussed further in **Section 5.4**.

BAEC were also selected for their efficacy in 3-D microcarrier cultures. Though 2-D assays are effective for studying certain tubulogenesis-related cellular activities in isolation, such as proliferation or migration, they do not mimic the *in vivo* 3-D configuration associated with tube formation [7, 8]. BAEC have proven to be particularly useful for such studies. For 3-D studies employing microcarrier bead endothelial cell cultures, complete bead coverage is essential to create an accurate model of *in vivo* sprouting angiogenesis in a microcarrier-based *in vitro* angiogenesis assay [8]. This is necessary to ensure that tubulogenic sprouting originates from confluent endothelial monolayers, similar to that which occurs in the *in vivo* tissue environment [8].

As described in the study by *Dietrich and Lelkes* (2006), BAEC both consistently exhibited high attachment rates to Cytodex3^{TM} microcarrier beads and were the only cell type, out of those tested (e.g., human aortic endothelial cells (HAEC), transformed human microvascular endothelial cells (HMEC-1), human microvascular endothelial cells

(HMVEC)), to form a confluent monolayer on bead surfaces within two to four days [8]. Specifically, with constant agitation during cell seeding (dynamic seeding), it has been shown that BAEC consistently form confluent monolayers on Cytodex3^{TM} microcarrier beads [8, 42]. As shown in *Figure 4.3a* in **Section 4.3**, the protocol used herein consistently produced confluent BAEC monolayers on Cytodex3^{TM} microcarrier beads.

Though the ability of BAEC to form monolayers on microcarrier beads is robust, the usefulness of large-vessel endothelial cells in modeling angiogenesis has been indeterminate [8]. However, BAEC, even though derived from the bovine aorta, have been shown to form capillary-like structures *in vitro* [8]. BAEC tube formation can be enabled by using the appropriate experimental setup, as demonstrated by several studies [8, 29, 43]. The ability of BAEC to form capillary-like tubular structures is also demonstrated by the present study as shown in **Section 4.11**.

The 3-D matrices for the migration and tube formation studies conducted herein were comprised of Type I collagen hydrogels. Two extracellular matrix materials are predominantly used in 3-D tubulogenic assays: collagen and fibrin. Collagen was selected as the extracellular matrix of choice as cells embedded in this type of gel tend to exhibit a phenotype typical of that found *in vivo* while cells maintained in fibrin tend to exhibit cellular activity associated with tubulogenesis that is a technical artifact of their exposure to fibrin [8]. Moreover, fibrin matrices intuitively model clotted tissues during wound healing processes.

5.3. Experimental Setup for Pressure Experiments

The experimental setup used in the present study was adapted from those used in previous studies by *Shin et al.* (2002) [31] and *Acevedo et al.* (1993) [14]. The pressure

system used in the present study was designed and calibrated to expose endothelial cells grown in standard multi-well tissue culture plates in either two- or 3-D configurations (described in **Section 3.8**) to hydrostatic pressures above atmospheric while maintaining a parallel culture of cells under standard pressure (i.e., 0 mmHg above atmospheric), but otherwise, similar experimental conditions. Whether cells were grown on a 2-D rigid polystyrene substrate or on the surface of a Cytodex3^{TM} bead embedded in collagen gel, the cells were directly exposed to a pressure level of 20 mmHg or 40 mmHg pressure in the absence of pressure-induced fluid flow. The only source of pressure variation was the depth to which Cytodex3^{TM} beads were submerged in the culture media, which was minimal (between 1 – 2 mmHg).

The system was capable of maintaining cultures under pressure and standard cell culture conditions for up to 6 days.[4] In the experiments conducted herein, however, pressurized and control cultures were maintained in humidified 37 degree C, 5% CO2/95% air environments for up to 4 days. The pressurized and control chambers were maintained in parallel with each chamber located in the same incubator and receiving the same constant supply of humidified 5% CO2 gas mixture. The combination of the resistance valve and relief valve described in **Section 3.5** allowed the control chamber to be maintained at atmospheric pressure (0 mmHg) while still receiving a constant supply of 5% CO2/95% air gas mixture. The pressurized chambers were maintained at either 20 mmHg or 40 mmHg sustained hydrostatic pressures by using the variable resistance valve on the 5% CO2 gas supply tank and the water column pressure head source to set the pressure for each experiment.

[4] The system is capable of maintaining cultures under pressure for longer periods of time, but 4 days was the longest that any experiment conducted as a part of this study was run.

The system employed for the research discussed herein is also capable of generating pulsatile pressures within a certain limits of pulse pressure magnitude and frequency. However, there is an upper limit to pulsatile pressure magnitudes to which cell cultures are exposed. The limitation on the magnitude of the pulse pressure is due to the maximum output force of the linear actuator that drives the bellows. If a more powerful linear motor were implemented, the system would be able to generate greater pulse pressures. The need for such measures will be addressed in the future when studies that expose cells to pulsatile pressures are conducted.

In each study performed, BAEC maintained under either pressurized or control conditions remained viable throughout the entirety of the study and exhibited normal cellular functions such as proliferation and morphological changes. Based on these observations, the experimental system and pressures used in this study neither killed nor damaged the cells over the duration of the experiments performed.

5.4. Confirmation of Cellular Responses of BAEC Grown in Two-Dimensional Culture to Sustained Hydrostatic Pressures

Pressure Upregulates Proliferation at 20 mmHg, but not 40 mmHg, After Three Days of Exposure

BAEC were cultured on 2-D tissue culture-treated polystyrene surfaces in cell culture flasks and multi-well cell culture plates. Microscopic imaging revealed that the cells attached and proliferated in the same manner demonstrated by other studies [44]. *Figure 4.1a* in **Section 4.1 – Culture of BAEC on Two-Dimensional Substrates** shows BAEC attached to the culture surface after seeding and overnight incubation (left image)

as well as after several days in culture (right image). The same process that yielded the images in *Figure 4.1a* was used each time BAEC were cultured on 2-D surfaces with similar results being observed.

Experiments were performed to verify the ability of the pressure exposure to elicit a proliferative response by the BAEC tested in the present study. *Acevedo et al.* (1993) showed that as little as 1 ng/mL exogenous basic fibroblast growth factor (FGF-2 or bFGF) upregulates bovine pulmonary artery endothelial cell (BPAE) proliferation and causes cytoskeletal reorganization [14, 40]. An experiment was performed as a part of this study to determine if exogenous FGF-2 would produce the expected increase in cell density when cells were grown under control conditions in the pressure system chambers. As shown in *Figure 4.6b*, cells grown in media supplemented with 2.5, but not 1, ng/mL FGF-2 also elicited a significant ($p = 0.017$) increase in cell density. The average fold-change observed in cells grown in media containing 2.5 ng/mL exogenous FGF-2 was approximately 2.0 times the density of controls. This is consistent with the results shown in the study by *Acevedo et al.* (1993), which showed comparable increases in cell density[5] [14]. It should, however, be noted that BAEC exposed to 1 ng/mL did not exhibit a statistically significant increase in proliferation. This discrepancy between the results of the present study and those of *Acevedo et al.* (1993) [14], however, may have been due to cell type differences (bovine aortic versus pulmonary artery endothelium).

The present study also verified that the pressure system used to assess the tubulogenic activity of BAEC was capable of eliciting a proliferative responses in these cells which were similar to those reported by previous studies. *Sumpio et al.* (1994)

[5] The experiment conducted in the study by *Acevedo et al.* (1993) showed an approximate fold-change of 1.8-2.0 times that of cells grown under control conditions (no FGF-2). It should be noted that their study employed bovine pulmonary endothelial cells (BPAEC) maintained in media containing 20% FBS.

showed that cells exposed to a 40 mmHg sustained pressure showed a significant increase in cell number after 9 days in culture; cells exposed to an 80 mmHg sustained pressure showed a significant increase in cell number after 7 days in culture; and cells exposed 120 mmHg showed a significant increase in cell number after 3 days [12].[6] In another similar experiment, *Acevedo et al.* (1993) showed significant increases in the cell numbers of BPAE grown under both 5 cmH_2O (1.1 mmHg) and 10 cmH_2O (7.4 mmHg) sustained hydrostatic pressures after 3, 5, and 7 days in culture. As shown in *Figure 4.6b*, cells maintained under a 20 mmHg, but not 40 mmHg, sustained pressure for 3 days showed a significant ($p = 0.018$ and $p = 0.077$, respectively) increase in cell density. The same experiment was performed with the addition of 1 ng/mL FGF-2 to the supernatant media for both control and pressurized cultures. With the addition of FGF-2, significant increases in cell density were observed for both 20 mmHg and 40 mmHg sustained pressures after 72 hours ($p = 0.049$ and $p = 0.042$, respectively). Interestingly, a pressure-induced proliferative response to 40 mmHg sustained pressure was not observed in the absence of FGF-2. In the study by *Sumpio et al.* (1994), exposure of BAEC to 40 mmHg did not exhibit a significant increase in cell number until after 9 days in culture. In the present study, cells were exposed to a 40 mmHg sustained pressure for only 3 days. Thus, the effect of a 40 mmHg pressure may take longer than 3 days to become apparent. It is clear, though, that exposure to 40 mmHg for 3 days does not appear to suppress the pro-proliferative effect of FGF-2. As shown in *Figure 4.6a* in **Section 4.6**, cells exposed to 40 mmHg and maintained in media containing 1 ng/mL FGF-2 exhibited a significant ($p = 0.042$) increase in cell density as compared with controls maintained under atmospheric

[6] The study by *Sumpio et al.* (1994) also showed that changes in cell number were not due to changes in pH or pCO_2.

(0 mmHg) pressure. Thus pressure stimulation may serve to sensitize BAEC to FGF-2 stimulation. This is consistent with the report of *Shin et al.* (2002) proposing that exposure to pressure facilitates FGF-2/FGFR-2 interactions [45].

Pressure Induces Morphological Changes in Endothelial Cells

It has been shown in several previous studies that exposure of endothelial cells to sustained hydrostatic pressure results in morphological changes and cytoskeletal reorganization [12, 14]. *Sumpio et al.* (1994) showed that endothelial cells exposed to static pressures became "more elongated and ellipsoidal in shape, but their long axes were randomly oriented" after exposure [12]. *Acevedo et al.* (1993) showed that pressure exposure induced "morphological, proliferative, and bi-layering responses" in endothelial cells, which consisted of a transformation from "a polygonal, 'cobblestone' arrangement to an elongated, randomly oriented cell cluster morphology" [14]. Microscopy results of the present study also indicate that cells exposed to pressure exhibit morphological changes (i.e., cell elongation) similar to those observed in previous studies. In the representative images in *Figure 4.6c* in **Section 4.6**, cells exposed to a 40 mmHg sustained pressure for 3 days appeared to elongate in randomly oriented directions as described in earlier studies. This response was also observed in BAEC cultures exposed to 20 mmHg (data not shown), but it is interesting to note that, even though exposure to 40 mmHg for 72 hours did not elicit a significant increase in cell density, it did elicit morphological changes.

MAZ-51 Inhibitor Blocks Increased Proliferation in Response to Pressure

It has been difficult to ascertain the role of VEGFR-3 expression in vascular endothelial tubulogenic processes because its ligand, VEGF-C, also binds strongly to

VEGFR-2 [29]. However, BAEC have been shown to express both VEGFR-2 and VEGFR-3. [29]. It has been shown that BAEC cultures uniformly express VEGFR-2, for which autophosphorylation is induced by binding of the VEGF-A, VEGF-C, VEGF-D, or VEGF-E ligands [29]. In contrast, studies have shown that expression of VEGFR-3 by vascular endothelial cells (specifically BAEC) is not uniform, but rather, heterogeneous [29]. *Persaud et al.* conducted a study similar to the one discussed herein in which BAEC were grown in 3-D collagen gels and exposed to exogenous growth factors and inhibitors [29]. They reported that BAEC gel invasion and tube formation could be induced using a proteolytically-modified VEGF-C analog, which was established as a ligand for both VEGFR-2 and VEGFR-3 (*Joukov et al.*, 1997; *Tille et al.*, 2003) [29, 46]. It was observed that invasive and tubulogenic responses of BAEC could be completely inhibited by antagonistic antibodies to VEGFR-2 when the inducing-agent was VEGF-A, which is not a ligand for VEGFR-3 [29]. When the exogenous inducing-agent was the VEGF-C analog, which binds to both VEGFR-2 and VEGFR-3, the response "could only be inhibited by a maximum of 67% by antagonizing VEGFR-2 [29, 46]. Therefore, the response must have been elicited through the VEGFR-3 pathway, indicating that some BAEC expressed VEGFR-3. *Persaud et al.* (2004) also analyzed BAEC VEGFR-3 expression using fluorescence-activated cell sorting (FACS) to determine VEGFR-3 expression levels in BAEC populations and determined that VEGFR-3-positive and VEGFR-2-negative BAEC subpopulations were approximately equal (i.e., VEGFR-3 expression will be observed in 50% of any given BAEC population) [29].

Having established that BAEC do express VEGFR-3, the present study determined whether its ligand, VEGF-C, plays a role in transducing pressures. It has been

shown that exposure of human vascular endothelial cells to cyclic pressure result in significant increases in proliferation that is mediated by VEGF-C [31]. In fact, *Shin et al.* (2002) showed that the VEGF-C gene in human umbilical vein endothelial cells (HUVEC) maintained under a 60/20 mmHg pulsatile pressure was the most highly upregulated gene [31]. Notably, it was established that HUVEC proliferation was upregulated in response to a 60/20 mmHg pulsatile pressure, but when HUVEC were incubated with mouse monoclonal VEGF-C antibody, this response was completely blocked [31]. Thus, VEGF-C appeared to serve as an autocrine signaling factor in the proliferative responses of endothelial cells to pressure stimulation.

In the present study, BAEC were incubated with varying concentrations of MAZ-51 and exposed to a 20 mmHg sustained hydrostatic pressure that had been shown to stimulate a statistically significant increase in BAEC proliferation (See **Section 4.6**). MAZ-51 is an indolinone, a class of molecules that have the ability to inhibit the activity of receptor tyrosine kinases, that potently blocks ligand-induced autophosphorylation of VEGFR-3 [47]. MAZ-51 also inhibits VEGFR-2 autophosphorylation, although less strongly [47]. Based on these properties, MAZ51 was used to explore the possibility that VEGFR-3 plays a role in the proliferative responses of endothelial cells to pressure.

As expected, exposure of BAEC to 20 mmHg sustained pressure produced a statistically significant ($N=5$, $p < 0.05$) increase in cell density as compared with controls (0 mmHg) in the absence of MAZ-51. Interestingly, exposure to 20 mmHg on average enhanced BAEC densities in the presence of both 1 μM and 5 μM concentrations of MAZ-51, although these effects were not statistically significant. However, pressure-dependent increases in cell density was completely blocked at concentrations of 10 μM

MAZ-51 or greater. Notably, VEGFR-2 blockade requires concentrations MAZ51 greater than 50 μM [47]. Thus, it would appear that VEGFR-3 is involved in the transduction of the bovine aortic endothelial cell response to sustained hydrostatic pressure.

Increased VEGF-C and VEGFR-3 Expression in Response to Sustained Pressure Exposure

To explore the possibility that pressure influences endothelial proliferation via the autocrine actions of VEGF-C, the present study assessed VEGF-C and VEGFR-3 expression by BAEC in response to exposure to sustained pressure. As shown in *Figure 4.7b* in **Section 4.7**, a significant increase was observed in BAEC expression of VEGF-C after exposure to 20 mmHg for 3 days. Exposure to both 20- and 40-mmHg sustained pressures produced significant increases in VEGFR-3 membrane expression after 3 days as compared with controls. These results further implicated VEGF-C and VEGFR-3 in the transduction of endothelial responses to sustained hydrostatic pressures. Since VEGF-C and VEGFR-3 have been implicated in vascular cell tubulogenesis [29, 30, 33, 38] and because the proliferative responses of endothelial cells to pressure appears to signal through the VEGF-C/VEGFR-3 pathway, it follows that pressure may stimulate endothelial tubulogenic activity. Thus, the present study examined the effects of pressure on two early tubulogenic processes: migration/matrix invasion and tube/sprout formation.

5.5. Investigation of the Effects of Sustained Pressure on Endothelial Migration and Invasion

The bi-layer gel study described in **Section 3.8** was employed to determine the effect of sustained hydrostatic pressures on the migratory and invasive behavior of

endothelial cells. Migration and invasion are but two cellular activities comprising the angiogenic cascade [22]. A scientific contribution of the present study was the development of a two-layer gel assay to assess the effects of pressure on endothelial migration in a 3-D format. Along this line, it was determined that endothelial cells grown on Cytodex3^{TM} tended to migrate from the bead into the surrounding gel within the plane between two distinct gel layers co-planer with the mid-plane of the bead as shown in *Figure 5.4a*.

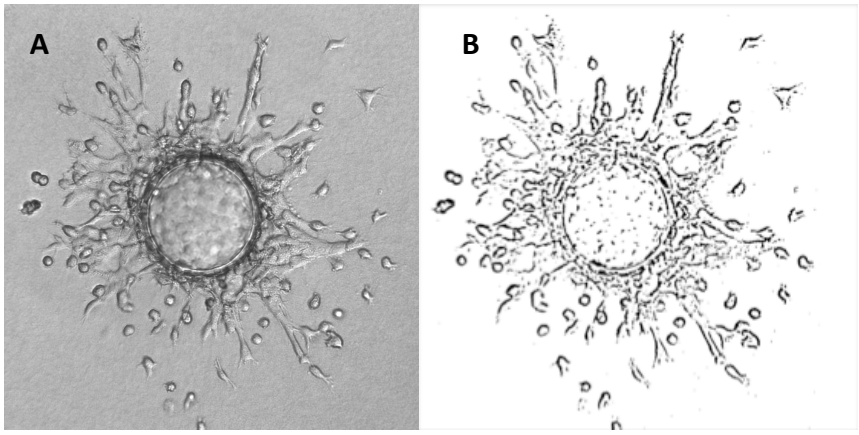

***Figure 5.5a* – Representative images of BAEC migrating from a Cytodex^{TM} bead in the bi-layer gel configuration. Shown are a phase-contrast image of a single bead with invading cells (Panel A) and the same image after processing using the InvasiQuant ImageJ macro. Cells migrated from the surface of the bead on the plane between the top and bottom gel layer, which is co-planar with the mid-plane of the bead. This allowed for all cellular activity to be captured on one microscopic focal plane and consistent image transformation using the InvasiQuant ImageJ macro. Images were captured at 100X magnification.**

Using this method, migratory and invasive activity of endothelial cells was compared between various pressures and growth factor treatments. To confirm the utility of this approach to assess endothelial migratory responses to pro-tubulogenic stimuli, the effect of FGF-2 and VEGF-A on endothelial migration and invasion into the extracellular space was assessed. Both of these molecules have been previously shown to enhance endothelial migration [7, 22]. Using a novel two-layer configuration and analysis method (see **Section 3.8**), the present study showed that both FGF-2 and VEGF-A induced

significant increases ($p < 0.05$) in BAEC migration and invasion between the two collagen gel layers. It should be noted that the effect of VEGF-A, however, was not observed until after 96 hours in culture (see *Figure 4.8b*) suggesting that FGF-2 was a more potent migratory stimulus. Nonetheless, these results collectively indicated the utility of the two-layer gel assay developed in the present study to assess the effects of pro-tubulogenic stimuli in modulating BAEC migration.

Interestingly, the only significant difference ($p < 0.05$) in migratory activity of BAEC in response to pressure observed in the present study was a decrease in the migration of cells maintained without growth factor supplementation under 40 mmHg for 96 hours. In other words, exposure to 20 or 40 mmHg sustained pressure for up to 96 hours did not enhance BAEC migration. It is possible that the image analysis method used to quantify the migration of BAEC populations was not sensitive enough to detect an effect of pressure on endothelial migration. A similar quantitative method has been used in previous studies to quantify angiogenesis [48]. *Boettcher et al.* (2010) developed a method for quantifying tube formation in mouse aortic ring experiments in which, after image processing, capillary-like sprouts are displayed in black pixels, which represent the area covered by invading cells that can be quantified easily by counting the number of black pixels [48]. Gray-scale images were processed by applying a high-pass filter to remove low frequency artifacts (e.g., structures out of focus or background inhomogeneities) and preserve high frequency gradients (i.e., capillary-like structures), then converting the image to a thresholded, binary-encoded image to allow for pixel-counting [48]. The method used herein to analyze images of BAEC invasion was adapted from this approach, as described in **Section 3.11**.

Since previous studies suggested that pressure sensitizes endothelial proliferative responses to growth factor (e.g., FGF-2) stimulation, endothelial migration responses to pressure were also examined in the presence of pro-tubulogenic growth factors. Though FGF-2 (bFGF) and VEGF-A operate through independent pathways, both have been implicated in the stimulation of endothelial migration [33]. FGF-2 and VEGF-A, in isolation, enable similar cellular functions including migration and each factor is essential for endothelial tubulogenesis. However, they likely affect tubulogenesis at different times during the process [22]. In combination, FGF-2 and VEGF-A have a synergistic affect on cell invasion and tube formation [22].

Previous studies have shown that FGF-2 is capable of inducing both cell mitogenesis and cell mobility [34]. FGF-2 binding activates a dual transduction pathway, with one pathway leading to a migratory phenotype and the other pathway leading to cell proliferation [34]. FGF-2 has been implicated in chemotactic endothelial cell migration [49]. Specifically, FGF-2 has been shown to drive endothelial invasion into collagen matrices by upregulating the expression of the plasminogen activators and matrix proteases necessary for dissolution of the basement membrane prior to migration and sprouting [32].

VEGF-A (also referred to as VEGF) is the pro-angiogenic monomer that binds to the VEGFR-1 and VEGFR-2 receptors. VEGF-A is a potent angiogenic agent that regulates *all* of the keys steps of the angiogenic process, including endothelial cell proliferation and migration [49]. Though VEGFR-1 is the high-affinity receptor for VEGF-A, the migratory response of endothelial cells is regulated by the binding of VEGF-A to VEGFR-2 [49].

It has also been reported that VEGF-C, which binds to both VEGFR-2 (low affinity) and VEGFR-3 (high affinity) in BAEC, induces endothelial migration in collagen matrices [29, 50]. Moreover, BAEC migration induced by exogenous VEGF-C can be completely blocked by the inhibition of VEGFR-3 [29]. Interestingly, *Persaud et al.* (2004) showed that BAEC migrated towards localized concentrations of a VEGF-C analog; a response that was abrogated in a dose-dependent manner by addition of a VEGFR-3 antagonistic antibody (mAb hF4-3C5) [29]. However, the study by *Persaud et al.* (2004) also revealed that the migratory response to VEGF-C could not be completely blocked by inhibition of binding to VEGFR-2, the low-affinity receptor for VEGF-C [29]. As explained in the study, the most obvious explanation for the increased migratory response of VEGFR-3-expressing BAEC is that the affinity of VEGF-C for VEGFR-3 is about fivefold higher than for VEGFR-2. [29]. Thus, stimulation of VEGFR-3 by VEGF-C is likely to be stronger and more sustained than that of VEGFR-2 [29]. Even though the expression of VEGFR-3 in normal cultures of BAEC is approximately 50% [29], the high-affinity binding of VEGF-C to VEGFR-3 is strongly indicative that the VEGF-C/VEGFR-3 pathway plays a role in BAEC migration and tube formation.

In summary, the methods used herein to quantify migration and invasion were able to detect increases in migration in response to FGF-2 and to VEGF-A under control conditions. As shown in *Figure 4.8b*, after 72 hours, significantly increased ($p > 0.05$) migration was observed in cultures exposed to 2.5 ng/mL FGF-2 as compared with cultures maintained under complete media without added growth factors. After 96 hours under atmospheric pressure (0 mmHg), significant increases in migration were observed in both the FGF-supplemented and VEGF-supplemented cultures as compared with

controls without added growth factor. This provides some evidence that the migration assay and method of analysis are capable of detecting expected changes in endothelial migration. The same methods and analysis were also applied to determine whether 20 or 40 mmHg sustained pressures affect endothelial migration. The only significant difference observed was a decrease in endothelial migration after 96-hour exposure to a 40 mmHg sustained pressure in the absence of added growth factors. Considering that a 40 mmHg sustained pressure was shown as having no significant effect on cellular levels of VEGF-C, the mechanism through which a 40 mmHg sustained pressure suppresses BAEC migration, if at all. It is likely that a more refined experiment and method of analysis may be required to detect subtle changes in endothelial migration.

5.6. Investigation of the Effects of Sustained Pressures on Endothelial Tube Formation

Tube formation experiments were performed according to the protocol in **Section 3.8** through **Section 3.12** in order to confirm the effects of known pro-tubulogenic growth factors on tube formation and to determine the effect, if any, of physiologic sustained pressures on tube formation. Many growth factors have been implicated in endothelial tube formation, however, none more so than those of the FGF and VEGF families. FGF-2 is one of the more studied pro-angiogenic factors and has been shown to be a potent mitogen and chemotactic factor capable of inducing endothelial cells to invade extracellular matrices and form capillary-like structures *in vitro* [17, 32]. FGF-2 has been shown to promote tubulogenesis by eliciting a variety of cellular activities such as cell elongation, proliferation, migration, and protease production and release [14, 22, 29, 32, 33, 49]. FGF-2 release has also been shown to be involved in the responses of endothelial

cells to pressure [14]. Additionally, exposure of endothelial cells to exogenous FGF-2 has been shown to induce autocrine expression of VEGF-A [29].

VEGF-A is also a potent mitogenic factor that is highly-specific to vascular and lymphatic endothelial cells and plays a multifunctional role in both angiogenesis and lymphangiogenesis [38, 51]. The role of VEGF-A in angiogenesis is central as it affects and regulates all of the key steps of the angiogenic (and lymphangiogenic) process [49]. VEGF-A has been shown to induce cell proliferation in both vascular and lymphatic endothelial cells [38, 49]. VEGF-A has also been implicated in the induction of cell survival, cytoskeletal reorganization, migration, tube formation, and branching morphogenesis [38, 49, 51]. Though VEGF-A is functionally essential for endothelial tubulogenesis, its release or expression, however, has not been shown to be affected by pressure exposure.

FGF-2 and VEGF-A were also used in combination in the tube formation experiments as it has been shown that "VEGF-A and FGF-2 synergize in the induction of endothelial cell invasion and tube formation in collagen gels [22]. It has been proposed that VEGF-A may promote early tubulogenic activity whereas FGF-2 might be involved in the later morphogenic and cellular remodeling activities [22]. *Cavallaro et al.* (2001) hypothesized that FGF-2 "triggers" tubulogenesis when VEGF-A is already present in the pericellular environment [22, 37]. *Mandriota and Pepper* (1997) showed that exogenous FGF-2 upregulates membrane expression of VEGFR-2 in BAEC [37]. However, as previously mentioned, basal levels of VEGFR-2 expression are not affected by blocking FGF-2 [37]. Combined, these findings support the possibility that FGF-2 may influence

the activities of endothelial cells under pressure hydrostatic pressures independent of VEGF-A.

Unlike for VEGF-A, VEGF-C expression has been shown to be upregulated by exposure of endothelial cells to pressure stimulation. In fact, the present study showed for the first time that exposure of BAEC to hydrostatic pressures selectively upregulated expression of VEGF-C and its high-affinity receptor for VEGFR-3. VEGF-C has been implicated in the stimulation of both angiogenesis and lymphangiogenesis through the enhancement of endothelial cell proliferation, migration, and tube formation [29, 38]. Interestingly, VEGFR-3 is associated predominantly with lymphangiogenesis, particularly in the developing embryo. Moreover, it has also been shown that both FGF-2 and VEGF-A plays an upstream role in VEGF-C expression by cultured vascular endothelial cells [15]. These factors, taken together, support the notion that the pro-tubulogenic effect of pressure on endothelial cells involves VEGF-C/VEGFR-3 interactions.

***Table 5.6a* – Summary of Significant ($p < 0.05$) Differences between Pressure and Control Cultures.** Summary table of the significant differences in the various tube formation measures between pressure-exposed and control cultures within each growth factor treatment group. Differences in which the measured value of the pressure-exposed group was significantly greater than that of the control group are marked with a plus (+) symbol and those where the pressure-exposed group was significantly less than the control group with a minus (-) symbol. Significant differences were determined by paired Student's t-test where $p < 0.05$ indicated a significant difference.

Summary of Significant Pressure/Control Differences									
		72 Hours				96 Hours			
		No GF	FGF-2	VEGF	FGF+ VEGF	No GF	FGF-2	VEGF	FGF+ VEGF
20 mmHg	Total (> 50	+	+						
	> 75 µm	+	+						
	> 150 µm			-				-	
	Mean Length			-	-			-	
40 mmHg	Total (> 50 µm)		+						+
	> 75 µm								
	> 150 µm								
	Mean Length								

As summarized in *Table 5.6a*, the number of sprouts greater than 50 µm (total) and 75 µm increased after 72-hour exposure to 20 mmHg. Interestingly, exposure to a 20 mmHg sustained pressure for 72 hours increased VEGF-C expression (*Figure 4.9*), VEGFR-3 expression (*Figure 4.9*), and proliferation (*Figure 4.6a, Figure 4.6b*) by BAEC. Previous studies have shown that the endothelial responses to pressure may also involve the upregulation of FGF-2 expression or release [14, 45], which may potentially cause an increase in VEGFR-2 expression. It also possible that pressure-sensitive tube formation involved the sensitivity of endothelial cells to FGF-2 stimulation. As shown in *Figure 4.10a* and *Figure 4.10b*, significant increases were observed in both the untreated and FGF-2 treatment groups after exposure to 20 mmHg for 72 hours as compared to

paired cultures maintained under control (0 mmHg) pressure but otherwise similar growth factor conditions. Notably, the FGF-2 group exhibited, on average, a greater mean fold-change in the number of tubes than the untreated group. This indicates that FGF-2 modulates the intensity of tubulogenic pressure response. The potential pathways by which pressure may influence endothelial tube formation is summarized in *Figure 5.6a* on the following page shows various pathways through which pressure transduction may occur.

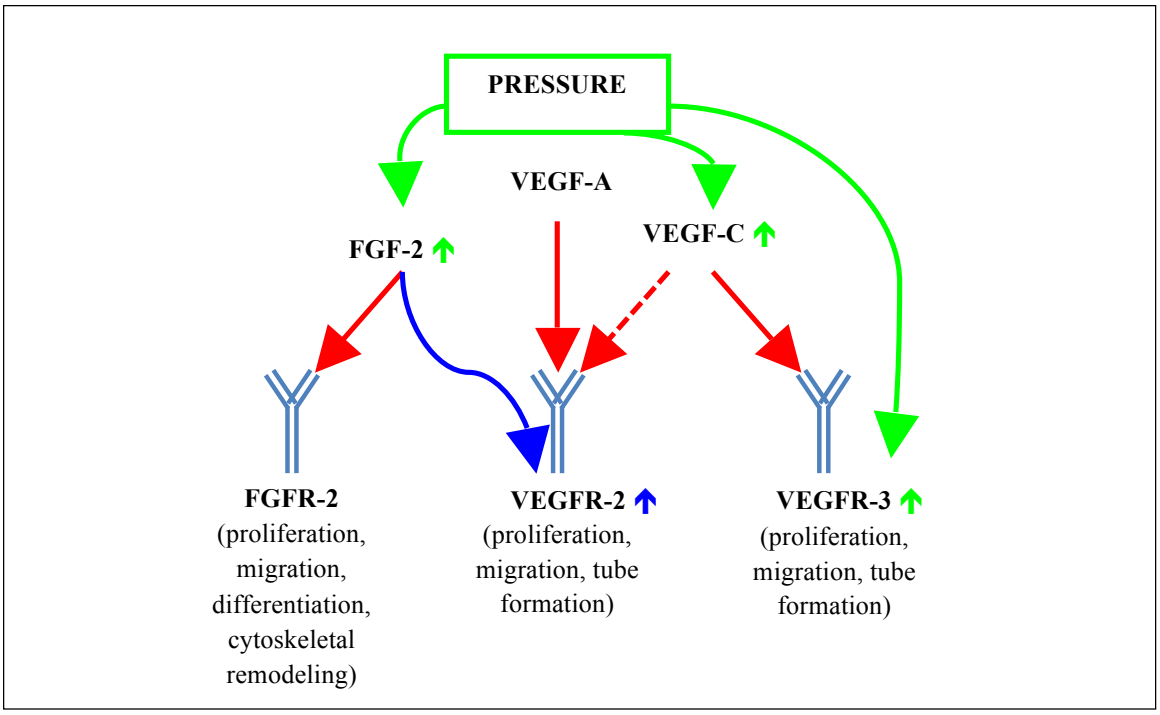

***Figure 5.6a* – The cumulative effects of pressure and growth factors on various other growth factors, growth factor receptors, and tubulogenic processes. Arrows indicate the effect that pressure has on the expression or release of each molecule. Up arrows next to growth factors or receptors indicate increases in that molecule. As shown, pressure causes increases (green) in FGF-2, VEGF-C, and VEGFR-3. Pressure also may, through the increases in FGF-2 expression or release (blue), increase VEGFR-2 expression. Dashed-line arrows indicate low-affinity interactions.**

The mechanisms by which pressure elicits these effects on tubulogenic growth factors and receptors are varied. Previous studies have shown that endothelial cells synthesize intracellular FGF-2 under normal culture conditions [14]. These intracellular stores, located in the nuclei and cytoplasm, were diminished by pressure exposure,

indicating cellular release of cytosolic FGF-2 stores in response to pressure [14]. Pressure-induced FGF-2 release increases the concentration of exogenous FGF-2, which acts in an autocrine and/or paracrine manner and elicits the morphological, proliferative, and tubulogenic effects associated with FGF-2/FGFR-1 binding. It has also been shown that pressure causes increases in VEGF-C transcription [31]. Increased transcription may also be the mechanism by which pressure increases membrane expression of VEGFR-3, the high affinity VEGF-C receptor.

A significant increase in sprouting was also observed after exposure of BAEC to 40 mmHg in the presence of FGF-2 for 72 hours. This also supports the hypothesis that FGF-2 "sensitizes" endothelial cells to pressure or is the "trigger" for tubulogenesis in response to pressure-induced VEGF-C expression since exposure to 40 mmHg pressure alone was not shown to induce increased proliferation (*Figure 4.6a* and *Figure 4.6b*). FGF-2 is a known mitogenic growth factor and its release has been shown to be induced by select pressure regimes [14]. Because increased proliferation was not observed in response to 72-hour exposure to a 40 mmHg sustained pressure, it is likely that a 40 mmHg sustained pressure does not elicit an effective increase in FGF-2 expression or signaling. This could explain why no significant difference in the total number of sprouts was observed in the untreated group ("No GF") after 72 hours of exposure to 40 mmHg, but a significant increase was observed when cultures were supplemented with 2.5 ng/mL of FGF-2.

Moreover, after 96 hours in culture, the combined effects of 40 mmHg pressure exposure and FGF-2 stimulation disappeared. In this regard, it is possible that BAEC cultures consumed the full doses of exogenous FGF-2 within the 96-hour duration of the

pressure experiments with the previously increased tubulogenic activity returning to basal levels. Prior studies have reported that the local microenvironmental concentration of growth factors and not the total dose is governs the resultant microvascular structure [17]. Therefore, it is possible that persistent increases in tubulogenic activity would be expected if FGF-2 levels in culture media were constantly replenished. Interestingly, *Ozawa et al.* (2003) reported that high initial doses of angiogenic factors, such as VEGF-A, result in aberrant blood vessels and abnormal tube formation [52]. Thus, it is also possible that low (optimal) levels of growth factors stimulate a persistent and normal microvascular response as compared to high (abnormal) levels [17]. Therefore, pressure may play a role in maintaining vascular development at a physiologic level.

It was also shown in the current study that BAEC stimulated with 2.5 ng/mL VEGF-A exhibited significant decreases in the number of tubes greater than 150 μm in length and a significant decrease in the mean tube length per bead after both 72- and 96-hour exposure to a 20 mmHg sustained pressure (*Figure 4.12e*). *Ozawa et al.* (2003) provided evidence that a threshold level of VEGF-A that supports physiologic levels of angiogenesis exists, and that exposure to levels of this growth factor in excess of this threshold concentration results in aberrant tube formation and are likely to result in capillary-like vessels displaying morphological and functional abnormalities [52]. As mentioned previously, it has been shown in this study that a 20 mmHg sustained pressure elicits significant increases in VEGF-C expression, which, in addition to promoting tubulogenic activity, has been shown to increase membrane expression of VEGFR-2 (the high-affinity receptor for VEGF-A) (*Figure 4.9*). Notably, a 72-hour exposure to 20 mmHg was also shown to increase membrane expression of the high-affinity VEGF-C

receptor, VEGFR-3. Taken together, these findings support the hypothesis that pressure, in combination with exogenous VEGF-A supplementation, may have caused a supra-physiologic expression level of vascular endothelial growth factor activity. This could explain why cultures supplemented with VEGF-A were unable to support sustained tube growth for 72 or 96 hours, which is in agreement with the results reported by *Ozawa et al.* (2003) [52].

5.7 Concluding Remarks

The results of the present study, combined with data from prior studies, suggest that hydrostatic pressure may play a role in endothelial tubulogenesis *in vivo* and be used as a modulating factor for neovascularization of tissues grown *in vitro*. This study suggests that the pressure modulation is actuated through a coupling of the FGF-2/FGFR-2 and VEGF- C/VEGFR-3 pathways.

Both FGF-2 and VEGF-C play significant roles in tubulogenesis in both vascular and lymphatic networks. It has been shown in this study as well as previous studies that exogenous FGF-2 and VEGF-family growth factors, specifically VEGF-A and VEGF-C, synergistically enhance *in vitro* BAEC tubulogenesis [37, 38, 53]. The present study presents evidence, consistent with previous studies [37], that FGF-2 signaling is a precursor to VEGF-C-mediated tubulogenesis. This finding is consistent with reports [37] that FGF-2 "triggers" the endothelial response to VEGF-family growth factors. Thus, pressure may be an effective modulator of vascular and lymphatic growth for its reported ability to upregulate the local activity levels of both FGF-2 and VEGF-C [2, 14, 19, 31, 45]. Thus, it is possible that FGF-2 "sensitizes" endothelial cells to pressure.

The current study also examined the effects of pressure on endothelial tubulogenesis defined in terms of a discrete set of endothelial activities: proliferation, migration into the extracellular matrix, and the assembly of capillary-like sprouts/tube. In this regard, BAEC seeded on polymeric microcarrier beads and embedded in collagenous matrices were capable of forming sprouts and doing so under a variety of conditions. Specifically, linear, multicellular sprout-like structures extended from the Cytodex3^{TM} bead surfaces. It should be noted that the present study did not investigate whether endothelial sprouts formed lumens *in vitro*. However, previous studies [54] have shown that endothelial sprouts typically do not form lumens after two to three days in culture and require other cell types such as pericytes or fibroblasts. Future studies should thus incorporate the use of other cell types to investigate lumen formation in a more physiological setting.

Despite this limitation, the observed robust tubulogenic response of BAEC to the 20 mmHg pressure stimulus was consistent with the magnitude-dependent effects of hydrostatic pressure on cell proliferation as well as on VEGF-C and VEGFR-3 expression reported in this and previous studies [31]. Also, the observations that FGF-2 promoted a detectable pressure-sensitive increase in endothelial sprouting under 40 mmHg is consistent with the effect of FGF-2 in the 40 mmHg cell proliferation experiments [12].

Taken together, this study focused on elucidating the effects of hydrostatic pressure on endothelial tube formation in the context of the potential use of this mechanical stimulus as an approach to modulate microvascular formation in synthetic or *in vitro*-grown tissue constructs. Given the known effects of fluid flow and substrate

strain on endothelial cells [2], it is important to point out that the hydrostatic pressure regimes used in these experiments were applied in the absence of fluid flow to the incompressible supernatant layer. BAEC responses also occurred in the absence of substrate strain, since the ability of the applied pressure to deform the porous, fully hydrated collagen gel matrix to significant levels is unlikely. Based on these, the present study suggests a role for pressure in early endothelial tubulogenic activity of bovine endothelial cells. Future work, however, is needed to validate human endothelial cells respond to pressure in a similar way, considering that the end application is the engineering of replacement human tissues.

In summary, the salient finding of the present Master's dissertation-related research is that early endothelial tubulogenic activity exhibits pressure sensitivity. It remains to be determined whether pressure-sensitive sprouting leads to the eventual establishment of lumen-containing tubular networks. However, our results provide new evidence substantiating pressure as a tubulogenic stimulus. The findings in this study have implications in a variety of areas. First, these findings add to those of previous studies in elucidating the pressure transduction mechanism of endothelial cells. Second, it has implications in pathological conditions where supraphysiologic pressures may cause erratic and abnormal vascular formation (e.g., glaucoma, cancer, and wound healing). And finally, this study advocates for the use of pressure to modulate neovascularization of tissues and synthetic tissue constructs *in vitro* so as to promote their ability to integrate and survive *in vivo*.

References

1. Carmielet, P., Angiogenesis in health and disease, Nature Medicine 9(6):653-660 (2003).
2. Shiu, Yang-Ting, et al., The Role of Mechanical Forces in Angiogenesis, *Critical Reviews in Biomedical Engineering* 33(5), 431-450 (2005).
3. Ikada, Yoshita (2006), *Tissue Engineering: Fundamentals and Principles*, Oxford, UK: Elsevier, Ltd.
4. ATP Focused Program: Tissue Engineering, National Institute of Standards and Technology, http://www.atp.nist.gov/focus/tissue.htm (visited on December 10, 2012)
5. Griffith et al., "Diffusion Limits of an *in Vitro* Thick Prevascularized Tissue," *Tissue Engineering*, 11, 257-265 (2005).
6. Schechner, J.S., A.K. Nath, L. Zheng, M.S. Kluger, C.C.W. Hughes, M.R. Sierra-Honigmann, M.I. Lorber, G. Tellides, M. Kashgarian, A.L.M. Bothwell, J.S. Pober, *In vivo* formation of complex microvessels lined by human endothelial cells in an immunodeficient mouse, Proc. Natl. Acad. Sci. 97(16):9191-9196 (2000).
7. Nehls, V. and D. Drenckhahn, "A microcarrier-based cocultivation system for the investigation of factors and cells involved in three-dimensional fibrin matrices in vitro," *Histochem Cell Biol* 104(6), 459-466 (1995).
8. Dietrich, F. and P. Lelkes, "Fine-tuning of a three-dimensional microcarrier-based angiogenesis assay for the analysis of endothelial-mesenchymal cell co-cultures in fibrin and collagen gels," *Angiogenesis* 9, 111-125 (2006).
9. The Organ Transplant Procurement Network, http://optn.transplant.hrsa.gov (visited on December 10, 2012).
10. Lokmik, Z. and G. Mitchell, Engineering the Microcirculation, Tissue Engineering 14(1):87-103 (2008).
11. Sumpio et al., Cells in focus: endothelial cell, Int'l. J. Biochem. and Cell Bio. 34:1508-1512 (2002).
12. Sumpio, B.E., M.D. Widmann, J. Ricotta, M.A. Awolesi, M. Watase, Increased Ambient Pressure Stimulates Proliferation and Morphological Changes in Cultured Endothelial Cells, J. Cell. Phys. 158:133-139 (1994).
13. Stoeltzing, Oliver et al., Angiopoietin-1 Inhibits Vascular Permeability, Angiogenesis, and Growth of Hepatic Colon Cancer Tumors, *Cancer Res.* 63:3370-3377 (2003).
14. Acevedo A.D., S.S. Bowser, M.E. Gerritsen, R. Bizios, Morphological and Proliferative Responses of Endothelial Cells to Hydrostatic Pressure: Role of Fibroblast Growth Factor, J Cell Phys. 153:603-614 (1993).
15. Skobe, M. and M. Detmar, Structure, Function, and Molecular Control of the Skin Lymphatic System, Skin Lymphatic System 5(1):14-19 (2000).
16. Vailhe, B., D. Vittet, J.J. Feige, In Vitro Models of Vasculogenesis and Angiogenesis, Laboratory Investigation 81(4):439-452 (2001).
17. Uriel, Shiri, Brey, Eric M., & Greisler, Howard P., Sustained low levels of fibroblast growth factor-1 promote persistent microvascular network formation, *The American Journal of Surgery* 192, 604-609 (2006).
18. Ucuzian, A.A., H.P. Greisler, In Vitro Models of Angiogenesis, World J. Surg. 31:654-663 (2007).

19. Shin, H.Y., R.M. Underwood, M.W. Fannon, Fluid Pressure Is a Magnitude-Dependent Modulator of Early Endothelial Activity: Implications Related to a Potential Tissue Engineering Control Parameter, Tissue Engineering Part A 18(23-24):2590-2600 (2012).
20. Folkman, J. and C. Haudenschild, Angiogenesis in vitro, Nature 288 (5791):551-556 (1980).
21. Montesano, R., M.S. Pepper, L. Orci, Angiogenesis In Vitro: Morphogenetic and Invasive Properties of Endothelial Cells, Physiology 5:75-79 (1990).
22. Cavallaro U., M. Tenan, V. Castelli, A. Perilli, N. Maggiano, E.G. Van Meir, R. Montesano, M.R. Soria, M.S. Pepper. Response of Bovine Endothelial Cells to FGF-2 and VEGF is Dependent on Their Site of Origin: Relevance to the Regulation of Angiogensis, J. Cell Biochem. 82:619-633 (2001).
23. Ferrara, N., Role of vascular endothelial growth factor in the regulation of angiogenesis, Kidney Int'l 56:794-814 (1999).
24. Cao, R., A. Eriksson, H. Kubo, K. Alitalo, Y. Cao, J. Thyberg, Comparative Evaluation of FGF-2-, VEGF-A-, and VEGF-C-Induced Angiogenesis, Lymphangiogenesis, Vascular Fenestrations, and Permeability, Circ. Res. 94:664-670 (2004).
25. Ferrara, N., K. Carver-Moore, H. Chen, M. Dowd, L. Lu, K.S. O'Shea, L. Powell-Braxton, K.J. Hillan, M.W. Moore, Heterozygous embryonic lethality induced by targeted inactivation of the VEGF gene, Nature 380:439-442 (1996).
26. Carmeliet, P., V. Ferreira, G. Breier, S. Pollefeyt, L. Kieckens, M. Gertenstein, M. Fahrig, A. Vandenhoeck, K. Harpal, C. Eberhardt, C DeClerco, J. Pawling, L. Moons, D. Collen, W. Risau, A. Nagy, Abnormal blood vessel development and lethality in embryos lacking a single VEGF allele, Nature 380:435-439 (1996).
27. Goldman, J., J.M. Rutkowski, J.D. Shields, M.C. Pasquier, Y. Cui, H.G. Schmokel, S. Willey, D.J. Hicklin, B. Pytowski, M.A. Swartz, Cooperative and redundant roles of VEGFR-2 and VEGFR-3 signaling in adult lymphangiogenesis, The FASEB Journal 21:1003-1012 (2007).
28. Tammela, T., G. Zarkada, E. Wallgard, A. Murtoma, S. Suchting, M. Wirzenius, M. Waltari, M. Hellstro, T. Schomber, R. Peltonen, C. Freitas, A. Duarte, H. Isoniemi, P. Laakkonen, G. Christofori, S. Y. Herttuala, M. Shibuya, B. Pytowski, A. Eichmann, C. Betsholtz, K. Alitalo, Blocking VEGFR-3 suppresses angiogenic sprouting and vascular network formation, Nature 454:656-663 (2008).
29. Persaud, K., J.C. Tille, M. Liu, Z. Zhu, X. Jiminez, D. Pereira, H.Q. Miao, L. Brennan, L. Witte, M.S. Pepper, B. Pytowski. Involvement of the VEGF receptor 3 in tubular morphogenesis demonstrated with a human anti-human VEGFR-3 monoclonal antibody that antagonizes receptor activation by VEGF-C, J. Cell Sci. 117:2745-2756 (2004).
30. Bauer, S.M., R.J. Bauer, Z.J. Liu, H. Chen, L. Goldstein, O.C. Velazquez, Vascular endothelial growth factor-C promotes vasculogenesis, angiogenesis, and collagen constriction in three-dimensional collagen gels, J. Vascular Surg. 41(4):699-706 (2005).
31. Shin, H.Y., VEGF-C mediates cyclic pressure-induced endothelial cell proliferation, Physiol. Genomics 11:245-251 (2002).

32. Montesano, R., J.D. Vassalli, A. Baird, R. Guillemin, L. Orci, Basic fibroblast growth factor induces angiogenesis in vitro, Proc. Natl. Acad. Sci. 83:7297-7301 (1986).
33. Cross, M.J. and L. Claesson-Welsh, FGF and VEGF function in angiogenesis: Signaling pathways, biological responses and therapeutic inhibition, Trends in Pharmacological Sci. 2(4):201-207 (2001).
34. Boilly, B., A.S. Vercoutter-Edouart, H. Hondermarck, V. Nurcombe, X. Le Bourhis, FGF signals for cell proliferation and migration through different pathways, Cytokine & Growth Factor Reviews 11:295-302 (2000).
35. Cao, R., J. Hong, N. Feng, Y. Zhang, X. Yang, P. Andersson, Y. Sun, K. Tritsaris, A.J. Hansen, S. Dissing, and Y. Cao, Collaborative interplay between FGF-2 and VEGF-C promotes lymphangiogenesis and metastasis, Proc. Nat'l Acad. Sci. 109(39):15894-15899 (2012).
36. Slavin, J., Fibroblast Growth Factors: At the Heart of Angiogenesis, Cell Bio. Int'l 19(5):431-444 (1995).
37. Mandriota, S.J. and M.S. Pepper, Vascular endothelial growth factor-induced in vitro angiogenesis and plasminogen activator expression are dependent on endogenous basic fibroblast growth factor, J. Cell Sci. 110:2293-2303 (1997).
38. Nagy, J.A., E. Vasile, D. Feng, C. Sundberg, L.F. Brown, M.J. Detmar, J.A. Lawitts, L. Benjamin, X. Tan, E.J. Manseau, A.M. Dvorak, H.F. Dvorak, Vascular Permeability Factor/Vascular Endothelial Growth Factor Induces Lymphangiogenesis as well as Angiogenesis, J. Exp. Med. 196(11):1497-1506 (2002).
39. Shin, H.Y., R. Bizios, M.E. Gerritsen, Cyclic Pressure Modulates Endothelial Barrier Function, Endothelium 10:179-187 (2003).
40. Shin, H.Y., E.A. Schwartz, R. Bizios, M.E. Gerritsen, Receptor-Mediated Basic Fibroblast Growth Factor Signaling Regulates Cyclic Pressure-Induced Human Endothelial Proliferation, Endothelium 11:285-291 (2004).
41. Ohashi, T., Y. Sugaya, N. Sakamoto, M. Sato, Hydrostatic pressure influences morphology and expression of VE-cadherin of vascular endothelial cells, J. Biomechanics 40:2399-2405 (2007).
42. Nakatsu, M. and C.W. Hughes, An Optimized Three-Dimensional *In Vitro* Model for the Analysis of Angiogenesis, Methods in Enzymology 443:65-82 (2008). The dynamic seeding protocol used herein to seed BAEC on Cytodex3^{TM} microcarrier beads was modeled after that used in *Nakatsu and Hughes* (2008).
43. Maeshima, K., A. Maeshima, Y. Hayashi, S. Kishi, I. Kojima, Crucial Role of Activin A in Tubulogenesis of Endothelial Cells Induced by Vascular Endothelial Growth Factor, Endocrinology 145(8):3739-3745 (2004).
44. Lincoln II, D.W., R.G. Whitney, J.R. Smith, *In Vitro* Proliferation and Lifespan of Bovine Aorta Endothelial Cells: Response to Conditioned Media, J. Cell. Sci. 56:281-292 (1982).
45. Shin, H.Y., M.E. Gerritsen, R. Bizios, Regulation of Endothelial Cell Proliferation and Apoptosis by Cyclic Pressure, Annals of Biomedical Eng. 30:297-304 (2002).
46. Tille, J.C., X. Wang, K.E. Lipson, G. McMahon, N. Ferrara, Z. Zhu, D.J. Hicklin, J.P. Sleeman, U. Eriksson, K. Alitalo, M.S. Pepper, Vascular endothelial growth factor (VEGF) receptor-2 signaling mediates VEGF-$C_{\Delta N \Delta C}$ and VEGF-A induced angiogenesis in vitro, Exp. Cell Res. 285(2):286-298 (2003).

47. Kirkin, V., W. Thiele, P. Baumann, R. Mazitzscheck, K. Rohde, G. Fellbrich, H. Weich, J. Waltenberger, A. Giannis, J. Sleeman. MAZ-51, an Indolinone that Inhibits Endothelial Cell and Tumor Cell Growth *In Vitro*, Suppresses Tumor Growth *In Vivo*, Int. J. Cancer 112:986-993 (2004).
48. Boettcher, M., T. Gloe, C. de Wit. Semiautomatic Quantification of Angiogenesis, J. Surg. Res. 162(1):132-139 (2010).
49. Lamalice, L., F. Le Boeuf, J. Huot, Endothelial Cell Migration During Angiogenesis, Circ. Res. 100:782-794 (2007).
50. Joukov, V., K. Pajusola, A. Kapainen, D. Chilov, I. Lahtinen, E. Kukk, O. Saksela, N. Kalkkinen, K. Alitalo. A novel vascular endothelial growth factor, VEGF-C, is a ligand for the Flt4 (VEGFR-2) receptor tyrosine kinases, The EMBO Journal 14(2):290-298 (1996).
51. Yang., S., X. Xin, C. Zlot, G. Ingle, G. Fuh, B. Li, B. Moffat, A. B. de Vos, M. Gerritsen, Vascular Endothelial Cell Growth Factor Driven Endothelial Cell Growth Factor Receptor-2, a Kinase Insert Domain-Containing Receptor, Arterioscler. Thomb. Vasc. Biol. 21:1934-1940 (2001).
52. Ozawa, C.R., A. Banfi, N.L. Glazer, et al., Microenvironmental VEGF concentration, not total dose, determines a threshold between normal and aberrant angiogenesis, J. Clin Inv. 15:516-527 (2003).
53. Ferrara, N., Role of vascular endothelial growth factor in the regulation of angiogenesis, Kidney Int'l. 56:794-814 (1999).
54. Montesano, R., L. Orci, P. Vassalli, In Vitro Rapid Organization of Endothelial Cells into Capillary-like Networks is Promoted by Collagen Matrices, J. Cell. Bio. 97:1648-1652 (1983).

Vita

RYAN MATTHEW UNDERWOOD

Education

B.S. **Mechanical Engineering**, Miami University, Oxford, Ohio 2008

B.S. **Engineering Management**, Miami University, Oxford, Ohio 2008

Work Experience

Law Clerk, Office of Risk Management, University of Kentucky Chandler Medical Center, Lexington, KY — Aug. 2012 – Dec. 2012

Summer Associate, Mannion & Gray, LPA, Fort Wright, KY — May 2012 – Aug. 2012

Law Clerk, Office of Entrepreneurship and Economic Development, University of Kentucky, Lexington, KY — May 2011 – Aug. 2011

Research Assistant, Cellular Mechanobiology Laboratory, Center for Biomedical Engineering, University of Kentucky, Lexington, KY — May 2008 – Aug. 2010

Research Assistant, Alternative Fuels Laboratory, Dept. of Mech. and Mfg. Engineering, Miami University, Oxford, OH — Sep. 2007 – Mar. 2008

Research and Development Co-Op, Ethicon Endo-Surgery, Johnson & Johnson, Cincinnati, OH — May 2007 – Sep. 2007

Engineering Intern, Ariel Corporation, Mount Vernon, OH — May 2006 – Aug. 2006

Engineering Intern, Milgard Manufacturing, Aurora, IL — May 2005 – Aug. 2005

Research Experience

Research Assistantship, Vascular Biology and Tissue Engineering, Center for Biomedical Engineering, University of Kentucky, Lexington, KY — 2008-2010

Undergraduate Research Assistantship, Alternative Fuels Development and Testing, Dept. of Mechanical and Manufacturing Engineering, Miami University, Oxford, OH — 2006-2008

Publications

H.Y. Shin, **R.M. Underwood**, M.W. Fannon. Fluid Pressure is a Magnitude-Dependent Modulator of Early Endothelial Tubulogenic Activity: Implications Related to a Potential Tissue Engineering Control Parameter. Tissue Engineering, Part A (2012) doi:10.1089/ten.tea.2011.0588 (in press)

Presentations

R.M. Underwood, H.Y. Shin, "Effects of Hydrostatic Pressure on Endothelial Tubulogenic Processes." Poster Session, Experimental Biology 2010, Anaheim, CA (Apr. 2010)

R.M. Underwood, H.Y. Shin, "The Effect of Sustained Hydrostatic Pressures on Endothelial Tubulogenesis." Invited Seminar, University of Kentucky Center for Biomedical Engineering, Lexington, KY (Mar. 2010)

R.M. Underwood, H.Y. Shin, "The Effect of Hydrostatic Pressure on Endothelial Angiogenesis and Lymphangiogenesis." Poster Session, Gill Heart Institute Cardiovascular Research Conference, Lexington, KY (Oct. 2009)

J.T. Van Kuren, **R.M. Underwood**, "An Alternative Fuels Testing Laboratory." Invited Presentation, ASME Dayton Engineering Sciences Symposium, Dayton, OH (Oct. 2007)

J.T. Van Kuren, **R.M. Underwood**, M. Mukai, M. Capalbo, R. Haas, J. Orbon, J. Sweeney, "Alternative Fuels Testing and Development." Invited Presentation, AIAA Joint Propulsion Conference, Cincinnati, OH (Feb. 2007)

Teaching Experience

Undergraduate Teaching Assistant, Fluid Mechanics, Dept. of Mechanical and Manufacturing Engineering, Miami University, Oxford, OH 2006-2007

Awards

Miami University Undergraduate Research Award, Grant-in-Aid 2007

Johnson Controls Robotics Scholarship, Recipient 2003

Professional Memberships & Affiliations

Kentucky Law Journal – *Senior Editor (2012-2013), Staff Editor (2011-2012)*

Phi Alpha Delta Law Fraternity, International – *President (Clay Chapter, 2011-2012), Member*

University of Kentucky Health Law Society – *Board Member*

University of Kentucky Student Health Advisory Committee (SHAC) – *Member*

American Bar Association (ABA) – *Student Member*

American Intellectual Property Law Association – *Student Member*

Biomedical Engineering Society (BMES) – *Vice President (University of Kentucky, 2009-2010), Member*

Federation of American Societies for Experimental Biology (FASEB) – *Member*

American Society for Mechanical Engineers (ASME) – *Member*

American Institute of Aeronautics and Astronautics (AIAA) – *Member*